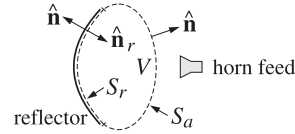


- 18.9 Consider a reflector antenna fed by a horn, as shown on the right. A closed surface $S = S_r + S_a$ is such that the portion S_r caps the reflector and the portion S_a is an aperture in front of the reflector. The feed lies outside the closed surface, so that the volume V enclosed by S is free of current sources.



Applying the Kottler version of the extinction theorem of Sec. 18.10 on the volume V , show that for points \mathbf{r} outside V , the field radiated by the induced surface currents on the reflector S_r is equal to the field radiated by the aperture fields on S_a , that is,

$$\begin{aligned} E_{\text{rad}}(\mathbf{r}) &= \frac{1}{j\omega\epsilon} \int_{S_r} [k^2 G \mathbf{J}_s + (\mathbf{J}_s \cdot \nabla') \nabla' G] dS' \\ &= \frac{1}{j\omega\epsilon} \int_{S_a} [k^2 G (\hat{\mathbf{n}} \times \mathbf{H}) + ((\hat{\mathbf{n}} \times \mathbf{H}) \cdot \nabla') \nabla' G + j\omega\epsilon (\hat{\mathbf{n}} \times \mathbf{E}) \times \nabla' G] dS' \end{aligned}$$

where the induced surface currents on the reflector are $\mathbf{J}_s = \hat{\mathbf{n}}_r \times \mathbf{H}$ and $\mathbf{J}_{ms} = -\hat{\mathbf{n}}_r \times \mathbf{E}$, and on the perfectly conducting reflector surface, we must have $\mathbf{J}_{ms} = 0$.

This result establishes the equivalence of the so-called aperture-field and current-distribution methods for reflector antennas [1686]. See also Sec. 21.9.

- 18.10 Consider an x -polarized uniform plane wave incident obliquely on the straight-edge aperture of Fig. 18.14.4, with a wave vector direction $\mathbf{k}_1 = \hat{\mathbf{z}} \cos \theta_1 + \hat{\mathbf{y}} \sin \theta_1$. First show that the tangential fields at an aperture point $\mathbf{r}' = x' \hat{\mathbf{x}} + y' \hat{\mathbf{y}}$ on the aperture above the straight-edge are given by:

$$E_a = \hat{\mathbf{x}} E_0 e^{-jk_y' \sin \theta_1}, \quad H_a = \hat{\mathbf{y}} \frac{E_0}{\eta_0} \cos \theta_1 e^{-jk_y' \sin \theta_1}$$

Then, using Kottler's formula (18.12.1), and applying the usual Fresnel approximations in the integrand, as was done for the point source in Fig. 18.14.4, show that the diffracted wave below the edge is given by Eqs. (18.14.23)–(18.14.25), except that the field at the edge is $E_{\text{edge}} = E_0$, and the focal lengths are in this case $F = l_2$ and $F' = l_2 / \cos^2 \theta_2$

Finally, show that the asymptotic diffracted field (when $l_2 \rightarrow \infty$), is given near the forward direction $\theta \approx 0$ by:

$$E = E_{\text{edge}} \frac{e^{-jkl_2}}{\sqrt{l_2}} \frac{1-j}{2\sqrt{\pi k} \theta}$$

- 18.11 Assume that the edge in the previous problem is a perfectly conducting screen. Using the field-equivalence principle with effective current densities on the aperture above the edge $\mathbf{J}_s = 0$ and $\mathbf{J}_{ms} = -2\hat{\mathbf{n}} \times \mathbf{E}_a$, and applying the usual Fresnel approximations, show that the diffracted field calculated by Eq. (18.4.1) is still given by Eqs. (18.14.23)–(18.14.25), except that the factor $\cos \theta_1 + \cos \theta_2$ is replaced now by $2 \cos \theta_2$, and that the asymptotic field and edge-diffraction coefficient are:

$$E = E_0 \frac{e^{-jkl_2}}{\sqrt{l_2}} D_{\text{edge}}, \quad D_{\text{edge}} = \frac{(1-j)2 \cos \theta_2}{4\sqrt{\pi k}(\sin \theta_1 + \sin \theta_2)}$$

Show that this expression agrees with the exact Sommerfeld solution (18.15.26) at normal incidence and near the forward diffracted direction.

Diffraction – Plane-Wave Spectrum

This chapter continues the previous one on radiation from apertures. The emphasis is on Rayleigh-Sommerfeld diffraction theory, plane-wave spectrum representation for scalar and vector fields, radiated and reactive power of apertures, integral equations for apertures in conducting screens, revisiting the Sommerfeld half-plane problem using Wiener-Hopf factorization techniques, the Bethe-Bouwkamp model of diffraction by small holes, and the Babinet principle.

19.1 Rayleigh-Sommerfeld Diffraction Theory

In this section, we recast Kirchhoff's diffraction formula in a form that uses a Dirichlet Green's function (i.e., one that vanishes on the boundary surface) and obtain the Rayleigh-Sommerfeld diffraction formula. In the next section, we show that this reformulation is equivalent to the *plane-wave spectrum* approach to diffraction, and use it to justify the modified forms (18.1.2) and (18.1.3) of the field equivalence principle. In Chap. 20, we use it to obtain the usual Fresnel and Fraunhofer approximations and discuss a few applications from Fourier optics.

We will work with the scalar case, but the same method can be used for the vector case. With reference to Fig. 19.1.1, we consider a scalar field $E(\mathbf{r})$ that satisfies the source-free Helmholtz equation, $(\nabla^2 + k^2)E(\mathbf{r}) = 0$, over the right half-space $z \geq 0$.

We consider a closed surface consisting of the surface S_∞ of a sphere of very large radius centered at the observation point \mathbf{r} and bounded on the left by its intersection S with the xy plane, as shown in the Fig. 19.1.1. Clearly, in the limit of infinite radius, the volume V bounded by $S + S_\infty$ is the right half-space $z \geq 0$, and S becomes the entire xy plane. Applying Eq. (18.10.3) to volume V , we have:

$$\int_V [G(\nabla'^2 E + k^2 E) - E(\nabla'^2 G + k^2 G)] dV' = - \oint_{S+S_\infty} \left[G \frac{\partial E}{\partial n'} - E \frac{\partial G}{\partial n'} \right] dS' \quad (19.1.1)$$

The surface integral over S_∞ can be ignored by noting that $\hat{\mathbf{n}}$ is the negative of the radial unit vector and therefore, we have after adding and subtracting the term $jkEG$:

$$- \int_{S_\infty} \left[G \frac{\partial E}{\partial n'} - E \frac{\partial G}{\partial n'} \right] dS' = \int_{S_\infty} \left[G \left(\frac{\partial E}{\partial r} + jkE \right) - E \left(\frac{\partial G}{\partial r} + jkG \right) \right] dS'$$

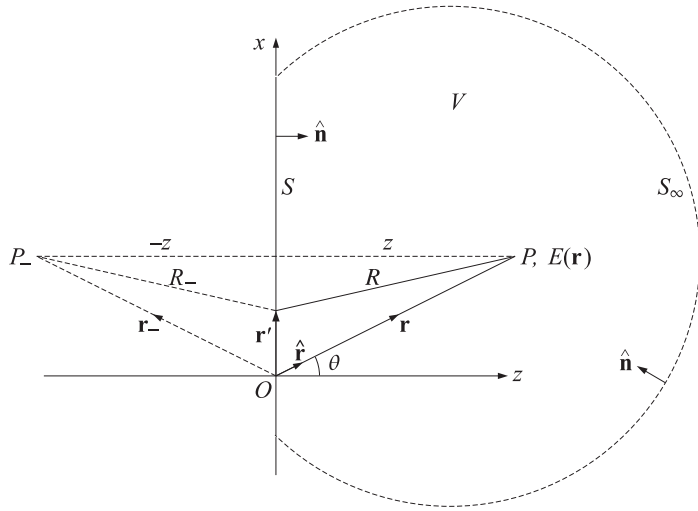


Fig. 19.1.1 Fields determined from their values on the xy-plane surface.

Assuming Sommerfeld's outgoing radiation condition:

$$r \left(\frac{\partial E}{\partial r} + jkE \right) \rightarrow 0, \text{ as } r \rightarrow \infty$$

and noting that $G = e^{-jk r} / 4\pi r$ also satisfies the same condition, it follows that the above surface integral vanishes in the limit of large radius r . Then, in the notation of Eq. (18.10.4), we obtain the standard Kirchhoff diffraction formula, where the planar surface S is the entire xy plane,

$$E(\mathbf{r}) u_V(\mathbf{r}) = \int_S \left[E \frac{\partial G}{\partial n'} - G \frac{\partial E}{\partial n'} \right] dS' \quad (19.1.2)$$

Thus, if \mathbf{r} lies in the right half-space, the left-hand side will be equal to $E(\mathbf{r})$, and if \mathbf{r} is in the left half-space, it will vanish. Given a point $\mathbf{r} = (x, y, z)$, we define its reflection relative to the xy plane by $\mathbf{r}_- = (x, y, -z)$. The distance between \mathbf{r}_- and a source point $\mathbf{r}' = (x', y', z')$ can be written in terms of the distance between the original point \mathbf{r} and the reflected source point $\mathbf{r}'_- = (x', y', -z')$:

$$R_- = |\mathbf{r}_- - \mathbf{r}'| = \sqrt{(x - x')^2 + (y - y')^2 + (z + z')^2} = |\mathbf{r} - \mathbf{r}'_-|$$

whereas

$$R = |\mathbf{r} - \mathbf{r}'| = \sqrt{(x - x')^2 + (y - y')^2 + (z - z')^2}$$

This leads us to define the reflected Green's function:

$$G_-(\mathbf{r}, \mathbf{r}') = \frac{e^{-jkR_-}}{4\pi R_-} = G(\mathbf{r} - \mathbf{r}'_-) = G(\mathbf{r}_- - \mathbf{r}') \quad (19.1.3)$$

and the Dirichlet Green's function:

$$G_d(\mathbf{r}, \mathbf{r}') = G(\mathbf{r}, \mathbf{r}') - G_-(\mathbf{r}, \mathbf{r}') = \frac{e^{-jkR}}{4\pi R} - \frac{e^{-jkR_-}}{4\pi R_-} \quad (19.1.4)$$

For convenience, we may choose the origin to lie on the xy plane. Then, as shown in Fig. 19.1.1, when the source point \mathbf{r}' lies on the xy plane (i.e., $z' = 0$), the function $G_d(\mathbf{r}, \mathbf{r}')$ will vanish because $R = R_-$. Next, we apply Eq. (19.1.2) at the observation point \mathbf{r} in the right half-space and at its reflection in the left half-plane, where (19.1.2) vanishes:

$$\begin{aligned} E(\mathbf{r}) &= \int_S \left[E \frac{\partial G}{\partial n'} - G \frac{\partial E}{\partial n'} \right] dS', \quad \text{at point } \mathbf{r} \\ 0 &= \int_S \left[E \frac{\partial G_-}{\partial n'} - G_- \frac{\partial E}{\partial n'} \right] dS', \quad \text{at point } \mathbf{r}_- \end{aligned} \quad (19.1.5)$$

where G_- stands for $G(\mathbf{r}_- - \mathbf{r}')$. But on the xy plane boundary, $G_- = G$ so that if we subtract the two expressions we may eliminate the term $\partial E / \partial n'$, which is the reason for using the Dirichlet Green's function:

$$E(\mathbf{r}) = \int_S E(\mathbf{r}') \frac{\partial}{\partial n'} (G - G_-) dS' = \int_S E(\mathbf{r}') \frac{\partial G_d}{\partial n'} dS'$$

On the xy plane, we have $\hat{\mathbf{n}} = \hat{\mathbf{z}}$, and therefore

$$\frac{\partial G}{\partial n'} = \frac{\partial G}{\partial z'} \Big|_{z'=0} \quad \text{and} \quad \frac{\partial G_-}{\partial n'} = \frac{\partial G_-}{\partial z'} \Big|_{z'=0} = - \frac{\partial G}{\partial z'} \Big|_{z'=0}$$

Then, the two derivative terms double resulting in the *Rayleigh-Sommerfeld* (type-1) diffraction integral [1286,1287]:

$$E(\mathbf{r}) = 2 \int_S E(\mathbf{r}') \frac{\partial G}{\partial z'} dS' = -2 \frac{\partial}{\partial z} \int_S E(\mathbf{r}') G dS' \quad (\text{Rayleigh-Sommerfeld}) \quad (19.1.6)$$

The indicated derivative of G can be expressed as follows:

$$- \frac{\partial G}{\partial z'} \Big|_{z'=0} = \frac{\partial G}{\partial z'} \Big|_{z'=0} = \frac{z}{R} \left(jk + \frac{1}{R} \right) \frac{e^{-jkR}}{4\pi R} \quad (19.1.7)$$

To clarify the notation, we may write Eq. (19.1.6) in the more explicit form using (19.1.7),

$$E(x, y, z) = 2 \iint_{-\infty}^{\infty} \frac{z}{R} \left(jk + \frac{1}{R} \right) \frac{e^{-jkR}}{4\pi R} E(x', y', 0) dx' dy' \quad (19.1.8)$$

where $R = \sqrt{(x - x')^2 + (y - y')^2 + z^2}$. For distances $R \gg \lambda$, or equivalently, $k \gg 1/R$, one obtains the approximation:

$$\frac{\partial G}{\partial z'} \Big|_{z'=0} = jk \frac{z}{R} \frac{e^{-jkR}}{4\pi R}, \quad \text{for } R \gg \lambda \quad (19.1.9)$$

This approximation will be used in Sec. 20.1 to obtain the standard Fresnel diffraction representation. The quantity z/R is an "obliquity" factor and is usually omitted for *paraxial* observation points that are near the z axis.

Equation (19.1.8) expresses the field at any point in the right half-space ($z \geq 0$) in terms of its values on the xy plane. For $z < 0$, the sign in the right-hand side of (19.1.6) must be reversed. This follows by using a left hemisphere enclosing the space $z < 0$, in the limit of large radius, and noting that now $\hat{\mathbf{n}} = -\hat{\mathbf{z}}$, and assuming that $E(x, y, z)$ still satisfies the Helmholtz equation in $z < 0$. Thus, we have more generally,

$$E(x, y, z) = \mp 2 \frac{\partial}{\partial z} \iint_{-\infty}^{\infty} E(x', y', 0) G(R) dx' dy' \quad \text{for } z \geq 0 \quad (19.1.10)$$

Because $R = \sqrt{(x-x')^2 + (y-y')^2 + z^2}$, it follows that $\int_S E(x', y', 0) G(R) dx' dy'$ will be an even function of z , and therefore, its z -derivative will be odd in z , and hence, $E(x, y, z)$ will be an *even* function of z . This is seen more explicitly by performing the z -differentiation in (19.1.10), and noting that, $\pm z = |z|$ for $z \geq 0$,

$$E(x, y, z) = 2 \iint_{-\infty}^{\infty} \frac{|z|}{R} \left(jk + \frac{1}{R} \right) \frac{e^{-jkR}}{4\pi R} E(x', y', 0) dx' dy', \quad \text{for all } z$$

By adding, instead of subtracting, the two integrals in (19.1.5), we obtain the alternative (Neumann-type) Green's function, $G_s = G + G_-$, having vanishing derivative on the boundary. This results in the so-called *type-2* Rayleigh-Sommerfeld diffraction integral that expresses $E(x, y, z)$ in terms of its derivative at $z = 0$,

$$E(x, y, z) = \mp 2 \iint_{-\infty}^{\infty} G(R) \frac{\partial E(x', y', 0)}{\partial z'} dx' dy' \quad \text{for } z \geq 0 \quad (19.1.11)$$

We will see in the next section that both Eqs. (19.1.10) and (19.1.11) follow from the *same* plane-wave spectrum representation.

The derivation of (19.1.10) and (19.1.11) implicitly assumed that $E(x, y, z)$ was continuous across the xy plane. When parts of the plane are replaced by a thin conducting sheet, then some of the electromagnetic field components develop discontinuities across the conducting parts. In such cases, where the limiting values $E(x', y', \pm 0)$ are different from the two sides of $z = 0$, the above diffraction integrals must be replaced by,

$$E(x, y, z) = \mp 2 \frac{\partial}{\partial z} \iint_{-\infty}^{\infty} E(x', y', \pm 0) G(R) dx' dy' \quad \text{for } z \geq 0 \quad (19.1.12)$$

$$E(x, y, z) = \mp 2 \iint_{-\infty}^{\infty} G(R) \frac{\partial E(x', y', \pm 0)}{\partial z'} dx' dy'$$

Eqs. (19.1.10) and (19.1.11) are also valid in the vectorial case for each component of the electric field $\mathbf{E}(\mathbf{r})$. However, these components are not independent of each other since they must satisfy $\nabla \cdot \mathbf{E} = 0$, and are also coupled to the magnetic field through Maxwell's equations. Taking into account these constraints, one arrives at the vectorial versions of (19.1.10) known as Smythe's diffraction formulas [1328], which are actually equivalent to the Franz formulas of Sec. 18.12. For example, assuming that the transverse components E_x, E_y are given by Eq. (19.1.10),

$$E_x(\mathbf{r}) = \mp 2 \int_S E_x(\mathbf{r}') \frac{\partial G}{\partial z} dS', \quad E_y(\mathbf{r}) = \mp 2 \int_S E_y(\mathbf{r}') \frac{\partial G}{\partial z} dS' \quad (19.1.13)$$

then, it is easy to verify that the following E_z component will satisfy the divergence condition, $\partial_x E_x + \partial_y E_y + \partial_z E_z = 0$,

$$E_z(\mathbf{r}) = \pm 2 \int_S \left[E_x(\mathbf{r}') \frac{\partial G}{\partial x} + E_y(\mathbf{r}') \frac{\partial G}{\partial y} \right] dS' \quad (19.1.14)$$

and indeed, Eqs. (19.1.13) and (19.1.14) are the Smythe formulas for the E field. We pursue these issues further in Sec. 19.5.

Kirchhoff Approximation

In the practical application of the Rayleigh-Sommerfeld formulas, the xy plane consists of an infinite opaque screen with an aperture A cut in it, as shown in Fig. 19.1.2.

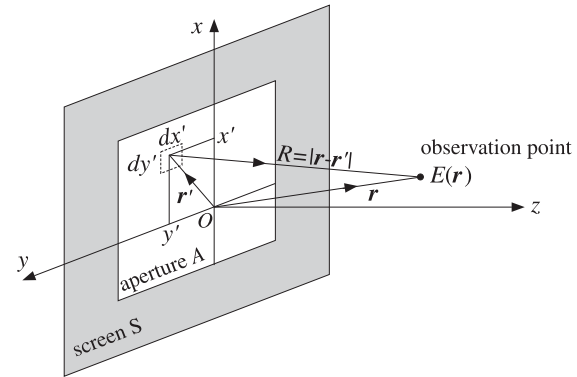


Fig. 19.1.2 Aperture geometry, with $R = |\mathbf{r} - \mathbf{r}'|$, $\mathbf{r} = \hat{\mathbf{x}}x + \hat{\mathbf{y}}y + \hat{\mathbf{z}}z$, $\mathbf{r}' = \hat{\mathbf{x}}x' + \hat{\mathbf{y}}y'$.

In the usual *Kirchhoff approximation* it is assumed that:

- (a) the field is zero over the opaque screen, so that the integration in (19.1.6) is restricted only over the aperture A .
- (b) the field, $E(\mathbf{r}')$, over the aperture is equal to the (known) incident field, say $E_{\text{inc}}(\mathbf{r})$, from the left.

This results in a computable approximation for the diffracted field into the right half-space $z > 0$,

$$E(\mathbf{r}) = -2 \frac{\partial}{\partial z} \int_A E_{\text{inc}}(\mathbf{r}') G(R) dS' \quad (\text{Kirchhoff approximation}) \quad (19.1.15)$$

Generally, such approximations work well for apertures whose dimensions are large compared to the wavelength λ . For apertures in conducting screens, the exact formulation requires that one must first determine the correct aperture fields by solving certain integral equations, and then apply the Rayleigh-Sommerfeld-Smythe formulas. We discuss these in Sec. 19.9.

19.2 Plane-Wave Spectrum Representation

The plane-wave spectrum representation builds up a single-frequency propagating wave $E(x, y, z)$ as a linear combination of plane waves $e^{-j(k_x x + k_y y + k_z z)}$.[†] The only assumption is that the field must satisfy the wave equation, which becomes the three-dimensional Helmholtz equation,

$$(\nabla^2 + k^2)E(x, y, z) = 0, \quad k = \frac{\omega}{c} = \omega \sqrt{\mu\epsilon} \quad (19.2.1)$$

where $c = 1/\sqrt{\mu\epsilon}$ is the speed of light in the propagation medium (assumed here to be homogeneous, isotropic, and lossless.) In solving the Helmholtz equation, one assumes initially a solution of the form:

$$E(x, y, z) = \hat{E}(k_x, k_y, z) e^{-jk_x x} e^{-jk_y y}$$

Inserting this into Eq. (19.2.1) and replacing, $\partial_x \rightarrow -jk_x$ and $\partial_y \rightarrow -jk_y$, we obtain:

$$\left(-k_x^2 - k_y^2 + \frac{\partial^2}{\partial z^2} + k^2\right) \hat{E}(k_x, k_y, z) = 0$$

or, defining $k_z^2 = k^2 - k_x^2 - k_y^2$, we have:

$$\frac{\partial^2 \hat{E}(k_x, k_y, z)}{\partial z^2} = -(k^2 - k_x^2 - k_y^2) \hat{E}(k_x, k_y, z) = -k_z^2 \hat{E}(k_x, k_y, z)$$

Its solution describing *forward-moving* waves ($z \geq 0$) is:

$$\hat{E}(k_x, k_y, z) = \hat{E}(k_x, k_y) e^{-jk_z z} \quad (19.2.2)$$

where $\hat{E}(k_x, k_y)$ is an arbitrary constant in the variable z .

If $k_x^2 + k_y^2 < k^2$, the wavenumber k_z is real-valued and the solution describes a *propagating* wave. If $k_x^2 + k_y^2 > k^2$, then k_z is imaginary and the solution describes an *evanescent* wave decaying with distance z . The two cases can be combined into one by defining k_z in terms of the *evanescent square-root* of Eq. (7.7.9) as follows:

$$k_z = \begin{cases} \sqrt{k^2 - k_x^2 - k_y^2}, & \text{if } k_x^2 + k_y^2 \leq k^2 \quad (\text{propagating}) \\ -j\sqrt{k_x^2 + k_y^2 - k^2}, & \text{if } k_x^2 + k_y^2 > k^2 \quad (\text{evanescent}) \end{cases} \quad (19.2.3)$$

and choose the square-root branch, $k_z = k$, when $k_x = k_y = 0$. In the evanescent case, we have the decaying solution:

$$\hat{E}(k_x, k_y, z) = \hat{E}(k_x, k_y) e^{-z\sqrt{k_x^2 + k_y^2 - k^2}}, \quad z \geq 0$$

Fig. 19.2.1 depicts the two regions on the $k_x k_y$ plane. The complete space dependence is $\hat{E}(k_x, k_y) e^{-jk_x x - jk_y y} e^{-jk_z z}$. The most general solution of Eq. (19.2.1) is obtained by

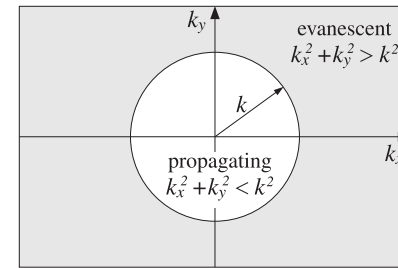


Fig. 19.2.1 Propagating and evanescent regions on the $k_x k_y$ plane.

adding up such plane-waves, that is, by the *spatial* two-dimensional inverse Fourier transform, for $z \geq 0$,

$$E(x, y, z) = \int_{-\infty}^{\infty} \int_{-\infty}^{\infty} \hat{E}(k_x, k_y) e^{-jk_x x - jk_y y} e^{-jk_z z} \frac{dk_x dk_y}{(2\pi)^2} \quad (19.2.4)$$

This is the *plane-wave spectrum representation*, also known as the *angular spectrum* representation, see [1415,1419], and some of the original papers [1601,1423-1425].

Because k_z is given by Eq. (19.2.3), this solution is composed, in general, of both propagating and evanescent modes. Of course, for large z , only the propagating modes survive. Setting $z = 0$, we recognize $\hat{E}(k_x, k_y)$ to be the spatial Fourier transform of the field, $E(x, y, 0)$, at $z = 0$ on the xy plane:

$$E(x, y, 0) = \int_{-\infty}^{\infty} \int_{-\infty}^{\infty} \hat{E}(k_x, k_y) e^{-jk_x x - jk_y y} \frac{dk_x dk_y}{(2\pi)^2} \quad (19.2.5)$$

$$\hat{E}(k_x, k_y) = \int_{-\infty}^{\infty} \int_{-\infty}^{\infty} E(x, y, 0) e^{jk_x x + jk_y y} dx dy$$

As in Chap. 3, we may give a system-theoretic interpretation to these results. Defining the “propagation” spatial filter, $\hat{h}(k_x, k_y, z) = e^{-jk_z z}$, then Eq. (19.2.2) reads:

$$\hat{E}(k_x, k_y, z) = e^{-jk_z z} \hat{E}(k_x, k_y) = \hat{h}(k_x, k_y, z) \hat{E}(k_x, k_y) \quad (19.2.6)$$

This multiplicative relationship in the wavenumber domain translates into a convolutional equation in the space domain. Let $h(x, y, z)$ denote the “impulse response” of this filter, that is, the spatial inverse Fourier transform of $\hat{h}(k_x, k_y, z) = e^{-jk_z z}$,

$$h(x, y, z) = \int_{-\infty}^{\infty} \int_{-\infty}^{\infty} e^{-jk_x x - jk_y y} e^{-jk_z z} \frac{dk_x dk_y}{(2\pi)^2} \quad (19.2.7)$$

then, we may write Eq. (19.2.4) in the convolutional form:

$$E(x, y, z) = \int_{-\infty}^{\infty} \int_{-\infty}^{\infty} h(x - x', y - y', z) E(x', y', 0) dx' dy' \quad (19.2.8)$$

[†]As always, we use $e^{j\omega t}$ harmonic time dependence.

Eq. (19.2.8) is equivalent to the Rayleigh-Sommerfeld formula (19.1.6). Indeed, it follows from Eq. (D.19) of Appendix D that

$$h(x-x', y-y', z) = -2 \frac{\partial G(R)}{\partial z} = 2 \frac{\partial G(R)}{\partial z'}, \quad G(R) = \frac{e^{-jkR}}{4\pi R}, \quad R = |\mathbf{r} - \mathbf{r}'| \quad (19.2.9)$$

with the understanding that $z' = 0$, so that $R = \sqrt{(x-x')^2 + (y-y')^2 + z^2}$. Thus, Eq. (19.2.8) takes the form of Eq. (19.1.6) or (19.1.8). The geometry was shown in Fig. 19.1.2. We note also that at $z = 0$, we have $h(x-x', y-y', 0) = \delta(x-x')\delta(y-y')$. This follows by setting $z = 0$ into (19.2.7), or from Eq. (D.21) of Appendix D. Thus, Eq. (19.2.8) is consistent at $z = 0$.

To summarize, the Rayleigh-Sommerfeld and plane-wave spectrum representations express a scalar field $E(x, y, z)$ in terms of its boundary values $E(x, y, 0)$ on the xy plane, or in terms of the 2-D Fourier transform $\hat{E}(k_x, k_y)$ of these boundary values,

$$\begin{aligned} E(x, y, z) &= -2 \frac{\partial}{\partial z} \iint_{-\infty}^{\infty} \frac{e^{-jkR}}{4\pi R} E(x', y', 0) dx' dy' \\ &= 2 \iint_{-\infty}^{\infty} \frac{z}{R} \left(jk + \frac{1}{R} \right) \frac{e^{-jkR}}{4\pi R} E(x', y', 0) dx' dy' \\ &= \iint_{-\infty}^{\infty} \hat{E}(k_x, k_y) e^{-jk_x x - jk_y y} e^{-jk_z z} \frac{dk_x dk_y}{(2\pi)^2} \end{aligned} \quad (19.2.10)$$

with $z \geq 0$ and $R = \sqrt{(x-x')^2 + (y-y')^2 + z^2}$. For arbitrary $z \geq 0$, we have,

$$\begin{aligned} E(x, y, z) &= \mp 2 \frac{\partial}{\partial z} \iint_{-\infty}^{\infty} \frac{e^{-jkR}}{4\pi R} E(x', y', 0) dx' dy' \\ &= 2 \iint_{-\infty}^{\infty} \frac{|z|}{R} \left(jk + \frac{1}{R} \right) \frac{e^{-jkR}}{4\pi R} E(x', y', 0) dx' dy' \\ &= \iint_{-\infty}^{\infty} \hat{E}(k_x, k_y) e^{-jk_x x - jk_y y} e^{-jk_z |z|} \frac{dk_x dk_y}{(2\pi)^2} \end{aligned} \quad (19.2.11)$$

Next, we show that the plane-wave representation (19.2.4) is equivalent to both the type-1 and the type-2 Rayleigh-Sommerfeld formulas, Eqs. (19.1.6) and (19.1.11). We note that Eq. (19.2.6) can be written as follows,

$$\hat{E}(k_x, k_y, z) = e^{-jk_z z} \cdot \hat{E}(k_x, k_y) = 2jk_z \cdot \left[\frac{e^{-jk_z z}}{2jk_z} \right] \cdot \hat{E}(k_x, k_y)$$

or,

$$\hat{E}(k_x, k_y, z) = 2jk_z \cdot \hat{G}(k_x, k_y, z) \cdot \hat{E}(k_x, k_y) \quad (19.2.12)$$

where $\hat{G}(k_x, k_y, z) = e^{-jk_z z} / (2jk_z)$ is the 2-D Fourier transform of the Green's function $G(r) = e^{-jkr} / (4\pi r)$, for $z \geq 0$. This follows from Eq. (D.11) of Appendix D. The factor $2jk_z$ can be associated either with $\hat{G}(k_x, k_y, z)$, leading to Eq. (19.1.6), or with $\hat{E}(k_x, k_y)$ leading to Eq. (19.1.11),

$$\hat{E}(k_x, k_y, z) = \underbrace{2jk_z \cdot \hat{G}(k_x, k_y, z)}_{\text{type-1}} \cdot \hat{E}(k_x, k_y) = \underbrace{2jk_z \cdot \hat{E}(k_x, k_y)}_{\text{type-2}} \cdot \hat{G}(k_x, k_y, z) \quad (19.2.13)$$

We recognize that $2jk_z \cdot \hat{E}(k_x, k_y)$ is the 2-D Fourier transform of the z -derivative of $E(x, y, z)$ at $z = 0$, indeed, by differentiating (19.2.4), we have,

$$-2 \frac{\partial E(x, y, z)}{\partial z} = \iint_{-\infty}^{\infty} 2jk_z \cdot \hat{E}(k_x, k_y) e^{-jk_x x - jk_y y} e^{-jk_z z} \frac{dk_x dk_y}{(2\pi)^2} \quad (19.2.14)$$

and at $z = 0$,

$$-2 \frac{\partial E(x, y, 0)}{\partial z} = \iint_{-\infty}^{\infty} 2jk_z \cdot \hat{E}(k_x, k_y) e^{-jk_x x - jk_y y} \frac{dk_x dk_y}{(2\pi)^2} \quad (19.2.15)$$

Thus, the inverse Fourier transform of the product of the transforms $\hat{G}(k_x, k_y, z)$ and $2jk_z \hat{E}(k_x, k_y)$ in (19.2.13) becomes the convolutional form of Eq. (19.1.11).

19.3 Far-Field Diffraction Pattern

The far-field, or Fraunhofer, diffraction pattern is obtained in the limit of a large radial distance r of the field observation point from the aperture. It can be derived using either the Rayleigh-Sommerfeld integrals or by applying the stationary-phase approximation to the plane-wave spectrum. We briefly discuss both approaches.

In Eq. (19.2.10), the quantity $R = |\mathbf{r} - \mathbf{r}'|$ is the distance between the field point at position \mathbf{r} and the aperture point \mathbf{r}' . If we assume that the aperture is finite, as in Fig. 19.1.2, and we choose $r \gg r'$, we may approximate R as follows,

$$R = |\mathbf{r} - \mathbf{r}'| = \sqrt{r^2 - 2\mathbf{r} \cdot \mathbf{r}' + r'^2} \approx r - \hat{\mathbf{r}} \cdot \mathbf{r}'$$

where $\hat{\mathbf{r}}$ is the unit vector in the direction of the observation point \mathbf{r} . We have used this approximation before in Sec. 15.7, see for example Fig. 15.7.1. The far-field approximation then consists of making the following replacements in Eq. (19.2.10), and assuming that $r \gg \lambda$, or, $k \gg 1/r$,

$$\frac{z}{R} \left(jk + \frac{1}{R} \right) \frac{e^{-jkR}}{4\pi R} \approx \frac{z}{r} \left(jk + \frac{1}{r} \right) \frac{e^{-jk(r - \hat{\mathbf{r}} \cdot \mathbf{r}')}}{4\pi r} \approx jk \frac{z}{r} \frac{e^{-jkr}}{4\pi r} e^{jk\hat{\mathbf{r}} \cdot \mathbf{r}'} \quad (19.3.1)$$

where we replaced $R \approx r$ in the denominators, but kept the approximation $R \approx r - \hat{\mathbf{r}} \cdot \mathbf{r}'$ in the phase exponential. The unit vector $\hat{\mathbf{r}}$ is uniquely defined by the corresponding polar and azimuthal angles θ, ϕ in the direction of \mathbf{r} . Thus, $z/r = \cos \theta$, and defining the wavevector $\mathbf{k} = k\hat{\mathbf{r}}$, we have,

$$\mathbf{k} = k\hat{\mathbf{r}} = k(\hat{\mathbf{x}} \sin \theta \cos \phi + \hat{\mathbf{y}} \sin \theta \sin \phi + \hat{\mathbf{z}} \cos \theta) \Rightarrow \begin{aligned} k_x &= k \sin \theta \cos \phi \\ k_y &= k \sin \theta \sin \phi \\ k_z &= k \cos \theta \end{aligned} \quad (19.3.2)$$

Since \mathbf{r}' is restricted to the xy plane, we have, $e^{jk\hat{\mathbf{r}} \cdot \mathbf{r}'} = e^{k_x x' + k_y y'}$. It follows that Eq. (19.2.10) can be approximated in this limit by,

$$E(x, y, z) \approx 2jk \cos \theta \frac{e^{-jkr}}{4\pi r} \iint_{-\infty}^{\infty} E(x', y', 0) e^{k_x x' + k_y y'} dx' dy'$$

but the last factor is the 2-D Fourier transform of $E(x', y', 0)$ evaluated at the directional wave vector, $\mathbf{k} = k \hat{\mathbf{r}}$,

$$E(x, y, z) \approx 2jk \cos \theta \frac{e^{-jkr}}{4\pi r} \hat{E}(k_x, k_y) \Big|_{\mathbf{k} = k\hat{\mathbf{r}}} \quad (\text{far-field diffraction pattern}) \quad (19.3.3)$$

The factor $\hat{E}(k_x, k_y)$ evaluated at $\mathbf{k} = k \hat{\mathbf{r}}$ is a function of the angles θ, ϕ , and represents the essential angular pattern of the diffracted wave. The factor $\cos \theta$ may be viewed as an obliquity factor.

The same result can be obtained by using the stationary-phase approximation for 2-D integrals discussed in Appendix H. Let us rewrite Eq. (19.2.4) in the form,

$$E(x, y, z) = \iint_{-\infty}^{\infty} \hat{E}(k_x, k_y) e^{j\varphi(k_x, k_y)} \frac{dk_x dk_y}{(2\pi)^2}, \quad (19.3.4)$$

where we defined the phase function,

$$\varphi(k_x, k_y) = -\mathbf{k} \cdot \mathbf{r} = -(k_x x + k_y y + k_z z) \quad (19.3.5)$$

The stationary-phase approximation to the integral in (19.3.4) is given by Eq. (H.6),

$$\iint_{-\infty}^{\infty} \hat{E}(k_x, k_y) e^{j\varphi(k_x, k_y)} \frac{dk_x dk_y}{(2\pi)^2} \approx e^{j(\sigma+1)\tau\frac{\pi}{4}} \frac{2\pi}{\sqrt{|\det \Phi|}} \frac{\hat{E}(k_x^0, k_y^0) e^{j\varphi(k_x^0, k_y^0)}}{(2\pi)^2} \quad (19.3.6)$$

where k_x^0, k_y^0 are the stationary points of the phase function $\varphi(k_x, k_y)$, that is, the solutions of the equations,

$$\frac{\partial \varphi}{\partial k_x} = 0, \quad \frac{\partial \varphi}{\partial k_y} = 0 \quad (19.3.7)$$

and where Φ is the matrix of second derivatives of φ evaluated at the stationary points k_x^0, k_y^0 , and σ, τ are the algebraic signs of the determinant and trace of Φ , that is,

$$\Phi = \begin{bmatrix} \frac{\partial^2 \varphi(k_x^0, k_y^0)}{\partial k_x^2} & \frac{\partial^2 \varphi(k_x^0, k_y^0)}{\partial k_x \partial k_y} \\ \frac{\partial^2 \varphi(k_x^0, k_y^0)}{\partial k_x \partial k_y} & \frac{\partial^2 \varphi(k_x^0, k_y^0)}{\partial k_y^2} \end{bmatrix}, \quad \sigma = \text{sign}(\det \Phi), \quad \tau = \text{sign}(\text{tr } \Phi) \quad (19.3.8)$$

Since $k_z^2 = k^2 - k_x^2 - k_y^2$, the conditions (19.3.7) become,

$$\begin{aligned} \frac{\partial \varphi}{\partial k_x} = -x - z \frac{\partial k_z}{\partial k_x} = -x + z \frac{k_x}{k_z} = 0 &\Rightarrow \frac{k_x^0}{k_z^0} = \frac{x}{z} \\ \frac{\partial \varphi}{\partial k_y} = -y - z \frac{\partial k_z}{\partial k_y} = -y + z \frac{k_y}{k_z} = 0 &\Rightarrow \frac{k_y^0}{k_z^0} = \frac{y}{z} \end{aligned} \quad (19.3.9)$$

Putting these back into $k_z^2 = k^2 - k_x^2 - k_y^2$, gives the following solution,

$$k_x^0 = k \frac{x}{r}, \quad k_y^0 = k \frac{y}{r}, \quad k_z^0 = k \frac{z}{r}, \quad r = \sqrt{x^2 + y^2 + z^2} \quad (19.3.10)$$

or, $\mathbf{k}^0 = k\mathbf{r}/r = k\hat{\mathbf{r}}$, which is the same as (19.3.2). Therefore, the phase function evaluated at \mathbf{k}^0 is, $\varphi(k_x^0, k_y^0) = -\mathbf{k}^0 \cdot \mathbf{r} = -k\hat{\mathbf{r}} \cdot \mathbf{r} = -kr$.

The second derivatives are obtained by differentiating (19.3.9) one more time and evaluating the result at \mathbf{k}^0 , for example,

$$\frac{\partial^2 \varphi}{\partial k_x^2} = z \frac{\partial}{\partial k_x} \left(\frac{k_x}{k_z} \right) = \frac{z}{k_z} \left(1 + \frac{k_x^2}{k_z^2} \right) \Big|_{\mathbf{k} = \mathbf{k}^0} = \frac{r}{k} \left(1 + \frac{x^2}{z^2} \right)$$

and similarly,

$$\frac{\partial^2 \varphi}{\partial k_x \partial k_y} = \frac{r}{k} \frac{xy}{z^2}, \quad \frac{\partial^2 \varphi}{\partial k_y^2} = \frac{r}{k} \left(1 + \frac{y^2}{z^2} \right)$$

It follows that, $\det \Phi, \sigma, \tau$ are,

$$\det \Phi = \frac{r^4}{k^2 z^2}, \quad \sigma = \tau = 1$$

and since $z > 0$, the approximation (19.3.6) yields the same answer as (19.3.3),

$$E(x, y, z) \approx e^{j(\sigma+1)\tau\frac{\pi}{4}} \frac{2\pi}{\sqrt{|\det \Phi|}} \frac{\hat{E}(k_x^0, k_y^0) e^{j\varphi(k_x^0, k_y^0)}}{(2\pi)^2} = e^{j(1+1)\frac{\pi}{4}} \frac{2\pi}{\sqrt{\frac{r^4}{k^2 z^2}}} \frac{\hat{E}(k_x^0, k_y^0) e^{-jkr}}{(2\pi)^2}$$

or,

$$E(x, y, z) = jk \frac{z}{r} \frac{e^{-jkr}}{2\pi r} \hat{E}(k_x^0, k_y^0) = 2jk \cos \theta \frac{e^{-jkr}}{4\pi r} \hat{E}(k_x^0, k_y^0)$$

19.4 One-Dimensional Apertures

The plane-wave spectrum representations and the Rayleigh-Sommerfeld diffraction formulas apply also to the special case of one-dimensional line sources and apertures, such as infinitely long narrow slits or strips, as shown for example in Fig. 19.4.1.

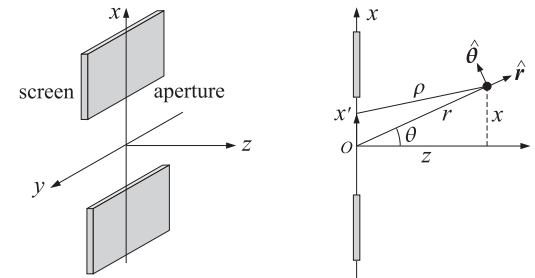


Fig. 19.4.1 Slit aperture with infinite length in the y-direction.

Specifically, we will assume that the one-dimensional aperture is along the x-direction and the fields, $E(x, z)$, depend only on the x, z coordinates and have no dependence on the y-coordinate. We recall from Eqs. (D.22) and (D.32) of Appendix D that the 2-D

outgoing Green's function can be derived by integrating out the y -variable of the 3-D Green's function, that is,

$$G_2(x - x', z) = -\frac{j}{4} H_0^{(2)}(k\rho) = \int_{-\infty}^{\infty} \frac{e^{-jkR}}{4\pi R} dy' \quad (19.4.1)$$

where, $\rho = \sqrt{(x - x')^2 + z^2}$ and $R = \sqrt{(x - x')^2 + (y - y')^2 + z^2}$.

Since $E(x', y', 0)$ does not depend on y' , we may integrate out the y' variable in Eq. (19.1.10) and use Eq. (19.4.1) to obtain the one-dimensional-aperture version of the Rayleigh-Sommerfeld diffraction integral, for $z > 0$,

$$E(x, z) = -2 \frac{\partial}{\partial z} \int_{-\infty}^{\infty} E(x', 0) G_2(x - x', z) dx' \quad (1\text{-D apertures}) \quad (19.4.2)$$

The corresponding 1-D plane-wave spectrum representation can be derived with the help of the Weyl representation of the G_2 Green's function derived in Eq. (D.30) of Appendix D, that is,

$$G_2(x, z) = -\frac{j}{4} H_0^{(2)}(k\sqrt{x^2 + z^2}) = \int_{-\infty}^{\infty} \frac{e^{-jk_x x} e^{-jk_z |z|}}{2jk_z} \frac{dk_x}{2\pi} \quad (19.4.3)$$

which implies that, for $z \geq 0$,

$$-2 \frac{\partial G_2(x, z)}{\partial z} = \int_{-\infty}^{\infty} e^{-jk_x x} e^{-jk_z z} \frac{dk_x}{2\pi} \quad (19.4.4)$$

with k_z defined as in Eq. (D.27) in terms of the evanescent square root,

$$k_z = \begin{cases} \sqrt{k^2 - k_x^2}, & \text{if } |k_x| < k \\ -j\sqrt{k_x^2 - k^2}, & \text{if } |k_x| > k \end{cases} \quad \begin{array}{c} \text{propagating} \\ \text{evanescent} \end{array} \quad (19.4.5)$$

It follows that the convolutional equation (19.4.2) can also be written as the inverse 1-D Fourier transform,

$$E(x, z) = \int_{-\infty}^{\infty} \hat{E}(k_x) e^{-jk_x x} e^{-jk_z z} \frac{dk_x}{2\pi} \quad (19.4.6)$$

where $\hat{E}(k_x)$ is the 1-D Fourier transform of $E(x, 0)$ at $z = 0$,

$$\begin{aligned} \hat{E}(k_x) &= \int_{-\infty}^{\infty} E(x, 0) e^{-jk_x x} dx \\ E(x, 0) &= \int_{-\infty}^{\infty} \hat{E}(k_x) e^{-jk_x x} \frac{dk_x}{2\pi} \end{aligned} \quad (19.4.7)$$

Replacing G_2 in terms of the Hankel function and noting the differentiation property, $dH_0^{(2)}(z)/dz = -H_1^{(2)}(z)$, we may summarize the above results as follows,

$$\begin{aligned} E(x, z) &= \frac{j}{2} \frac{\partial}{\partial z} \int_{-\infty}^{\infty} H_0^{(2)}(k\rho) E(x', 0) dx' \\ &= -\frac{j}{2} \int_{-\infty}^{\infty} \frac{kz}{\rho} H_1^{(2)}(k\rho) E(x', 0) dx' \\ &= \int_{-\infty}^{\infty} \hat{E}(k_x) e^{-jk_x x} e^{-jk_z z} \frac{dk_x}{2\pi} \end{aligned} \quad \begin{array}{l} z \geq 0 \\ \rho = \sqrt{(x - x')^2 + z^2} \end{array} \quad (19.4.8)$$

The far-field approximation easily follows from (19.4.8), for large $r = \sqrt{x^2 + z^2}$,

$$E(x, z) \approx e^{j\frac{\pi}{4}} \cos \theta \sqrt{\frac{k}{2\pi r}} e^{-jkr} \hat{E}(k_x^0) \quad (\text{far-field approximation}) \quad (19.4.9)$$

where $k_x^0 = kx/r = k \sin \theta$, $k_z^0 = kz/r = k \cos \theta$, $\cos \theta = z/r$. Eq. (19.4.9) can be derived either by applying the stationary-phase method to the one-dimensional Fourier integral (19.4.6), that is, Eq. (H.4) of Appendix H, or, by using the following asymptotic expression for the Hankel function $H_1^{(2)}$ in (19.4.8),

$$H_1^{(2)}(k\rho) \approx \sqrt{\frac{2}{\pi k\rho}} e^{-j(k\rho - \frac{3\pi}{4})}, \quad \text{for large } \rho$$

and replacing the ρ in the exponential $e^{-jk\rho}$ by the approximation,

$$\rho = \sqrt{(x - x')^2 + z^2} = \sqrt{r^2 - 2xx' + x'^2} \approx r - \frac{x}{r} x'$$

and also replacing ρ by r in the other factors of (19.4.8).

In both the 3-D and 2-D cases, the radial dependence of the far field describes an outgoing spherical or cylindrical wave, while the angular pattern is given by the product of the obliquity factor $\cos \theta$ and the spatial Fourier transform of the aperture distribution evaluated at the wavenumber $\mathbf{k} = k\hat{\mathbf{i}}$.

19.5 Plane-Wave Spectrum-Vector Case

Next, we discuss the vector case for electromagnetic fields. To simplify the notation, we define the two-dimensional transverse vectors $\mathbf{r}_\perp = \hat{\mathbf{x}}x + \hat{\mathbf{y}}y$ and $\mathbf{k}_\perp = \hat{\mathbf{x}}k_x + \hat{\mathbf{y}}k_y$, as well as the transverse gradient $\nabla_\perp = \hat{\mathbf{x}}\partial_x + \hat{\mathbf{y}}\partial_y$, so that the full three-dimensional gradient is,

$$\nabla = \hat{\mathbf{x}}\partial_x + \hat{\mathbf{y}}\partial_y + \hat{\mathbf{z}}\partial_z = \nabla_\perp + \hat{\mathbf{z}}\partial_z$$

In this notation, Eq. (19.2.6) reads, $\hat{E}(\mathbf{k}_\perp, z) = \hat{h}(\mathbf{k}_\perp, z) \hat{E}(\mathbf{k}_\perp)$, with $\hat{h}(\mathbf{k}_\perp, z) = e^{-jk_z z}$. The plane-wave spectrum representations (19.2.4) and (19.2.8) now are,[†]

$$\begin{aligned} E(\mathbf{r}_\perp, z) &= \int_{-\infty}^{\infty} \hat{E}(\mathbf{k}_\perp) e^{-jk_z z} e^{-j\mathbf{k}_\perp \cdot \mathbf{r}_\perp} \frac{d^2 \mathbf{k}_\perp}{(2\pi)^2} \\ &= \int_{-\infty}^{\infty} E(\mathbf{r}'_\perp, 0) h(\mathbf{r}_\perp - \mathbf{r}'_\perp, z) d^2 \mathbf{r}'_\perp \end{aligned} \quad \begin{array}{c} E(\mathbf{r}_\perp, 0) \\ \xrightarrow{\quad} \\ \boxed{h(\mathbf{r}_\perp, z)} \\ \xrightarrow{\quad} \\ E(\mathbf{r}_\perp, z) \end{array} \quad (19.5.1)$$

for $z \geq 0$, where

$$\hat{E}(\mathbf{k}_\perp) = \int_{-\infty}^{\infty} e^{j\mathbf{k}_\perp \cdot \mathbf{r}_\perp} E(\mathbf{r}_\perp, 0) d^2 \mathbf{r}_\perp \quad (19.5.2)$$

and

[†]where the integral sign represents double integration; note also that in the literature one often sees the notation $\mathbf{k}_\parallel, \mathbf{r}_\parallel$, with the subscript \parallel meaning "parallel" to the interface, whereas our notation $\mathbf{k}_\perp, \mathbf{r}_\perp$ means "perpendicular" to z .

$$h(\mathbf{r}_\perp, z) = \int_{-\infty}^{\infty} e^{-jk_z z} e^{-j\mathbf{k}_\perp \cdot \mathbf{r}_\perp} \frac{d^2 \mathbf{k}_\perp}{(2\pi)^2} = -2 \frac{\partial}{\partial z} \left(\frac{e^{-jkr}}{4\pi r} \right), \quad r = \sqrt{\mathbf{r}_\perp \cdot \mathbf{r}_\perp + z^2} \quad (19.5.3)$$

In the vectorial case, $E(\mathbf{r}_\perp, z)$ is replaced by a three-dimensional field, which can be decomposed into its transverse x, y components and its longitudinal part along z :

$$\mathbf{E} = \underbrace{\hat{\mathbf{x}}E_x + \hat{\mathbf{y}}E_y}_{\text{transverse part}} + \hat{\mathbf{z}}E_z \equiv \mathbf{E}_\perp + \hat{\mathbf{z}}E_z$$

The plane-wave spectrum representations apply separately to each component of \mathbf{E} and \mathbf{H} , and can be written vectorially as follows, for $z \geq 0$,

$$\begin{aligned} \mathbf{E}(\mathbf{r}_\perp, z) &= \int_{-\infty}^{\infty} \hat{\mathbf{E}}(\mathbf{k}_\perp) e^{-jk_z z} e^{-j\mathbf{k}_\perp \cdot \mathbf{r}_\perp} \frac{d^2 \mathbf{k}_\perp}{(2\pi)^2} \\ \mathbf{H}(\mathbf{r}_\perp, z) &= \int_{-\infty}^{\infty} \hat{\mathbf{H}}(\mathbf{k}_\perp) e^{-jk_z z} e^{-j\mathbf{k}_\perp \cdot \mathbf{r}_\perp} \frac{d^2 \mathbf{k}_\perp}{(2\pi)^2} \end{aligned} \quad (19.5.4)$$

where $\hat{\mathbf{E}}(\mathbf{k}_\perp), \hat{\mathbf{H}}(\mathbf{k}_\perp)$ are the 2-D Fourier transforms,

$$\begin{aligned} \hat{\mathbf{E}}(\mathbf{k}_\perp) &= \int_{-\infty}^{\infty} e^{j\mathbf{k}_\perp \cdot \mathbf{r}_\perp} \mathbf{E}(\mathbf{r}_\perp, 0) d^2 \mathbf{r}_\perp \\ \hat{\mathbf{H}}(\mathbf{k}_\perp) &= \int_{-\infty}^{\infty} e^{j\mathbf{k}_\perp \cdot \mathbf{r}_\perp} \mathbf{H}(\mathbf{r}_\perp, 0) d^2 \mathbf{r}_\perp \end{aligned} \quad (19.5.5)$$

Because \mathbf{E} must satisfy the source-free Gauss's law, $\nabla \cdot \mathbf{E} = 0$, this imposes certain constraints among the Fourier components, $\hat{\mathbf{E}}(\mathbf{k}_\perp)$, that must be taken into account in writing (19.5.4). Indeed, we have from (19.5.4)

$$\nabla \cdot \mathbf{E} = -j \int_{-\infty}^{\infty} \mathbf{k} \cdot \hat{\mathbf{E}}(\mathbf{k}_\perp) e^{-jk_z z} e^{-j\mathbf{k}_\perp \cdot \mathbf{r}_\perp} \frac{d^2 \mathbf{k}_\perp}{(2\pi)^2} = 0$$

which requires that $\mathbf{k} \cdot \hat{\mathbf{E}}(\mathbf{k}_\perp) = 0$. Separating this into its transverse and longitudinal parts, we have:

$$\mathbf{k} \cdot \hat{\mathbf{E}} = \mathbf{k}_\perp \cdot \hat{\mathbf{E}}_\perp + k_z \hat{E}_z = 0, \quad \text{or,}$$

$$\hat{E}_z(\mathbf{k}_\perp) = -\frac{\mathbf{k}_\perp \cdot \hat{\mathbf{E}}_\perp(\mathbf{k}_\perp)}{k_z} = -\frac{k_x \hat{E}_x(\mathbf{k}_\perp) + k_y \hat{E}_y(\mathbf{k}_\perp)}{k_z} \quad (19.5.6)$$

It follows that the Fourier vector $\hat{\mathbf{E}}(\mathbf{k}_\perp)$ must have the form:

$$\hat{\mathbf{E}}(\mathbf{k}_\perp) = \hat{\mathbf{E}}_\perp(\mathbf{k}_\perp) + \hat{\mathbf{z}} \hat{E}_z(\mathbf{k}_\perp) = \hat{\mathbf{E}}_\perp(\mathbf{k}_\perp) - \hat{\mathbf{z}} \frac{\mathbf{k}_\perp \cdot \hat{\mathbf{E}}_\perp(\mathbf{k}_\perp)}{k_z} \quad (19.5.7)$$

and it is expressible only in terms of its transverse components $\hat{\mathbf{E}}_\perp(\mathbf{k}_\perp)$. Thus, the correct plane-wave spectrum representation for the \mathbf{E} -field as well as that for the \mathbf{H} -

field become in the vector case, for $z \geq 0$,

$$\begin{aligned} \mathbf{E}(\mathbf{r}_\perp, z) &= \int_{-\infty}^{\infty} \left[\hat{\mathbf{E}}_\perp(\mathbf{k}_\perp) - \hat{\mathbf{z}} \frac{\mathbf{k}_\perp \cdot \hat{\mathbf{E}}_\perp(\mathbf{k}_\perp)}{k_z} \right] e^{-jk_z z} e^{-j\mathbf{k}_\perp \cdot \mathbf{r}_\perp} \frac{d^2 \mathbf{k}_\perp}{(2\pi)^2} \\ \mathbf{H}(\mathbf{r}_\perp, z) &= \frac{1}{\eta k} \int_{-\infty}^{\infty} \mathbf{k} \times \left[\hat{\mathbf{E}}_\perp(\mathbf{k}_\perp) - \hat{\mathbf{z}} \frac{\mathbf{k}_\perp \cdot \hat{\mathbf{E}}_\perp(\mathbf{k}_\perp)}{k_z} \right] e^{-jk_z z} e^{-j\mathbf{k}_\perp \cdot \mathbf{r}_\perp} \frac{d^2 \mathbf{k}_\perp}{(2\pi)^2} \end{aligned} \quad (19.5.8)$$

where, $\mathbf{k} = \mathbf{k}_\perp + \hat{\mathbf{z}}k_z = \hat{\mathbf{x}}k_x + \hat{\mathbf{y}}k_y + \hat{\mathbf{z}}k_z$. The magnetic field was obtained from Faraday's law, $\nabla \times \mathbf{E} = -j\omega\mu\mathbf{H}$. Replacing, $\omega\mu = k\eta$, since $k = \omega\sqrt{\mu\epsilon}$ and $\eta = \sqrt{\mu/\epsilon}$, we have, $\mathbf{H} = \nabla \times \mathbf{E} / (-jk\eta)$, which leads to the above expression for \mathbf{H} by bringing the gradient ∇ inside the Fourier integral for \mathbf{E} , and replacing it by $\nabla \rightarrow -j\mathbf{k}$.

The plane-wave Fourier components for \mathbf{E} and \mathbf{H} form a right-handed vector triplet together with the vector \mathbf{k} ,

$$\begin{aligned} \hat{\mathbf{E}}(\mathbf{k}_\perp) &= \hat{\mathbf{E}}_\perp(\mathbf{k}_\perp) - \hat{\mathbf{z}} \frac{\mathbf{k}_\perp \cdot \hat{\mathbf{E}}_\perp(\mathbf{k}_\perp)}{k_z} \\ \hat{\mathbf{H}}(\mathbf{k}_\perp) &= \frac{1}{\eta k} \mathbf{k} \times \left[\hat{\mathbf{E}}_\perp(\mathbf{k}_\perp) - \hat{\mathbf{z}} \frac{\mathbf{k}_\perp \cdot \hat{\mathbf{E}}_\perp(\mathbf{k}_\perp)}{k_z} \right] = \frac{1}{\eta k} \mathbf{k} \times \hat{\mathbf{E}}(\mathbf{k}_\perp) \end{aligned} \quad (19.5.9)$$

Albeit complex-valued because of Eq. (19.2.3), the normalized vector $\hat{\mathbf{k}} = \mathbf{k}/k$ can be thought of as a unit vector, indeed, satisfying, $\mathbf{k} \cdot \mathbf{k} = k_x^2 + k_y^2 + k_z^2 = k^2$, or, $\hat{\mathbf{k}} \cdot \hat{\mathbf{k}} = 1$.

It follows from (19.5.9), that $\mathbf{k} \cdot \hat{\mathbf{H}}(\mathbf{k}_\perp) = 0$ and $\mathbf{k} \times \hat{\mathbf{H}}(\mathbf{k}_\perp) = -k \hat{\mathbf{E}}(\mathbf{k}_\perp) / \eta = -\omega\epsilon \hat{\mathbf{E}}(\mathbf{k}_\perp)$, which imply that Eqs. (19.5.8) satisfy the remaining Maxwell equations, that is, $\nabla \cdot \mathbf{H} = 0$ and $\nabla \times \mathbf{H} = j\omega\epsilon \mathbf{E}$, in the right half-space $z \geq 0$.

We could equally well have started with the tangential components of the magnetic field on the aperture, $\mathbf{H}_\perp(\mathbf{r}'_\perp, 0)$, and the corresponding Fourier transform, $\hat{\mathbf{H}}_\perp(\mathbf{k}_\perp)$, and have used the constraint $\nabla \cdot \mathbf{H} = 0$, or, $\mathbf{k}_\perp \cdot \hat{\mathbf{H}}_\perp(\mathbf{k}_\perp) + k_z \hat{H}_z(\mathbf{k}_\perp) = 0$, to obtain the following alternative plane-wave spectrum representation, with the electric field derived from, $j\omega\epsilon \mathbf{E} = \nabla \times \mathbf{H}$, or, $\mathbf{E} = (\eta/jk) \nabla \times \mathbf{H}$, for $z \geq 0$,

$$\begin{aligned} \mathbf{H}(\mathbf{r}_\perp, z) &= \int_{-\infty}^{\infty} \left[\hat{\mathbf{H}}_\perp(\mathbf{k}_\perp) - \hat{\mathbf{z}} \frac{\mathbf{k}_\perp \cdot \hat{\mathbf{H}}_\perp(\mathbf{k}_\perp)}{k_z} \right] e^{-jk_z z} e^{-j\mathbf{k}_\perp \cdot \mathbf{r}_\perp} \frac{d^2 \mathbf{k}_\perp}{(2\pi)^2} \\ \mathbf{E}(\mathbf{r}_\perp, z) &= -\frac{\eta}{k} \int_{-\infty}^{\infty} \mathbf{k} \times \left[\hat{\mathbf{H}}_\perp(\mathbf{k}_\perp) - \hat{\mathbf{z}} \frac{\mathbf{k}_\perp \cdot \hat{\mathbf{H}}_\perp(\mathbf{k}_\perp)}{k_z} \right] e^{-jk_z z} e^{-j\mathbf{k}_\perp \cdot \mathbf{r}_\perp} \frac{d^2 \mathbf{k}_\perp}{(2\pi)^2} \end{aligned} \quad (19.5.10)$$

The plane-wave Fourier components still form a right-handed triplet with \mathbf{k} ,

$$\begin{aligned} \hat{\mathbf{H}}(\mathbf{k}_\perp) &= \hat{\mathbf{H}}_\perp(\mathbf{k}_\perp) - \hat{\mathbf{z}} \frac{\mathbf{k}_\perp \cdot \hat{\mathbf{H}}_\perp(\mathbf{k}_\perp)}{k_z} \\ \hat{\mathbf{E}}(\mathbf{k}_\perp) &= -\frac{\eta}{k} \mathbf{k} \times \left[\hat{\mathbf{H}}_\perp(\mathbf{k}_\perp) - \hat{\mathbf{z}} \frac{\mathbf{k}_\perp \cdot \hat{\mathbf{H}}_\perp(\mathbf{k}_\perp)}{k_z} \right] = -\frac{\eta}{k} \mathbf{k} \times \hat{\mathbf{H}}(\mathbf{k}_\perp) \end{aligned} \quad (19.5.11)$$

Eqs. (19.5.11) are entirely equivalent to (19.5.9), hence (19.5.10) are equivalent to (19.5.8). Eqs. (19.5.10) could also be obtained quickly from (19.5.8) by a duality transformation, that is, $\mathbf{E} \rightarrow \mathbf{H}, \mathbf{H} \rightarrow -\mathbf{E}, \eta \rightarrow \eta^{-1}$.

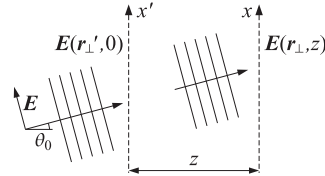
Example 19.5.1: Oblique Plane Wave. Here, we show that the plane-wave spectrum method correctly generates an ordinary plane wave from its transverse values at an input plane. Consider a TM electromagnetic wave propagating at an angle θ_0 with respect to the z axis, as shown in the figure below. The electric field at an arbitrary point, and its transverse part evaluated on the plane $z' = 0$, are given by

$$E(\mathbf{r}_\perp, z) = E_0 (\hat{\mathbf{x}} \cos \theta_0 - \hat{\mathbf{z}} \sin \theta_0) e^{-j(k_x^0 x + k_z^0 z)}$$

$$E_\perp(\mathbf{r}'_\perp, 0) = \hat{\mathbf{x}} E_0 \cos \theta_0 e^{-jk_x^0 x'} = \hat{\mathbf{x}} E_0 \cos \theta_0 e^{-jk_x^0 \cdot \mathbf{r}'_\perp}$$

$$k_x^0 = k \sin \theta_0, \quad k_y^0 = 0, \quad k_z^0 = k \cos \theta_0$$

$$\mathbf{k}_\perp^0 = \hat{\mathbf{x}} k_x^0 + \hat{\mathbf{y}} k_y^0 = \hat{\mathbf{x}} k \sin \theta_0$$



It follows that the spatial Fourier transform of $E_\perp(\mathbf{r}'_\perp, 0)$ will be

$$\hat{E}_\perp(\mathbf{k}_\perp, 0) = \int_{-\infty}^{\infty} \hat{\mathbf{x}} E_0 \cos \theta_0 e^{-jk_x^0 \cdot \mathbf{r}'_\perp} e^{j\mathbf{k}_\perp \cdot \mathbf{r}'_\perp} d^2 \mathbf{r}'_\perp = \hat{\mathbf{x}} E_0 \cos \theta_0 (2\pi)^2 \delta(\mathbf{k}_\perp - \mathbf{k}_\perp^0)$$

Then, the integrand of Eq. (19.5.8) becomes

$$\hat{E}_\perp - \hat{\mathbf{z}} \frac{\mathbf{k}_\perp \cdot \hat{E}_\perp}{k_z} = E_0 (\hat{\mathbf{x}} \cos \theta_0 - \hat{\mathbf{z}} \sin \theta_0) (2\pi)^2 \delta(\mathbf{k}_\perp - \mathbf{k}_\perp^0)$$

and Eq. (19.5.8) gives

$$E(\mathbf{r}_\perp, z) = \int_{-\infty}^{\infty} E_0 (\hat{\mathbf{x}} \cos \theta_0 - \hat{\mathbf{z}} \sin \theta_0) (2\pi)^2 \delta(\mathbf{k}_\perp - \mathbf{k}_\perp^0) e^{-jk_z z} e^{-j\mathbf{k}_\perp \cdot \mathbf{r}_\perp} \frac{d^2 \mathbf{k}_\perp}{(2\pi)^2} = E_0 (\hat{\mathbf{x}} \cos \theta_0 - \hat{\mathbf{z}} \sin \theta_0) e^{-j(k_x^0 x + k_z^0 z)}$$

which is the correct expression for the plane wave. For a TE wave a similar result holds. \square

One-Dimensional Apertures

As in Sec. 19.4, we assume that there is no y -dependence in the fields (see Fig. 19.4.1 for the geometry). The 2-D Fourier transforms of the 2-D aperture fields reduce to 1-D Fourier transforms of 1-D fields:

$$\begin{aligned} \hat{E}_\perp(k_x, k_y) &= \int_{-\infty}^{\infty} E_\perp(x, 0) e^{-jk_x x - jk_y y} dx dy \\ &= \int_{-\infty}^{\infty} E_\perp(x, 0) e^{jk_x x} dx \cdot \int_{-\infty}^{\infty} e^{jk_y y} dy = \hat{E}(k_x) \cdot 2\pi \delta(k_y) \end{aligned}$$

The $\delta(k_y)$ factor effectively sets $k_y = 0$ in the 2-D expressions and eliminates the k_y integrations, replacing (19.5.8) by,

$$\begin{aligned} E(x, z) &= \int_{-\infty}^{\infty} \left[\hat{E}_\perp(k_x) - \hat{\mathbf{z}} \frac{k_x \hat{E}_x(k_x)}{k_z} \right] e^{-jk_z z} e^{-jk_x x} \frac{dk_x}{2\pi} \\ \mathbf{H}(x, z) &= \frac{1}{\eta k} \int_{-\infty}^{\infty} \mathbf{k} \times \left[\hat{E}_\perp(k_x) - \hat{\mathbf{z}} \frac{k_x \hat{E}_x(k_x)}{k_z} \right] e^{-jk_z z} e^{-jk_x x} \frac{dk_x}{2\pi} \end{aligned} \quad (19.5.12)$$

where now, $\mathbf{k} = \mathbf{k}_\perp + \hat{\mathbf{z}} k_z = \hat{\mathbf{x}} k_x + \hat{\mathbf{z}} k_z$, and hence, the constraint, $\mathbf{k} \cdot \hat{E} = 0$, implies,

$$\hat{E}_z = -\frac{\mathbf{k}_\perp \cdot \hat{E}_\perp}{k_z} = -\frac{k_x \hat{E}_x}{k_z} \quad (19.5.13)$$

We may rewrite (19.5.12) more explicitly in terms of the transverse E_x, E_y components,

$$\begin{aligned} E(x, z) &= \int_{-\infty}^{\infty} \left[\hat{y} \hat{E}_y(k_x) + \frac{1}{k_z} (\hat{\mathbf{x}} k_z - \hat{\mathbf{z}} k_x) \hat{E}_x(k_x) \right] e^{-jk_x x - jk_z z} \frac{dk_x}{2\pi} \\ \mathbf{H}(x, z) &= \frac{1}{\eta k} \int_{-\infty}^{\infty} \left[(\hat{\mathbf{z}} k_x - \hat{\mathbf{x}} k_z) \hat{E}_y(k_x) + \hat{y} \frac{k^2}{k_z} \hat{E}_x(k_x) \right] e^{-jk_x x - jk_z z} \frac{dk_x}{2\pi} \end{aligned} \quad (19.5.14)$$

Thus, the Fourier components of the magnetic field are,

$$\hat{H}_x = -\frac{k_z}{\eta k} \hat{E}_y, \quad \hat{H}_y = \frac{k}{\eta k_z} \hat{E}_x, \quad \hat{H}_z = \frac{k_x}{\eta k} \hat{E}_y \quad (19.5.15)$$

19.6 Far-Field Approximation, Radiation Pattern

The far-field approximation for the vector case is easily obtained by applying Eq. (19.3.3) to each component of the \mathbf{E}, \mathbf{H} fields, that is, for large r ,

$$\mathbf{E}(\mathbf{r}) \approx 2jk \cos \theta \frac{e^{-jkr}}{4\pi r} \hat{E}(\mathbf{k}_\perp) \Big|_{\mathbf{k} = k\hat{\mathbf{r}}} \quad (\text{far-field radiation pattern}) \quad (19.6.1)$$

and similarly for \mathbf{H} . Since $\mathbf{k} \cdot \hat{E} = 0$ and $\mathbf{k} = k\hat{\mathbf{r}}$, it follows that, $\hat{\mathbf{r}} \cdot \mathbf{E}(r) = 0$, thus, the far field has no radial component. The azimuthal and polar components are easily worked out from (19.6.1) to be,

$$\begin{aligned} E_\phi &= 2jk \frac{e^{-jkr}}{4\pi r} \cos \theta [\hat{E}_y \cos \phi - \hat{E}_x \sin \phi] \\ E_\theta &= 2jk \frac{e^{-jkr}}{4\pi r} [\hat{E}_x \cos \phi + \hat{E}_y \sin \phi] \\ \mathbf{H} &= \frac{1}{\eta} \hat{\mathbf{r}} \times \mathbf{E} \Rightarrow H_\phi = \frac{1}{\eta} E_\theta, \quad H_\theta = -\frac{1}{\eta} E_\phi \end{aligned} \quad (19.6.2)$$

These are the same as Eqs. (18.4.10) and (18.4.12) of Chap. 18, if we recognize that the quantity $f(\theta, \phi)$ in those equations is nothing but $f(\theta, \phi) = \hat{E}_\perp(\mathbf{k}_\perp)$ evaluated at $\mathbf{k} = k\hat{\mathbf{r}}$. In a similar fashion, we can show that the far-field approximation based on (19.5.10) is equivalent to (18.4.11), where now we have, $g(\theta, \phi) = \hat{\mathbf{H}}_\perp(\mathbf{k}_\perp)$.

The $\cos \theta$ factor is an obliquity factor and is sometimes referred to as an *element factor* [1447]. The factors, $[\hat{E}_y \cos \phi - \hat{E}_x \sin \phi]$ and $[\hat{E}_x \cos \phi + \hat{E}_y \sin \phi]$, are referred to as *pattern space factors*.

For the 1-D case described by Eq. (19.5.12), the far-field approximation follows by applying the scalar result (19.4.9) to each component, that is, for large $r = \sqrt{x^2 + z^2}$,

$$\mathbf{E}(r, \theta) \approx e^{j\frac{\pi}{4}} \cos \theta \sqrt{\frac{k}{2\pi r}} e^{-jkr} \hat{E}(k_x^0) \quad (\text{far-field approximation}) \quad (19.6.3)$$

where, $k_x^0 = k \sin \theta$, $k_z^0 = k \cos \theta$, $\cos \theta = z/r$. Resolving these into the cylindrical coordinate directions, $\hat{\mathbf{r}}, \hat{\boldsymbol{\theta}}, \hat{\boldsymbol{\phi}}$, shown in Fig. 19.4.1, we have, $\mathbf{E} = \hat{\boldsymbol{\theta}} E_\theta + \hat{\boldsymbol{\phi}} E_\phi$,

$$\begin{aligned} E_\phi(r, \theta) &= e^{j\frac{\pi}{4}} \sqrt{\frac{k}{2\pi r}} e^{-jkr} \cos \theta \hat{E}_\phi(k_x^0) \\ E_\theta(r, \theta) &= e^{j\frac{\pi}{4}} \sqrt{\frac{k}{2\pi r}} e^{-jkr} \hat{E}_\theta(k_x^0) \end{aligned} \quad (19.6.4)$$

For the magnetic field, we have, $\mathbf{H} = \hat{\mathbf{r}} \times \mathbf{E} / \eta = (\hat{\boldsymbol{\phi}} E_\phi - \hat{\boldsymbol{\theta}} E_\theta) / \eta$,

$$\begin{aligned} H_\theta(r, \theta) &= -\frac{1}{\eta} E_\phi = -\frac{1}{\eta} e^{j\frac{\pi}{4}} \sqrt{\frac{k}{2\pi r}} e^{-jkr} \cos \theta \hat{E}_\phi(k_x^0) \\ H_\phi(r, \theta) &= \frac{1}{\eta} E_\theta = \frac{1}{\eta} e^{j\frac{\pi}{4}} \sqrt{\frac{k}{2\pi r}} e^{-jkr} \hat{E}_\theta(k_x^0) \end{aligned} \quad (19.6.5)$$

19.7 Radiated and Reactive Power, Directivity

The z-component of the Poynting vector at the $z = 0$ plane is given by,

$$S_z = \frac{1}{2} \mathbf{E}(\mathbf{r}_\perp, 0) \times \mathbf{H}^*(\mathbf{r}_\perp, 0) \cdot \hat{\mathbf{z}} \quad (19.7.1)$$

The total power P_{rad} transmitted through the aperture at $z = 0$, and radiated into the right half-space, can be obtained by integrating the real part, $\text{Re}[S_z]$, over the aperture. Similarly, the integral of the imaginary part, $\text{Im}[S_z]$, gives the reactive power P_{react} at the aperture. Thus, we have,

$$P_{\text{rad}} + jP_{\text{react}} = \int_{-\infty}^{\infty} S_z d^2\mathbf{r}_\perp = \frac{1}{2} \int_{-\infty}^{\infty} \mathbf{E}(\mathbf{r}_\perp, 0) \times \mathbf{H}^*(\mathbf{r}_\perp, 0) \cdot \hat{\mathbf{z}} d^2\mathbf{r}_\perp \quad (19.7.2)$$

Applying the vectorial version of Parseval's identity, we may express Eq. (19.7.2) as an integral in the wavenumber domain of the corresponding 2-D Fourier transforms $\hat{\mathbf{E}}, \hat{\mathbf{H}}$ of \mathbf{E}, \mathbf{H} , which are defined in Eq. (19.5.8). Thus, we find,

$$\begin{aligned} P_{\text{rad}} + jP_{\text{react}} &= \frac{1}{2} \int_{-\infty}^{\infty} \mathbf{E}(\mathbf{r}_\perp, 0) \times \mathbf{H}^*(\mathbf{r}_\perp, 0) \cdot \hat{\mathbf{z}} d^2\mathbf{r}_\perp \\ &= \frac{1}{2} \int_{-\infty}^{\infty} \hat{\mathbf{E}}(\mathbf{k}_\perp) \times \hat{\mathbf{H}}^*(\mathbf{k}_\perp) \cdot \hat{\mathbf{z}} \frac{d^2\mathbf{k}_\perp}{(2\pi)^2} \end{aligned} \quad (19.7.3)$$

But the plane-wave Fourier components satisfy, $\hat{\mathbf{H}} = \mathbf{k} \times \hat{\mathbf{E}} / \eta k$, where $\mathbf{k} = \mathbf{k}_\perp + \hat{\mathbf{z}} k_z$. The vector \mathbf{k}_\perp is real-valued but k_z becomes imaginary in the evanescent part of the integral. Therefore, we may write, $\mathbf{k}^* = \mathbf{k}_\perp + \hat{\mathbf{z}} k_z^* = \mathbf{k} + \hat{\mathbf{z}} (k_z^* - k_z)$. Using the constraint, $\mathbf{k} \cdot \hat{\mathbf{E}} = 0$, which implies, $\mathbf{k}^* \cdot \hat{\mathbf{E}} = \hat{E}_z (k_z^* - k_z)$, it follows that,

$$\begin{aligned} \hat{\mathbf{E}} \times \hat{\mathbf{H}}^* \cdot \hat{\mathbf{z}} &= \frac{1}{\eta k} \hat{\mathbf{E}} \times (\mathbf{k}^* \times \hat{\mathbf{E}}^*) \cdot \hat{\mathbf{z}} = \frac{1}{\eta k} [\mathbf{k}^* |\hat{\mathbf{E}}|^2 - \hat{\mathbf{E}}^* (\mathbf{k}^* \cdot \hat{\mathbf{E}})] \cdot \hat{\mathbf{z}} \\ &= \frac{1}{\eta k} [k_z^* |\hat{\mathbf{E}}|^2 - \hat{E}_z^* \hat{E}_z (k_z^* - k_z)] = \frac{1}{\eta k} [k_z^* |\hat{\mathbf{E}}_\perp|^2 + k_z |\hat{E}_z|^2] \end{aligned}$$

Thus, Eq. (19.7.3) becomes,

$$P_{\text{rad}} + jP_{\text{react}} = \frac{1}{2\eta k} \int_{-\infty}^{\infty} [k_z^* |\hat{\mathbf{E}}_\perp|^2 + k_z |\hat{E}_z|^2] \frac{d^2\mathbf{k}_\perp}{(2\pi)^2} \quad (19.7.4)$$

Splitting the integration over the visible/propagating region, $|\mathbf{k}_\perp| = \sqrt{k_x^2 + k_y^2} \leq k$, and over the invisible/evanescent region, $|\mathbf{k}_\perp| = \sqrt{k_x^2 + k_y^2} > k$, and noting that k_z is real over the former, and imaginary, over the latter region, we may separate $P_{\text{rad}}, P_{\text{react}}$,

$$P_{\text{rad}} + jP_{\text{react}} = \frac{1}{2\eta k} \left[\int_{|\mathbf{k}_\perp| \leq k} + \int_{|\mathbf{k}_\perp| > k} \right] [k_z^* |\hat{\mathbf{E}}_\perp|^2 + k_z |\hat{E}_z|^2] \frac{d^2\mathbf{k}_\perp}{(2\pi)^2}$$

$$\begin{aligned} P_{\text{rad}} &= \frac{1}{2\eta} \int_{|\mathbf{k}_\perp| \leq k} [|\hat{\mathbf{E}}_\perp|^2 + |\hat{E}_z|^2] \frac{k_z}{k} \frac{d^2\mathbf{k}_\perp}{(2\pi)^2} & k_z &= \sqrt{k^2 - |\mathbf{k}_\perp|^2} \\ P_{\text{react}} &= \frac{1}{2\eta} \int_{|\mathbf{k}_\perp| > k} [|\hat{\mathbf{E}}_\perp|^2 - |\hat{E}_z|^2] \frac{jk_z}{k} \frac{d^2\mathbf{k}_\perp}{(2\pi)^2} & jk_z &= \sqrt{|\mathbf{k}_\perp|^2 - k^2} \end{aligned} \quad (19.7.5)$$

In Sec. 18.6, we assumed that the transverse aperture fields were Huygens sources, that is, $\mathbf{H}_\perp(\mathbf{r}_\perp, 0) = \hat{\mathbf{z}} \times \mathbf{E}_\perp(\mathbf{r}_\perp, 0) / \eta$. Under this assumption, the radiated power is given approximately by,

$$\begin{aligned} P_{\text{rad}} &= \frac{1}{2} \int_{-\infty}^{\infty} \text{Re}[\mathbf{E}_\perp(\mathbf{r}_\perp, 0) \times \mathbf{H}_\perp^*(\mathbf{r}_\perp, 0)] \cdot \hat{\mathbf{z}} d^2\mathbf{r}_\perp \\ &= \frac{1}{2\eta} \int_{-\infty}^{\infty} |\mathbf{E}_\perp(\mathbf{r}_\perp, 0)|^2 d^2\mathbf{r}_\perp = \frac{1}{2\eta} \int_{-\infty}^{\infty} |\hat{\mathbf{E}}_\perp|^2 \frac{d^2\mathbf{k}_\perp}{(2\pi)^2} \end{aligned} \quad (19.7.6)$$

where we used Parseval's identity in the last two integrals. Eq. (19.7.6) approximates (19.7.5) for large apertures [19]. Indeed, $\hat{\mathbf{E}}_\perp$ is typically highly peaked in the forward direction, $\mathbf{k}_\perp = 0$, or, $k_z = k$, and hence, $\hat{E}_z = -\mathbf{k}_\perp \cdot \hat{\mathbf{E}}_\perp / k_z$ is small compared to $\hat{\mathbf{E}}_\perp$ in (19.7.5). Thus, the two expressions will agree, if we also assume that the contribution of the invisible/evanescent region, $|\mathbf{k}_\perp| > k$, in (19.7.6) is small. However, such assumption is not warranted in the so-called super-directive apertures where a huge amount of reactive power resides in the invisible region.

An alternative way of calculating the radiated power is by integrating the radial component of the Poynting vector over a hemisphere of very large radius in the right half-space. At large radial distances, we may use the radiated fields given in (19.6.1),

$$\mathbf{E}_{\text{rad}}(\mathbf{r}) = 2jk \cos \theta \frac{e^{-jkr}}{4\pi r} \hat{\mathbf{E}}(\mathbf{k}_\perp^0) \Big|_{k^0 = k\hat{\mathbf{r}}}, \quad \mathbf{H}_{\text{rad}}(\mathbf{r}) = \frac{1}{\eta} \hat{\mathbf{r}} \times \mathbf{E}_{\text{rad}} \quad (19.7.7)$$

The corresponding Poynting vector has only a radial component, since, $\hat{\mathbf{r}} \cdot \mathbf{E}_{\text{rad}} = 0$,

$$\mathcal{P} = \frac{1}{2} \text{Re}[\mathbf{E}_{\text{rad}} \times \mathbf{H}_{\text{rad}}^*] = \frac{1}{2\eta} \text{Re}[\mathbf{E}_{\text{rad}} \times (\hat{\mathbf{r}} \times \mathbf{E}_{\text{rad}}^*)] = \hat{\mathbf{r}} \frac{1}{2\eta} |\mathbf{E}_{\text{rad}}|^2 = \hat{\mathbf{r}} \mathcal{P}_r \quad (19.7.8)$$

Using spherical coordinates, the net power transmitted through the right-half hemisphere of radius r will be given as follows,

$$\begin{aligned}
 P_{\text{rad}} &= \int \mathcal{P}_r dS = \int_0^{\pi/2} \int_0^{2\pi} \mathcal{P}_r r^2 \sin \theta d\theta d\phi = \int_0^{\pi/2} \int_0^{2\pi} \frac{1}{2\eta} |\mathbf{E}_{\text{rad}}|^2 r^2 \sin \theta d\theta d\phi \\
 &= \int_0^{\pi/2} \int_0^{2\pi} \frac{1}{2\eta} \left| 2jk \cos \theta \frac{e^{-jkr}}{4\pi r} \hat{\mathbf{E}}(\mathbf{k}_\perp^0) \right|^2 r^2 \sin \theta d\theta d\phi \\
 &= \frac{1}{2\eta (2\pi)^2} \int_0^{\pi/2} \int_0^{2\pi} |\hat{\mathbf{E}}(\mathbf{k}_\perp^0)|^2 k^2 \cos^2 \theta \sin \theta d\theta d\phi
 \end{aligned}$$

Changing variables from θ, ϕ to $k_x = k \sin \theta \cos \phi, k_y = k \sin \theta \sin \phi$, and noting that, $dk_x dk_y = k^2 \cos \theta \sin \theta d\theta d\phi$, and, $k_z = k \cos \theta$, it follows that the last integral can be transformed into that of Eq. (19.7.5).

The directivity in direction, θ, ϕ , is defined as follows in terms of the radiation intensity (radiated power per unit solid angle), $dP/d\Omega = r^2 dP/dS = r^2 \mathcal{P}_r$,

$$D(\theta, \phi) = \frac{dP/d\Omega}{P_{\text{rad}}/4\pi} = 4\pi \frac{r^2 \mathcal{P}_r}{P_{\text{rad}}} = \frac{k^2}{\pi} \frac{\cos^2 \theta |\hat{\mathbf{E}}(\mathbf{k}_\perp^0)|^2}{\int_{|\mathbf{k}_\perp| \leq k} |\hat{\mathbf{E}}(\mathbf{k}_\perp)|^2 \frac{k_z}{k} \frac{d^2 \mathbf{k}_\perp}{(2\pi)^2}} \quad (19.7.9)$$

Assuming that the maximum directivity is in the forward direction, $\mathbf{k}_\perp = 0$, we have,

$$D_{\text{max}} = \frac{4\pi}{\lambda^2} \frac{|\hat{\mathbf{E}}_\perp(0)|^2}{\int_{|\mathbf{k}_\perp| \leq k} |\hat{\mathbf{E}}(\mathbf{k}_\perp)|^2 \frac{k_z}{k} \frac{d^2 \mathbf{k}_\perp}{(2\pi)^2}} \quad (19.7.10)$$

where we replaced, $k^2/\pi = 4\pi/\lambda^2$, and $|\hat{\mathbf{E}}(0)|^2 = |\hat{\mathbf{E}}_\perp(0)|^2$, since, $\hat{\mathbf{E}}_z = -\mathbf{k}_\perp \cdot \hat{\mathbf{E}}_\perp/k_z = 0$, at $\mathbf{k}_\perp = 0$. By comparison, the approximate expression (18.6.10) in Sec. 18.6 was,

$$D_{\text{max}} = \frac{4\pi}{\lambda^2} \frac{|\hat{\mathbf{E}}_\perp(0)|^2}{\int_{-\infty}^{\infty} |\hat{\mathbf{E}}_\perp(\mathbf{k}_\perp)|^2 \frac{d^2 \mathbf{k}_\perp}{(2\pi)^2}} = \frac{4\pi}{\lambda^2} \frac{\left| \int_{-\infty}^{\infty} \mathbf{E}_\perp(\mathbf{r}_\perp, 0) d^2 \mathbf{r}_\perp \right|^2}{\int_{-\infty}^{\infty} |\mathbf{E}_\perp(\mathbf{r}_\perp, 0)|^2 d^2 \mathbf{r}_\perp} \quad (19.7.11)$$

Quite similar expressions hold also in the 1-D aperture case. The total radiated and reactive powers (per unit y -length) are defined by integrating the z -component of the Poynting vector over the x -aperture only. This gives,

$$P'_{\text{rad}} + jP'_{\text{react}} = \int_{-\infty}^{\infty} S_z dx = \frac{1}{2\eta k} \int_{-\infty}^{\infty} [k_z^* |\hat{\mathbf{E}}_\perp|^2 + k_z |\hat{\mathbf{E}}_z|^2] \frac{dk_x}{2\pi} \quad (19.7.12)$$

where the prime means “per unit y -length.” Then, (19.7.12) separates as,

$$\begin{aligned}
 P'_{\text{rad}} &= \frac{1}{2\eta} \int_{|k_x| \leq k} [|\hat{\mathbf{E}}_\perp|^2 + |\hat{\mathbf{E}}_z|^2] \frac{k_z}{k} \frac{dk_x}{2\pi} & k_z &= \sqrt{k^2 - k_x^2} \\
 P'_{\text{react}} &= \frac{1}{2\eta} \int_{|k_x| > k} [|\hat{\mathbf{E}}_\perp|^2 - |\hat{\mathbf{E}}_z|^2] \frac{jk_z}{k} \frac{dk_x}{2\pi} & jk_z &= \sqrt{k_x^2 - k^2}
 \end{aligned} \quad (19.7.13)$$

It is convenient to rewrite these in a form that explicitly separates the TE and TM components, that is, E_y and H_y , Using Eqs. (19.5.15), we find,

$$\begin{aligned}
 P'_{\text{rad}} &= \frac{1}{2\eta} \int_{|k_x| \leq k} [|\hat{E}_y|^2 + |\eta \hat{H}_y|^2] \frac{k_z}{k} \frac{dk_x}{2\pi} & k_z &= \sqrt{k^2 - k_x^2} \\
 P'_{\text{react}} &= \frac{1}{2\eta} \int_{|k_x| > k} [|\hat{E}_y|^2 - |\eta \hat{H}_y|^2] \frac{jk_z}{k} \frac{dk_x}{2\pi} & jk_z &= \sqrt{k_x^2 - k^2}
 \end{aligned} \quad (19.7.14)$$

Indeed, using Eqs. (19.5.15), we have in the visible region, $|k_x| \leq k$,

$$|\hat{\mathbf{E}}|^2 = |\hat{E}_x|^2 + |\hat{E}_y|^2 + |\hat{E}_z|^2 = |\hat{E}_y|^2 + |\hat{E}_x|^2 + \frac{k_x^2}{k_z^2} |\hat{E}_x|^2 = |\hat{E}_y|^2 + \frac{k^2}{k_z^2} |\hat{E}_x|^2 = |\hat{E}_y|^2 + |\eta \hat{H}_y|^2$$

Similarly, in the invisible region, $|k_x| > k$, we have noting that $|k_z|^2 = k_x^2 - k^2$,

$$|\hat{E}_\perp|^2 - |\hat{E}_z|^2 = |\hat{E}_y|^2 + |\hat{E}_x|^2 - \frac{k_x^2}{|k_z|^2} |\hat{E}_x|^2 = |\hat{E}_y|^2 - \frac{k^2}{k_z^2} |\hat{E}_x|^2 = |\hat{E}_y|^2 - |\eta \hat{H}_y|^2$$

The same expression for P'_{rad} can also be obtained by integrating the radial component \mathcal{P}_r of the Poynting vector over a semi-cylindrical surface of large radius r and using the radiation fields (19.6.3). Fig. 19.7.1 illustrates the surface conventions in the 1-D and 2-D cases.

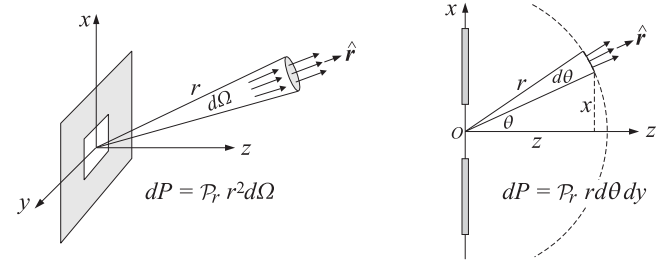


Fig. 19.7.1 Radiated power from 2-D and 1-D apertures.

The directivity may be defined in terms of the power density through the cylindrical surface $dS = rd\theta dy$, that is,,

$$dP = \mathcal{P}_r rd\theta dy$$

or, with $P' = dP/dy$, using (19.6.3),

$$\frac{dP}{d\theta dy} = \frac{dP'}{d\theta} = r \mathcal{P}_r = r \frac{1}{2\eta} |\mathbf{E}_{\text{rad}}|^2 = r \frac{1}{2\eta} \left| e^{j\pi/4} \cos \theta \sqrt{\frac{k}{2\pi r}} e^{-jkr} \hat{\mathbf{E}}(\mathbf{k}_x^0) \right|^2$$

which gives for the directivity towards the θ -direction,

$$D(\theta) = \frac{dP'/d\theta}{P'_{\text{rad}}/2\pi} = k \frac{\cos^2 \theta |\hat{\mathbf{E}}(\mathbf{k}_x^0)|^2}{\int_{-k}^k |\hat{\mathbf{E}}(\mathbf{k}_x)|^2 \frac{k_z}{k} \frac{dk_x}{2\pi}} \quad (19.7.15)$$

where $k_x^0 = k \sin \theta$. We note that the denominator $P'_{\text{rad}}/2\pi$ in the above definition represents the radiation intensity in the ideal cylindrically-isotropic case, that is,

$$\left(\frac{dP'}{d\theta}\right)_{\text{isotropic}} = \frac{P'_{\text{rad}}}{2\pi}$$

If the maximum directivity is towards the forward direction, $\theta = 0$, or, $k_x^0 = 0$, then, $\hat{E}_z = 0$, and we find the following expression for the maximum directivity, expressible also in terms of the TE and TM components,

$$D_{\text{max}} = k \frac{\int_{-k}^k |\hat{E}_\perp(k_x)|^2 \frac{k_z}{k} \frac{dk_x}{2\pi}}{\int_{-k}^k [|\hat{E}_y(k_x)|^2 + |\eta \hat{H}_y(k_x)|^2] \frac{k_z}{k} \frac{dk_x}{2\pi}} = \frac{2\pi}{\lambda} \frac{|\hat{E}_y(0)|^2 + |\eta \hat{H}_y(0)|^2}{\int_{-k}^k [|\hat{E}_y(k_x)|^2 + |\eta \hat{H}_y(k_x)|^2] \frac{k_z}{k} \frac{dk_x}{2\pi}} \quad (19.7.16)$$

Finally, had we assumed that the aperture fields were Huygens sources, the maximum directivity would be given by the analogous expression to (19.7.11),

$$D_{\text{max}} = \frac{2\pi}{\lambda} \frac{|\hat{E}_\perp(0)|^2}{\int_{-\infty}^{\infty} |\hat{E}_\perp(k_x)|^2 \frac{dk_x}{2\pi}} = \frac{2\pi}{\lambda} \frac{\left| \int_{-\infty}^{\infty} E_\perp(x, 0) dx \right|^2}{\int_{-\infty}^{\infty} |E_\perp(x, 0)|^2 dx} \quad (19.7.17)$$

For a finite-aperture of length L , extending over $-L/2 \leq x \leq L/2$, Eq. (19.7.17) is maximized when the aperture distribution $E_\perp(x, 0)$ is uniform, resulting in the maximum value, $D_{\text{max}} = 2\pi L/\lambda$. This is the 1-D version of the 2-D result, $D_{\text{max}} = 4\pi A/\lambda^2$, for uniform apertures that we derived in Sec. 18.6, under the approximation of Eq. (19.7.6).

19.8 Smythe Diffraction Formulas

The plane-wave representations Eqs. (19.5.8) or Eq. (19.5.10), can also be written convolutionally in terms of the transverse components, $E_\perp(\mathbf{r}'_\perp, 0)$, $H_\perp(\mathbf{r}'_\perp, 0)$, on the $z = 0$ aperture plane. The resulting Rayleigh-Sommerfeld type formulas are known as Smythe's formulas [1328].

From the Weyl representations (D.18) and (D.20) of Appendix D, we have with $G(r) = e^{-jk_r r}/4\pi r$, and $r = |\mathbf{r}| = \sqrt{x^2 + y^2 + z^2}$, and for $z \geq 0$,

$$-2 \frac{\partial G}{\partial z} = \int_{-\infty}^{\infty} e^{-jk_z z} e^{-jk_\perp \cdot \mathbf{r}_\perp} \frac{d^2 \mathbf{k}_\perp}{(2\pi)^2}, \quad -2 \nabla_\perp G = \int_{-\infty}^{\infty} \frac{\mathbf{k}_\perp}{k_z} e^{-jk_z z} e^{-jk_\perp \cdot \mathbf{r}_\perp} \frac{d^2 \mathbf{k}_\perp}{(2\pi)^2}$$

that is, we have the 2-D Fourier transforms with respect to \mathbf{r}_\perp ,

$$\hat{G}(\mathbf{k}_\perp, z) = \frac{e^{-jk_z z}}{2jk_z}, \quad -2 \frac{\partial \hat{G}}{\partial z} = e^{-jk_z z}, \quad -2 \widehat{\nabla_\perp G} = \frac{\mathbf{k}_\perp}{k_z} e^{-jk_z z} \quad (19.8.1)$$

We observe that in (19.5.8) the following products of Fourier transforms (in \mathbf{k}_\perp) appear, which will become convolutions in the \mathbf{r}_\perp domain:

$$\hat{E}_\perp(\mathbf{k}_\perp) \cdot e^{-jk_z z} = \hat{E}_\perp(\mathbf{k}_\perp) \cdot \left(-2 \frac{\partial \hat{G}}{\partial z}\right)$$

$$\hat{E}_\perp(\mathbf{k}_\perp) \cdot \left(\frac{\mathbf{k}_\perp}{k_z} e^{-jk_z z}\right) = \hat{E}_\perp(\mathbf{k}_\perp) \cdot \left(-2 \widehat{\nabla_\perp G}\right)$$

$$E(\mathbf{r}_\perp, z) = \int_{-\infty}^{\infty} \left[\hat{E}_\perp(\mathbf{k}_\perp) \cdot \left(-2 \frac{\partial \hat{G}}{\partial z}\right) - \hat{z} \left[\hat{E}_\perp(\mathbf{k}_\perp) \cdot \left(-2 \widehat{\nabla_\perp G}\right) \right] \right] e^{-jk_\perp \cdot \mathbf{r}_\perp} \frac{d^2 \mathbf{k}_\perp}{(2\pi)^2}$$

It follows that (19.5.8) can be written convolutionally in the form:

$$E(\mathbf{r}_\perp, z) = -2 \int_{-\infty}^{\infty} \left[E_\perp(\mathbf{r}'_\perp, 0) \frac{\partial G(R)}{\partial z} - \hat{z} \left(E_\perp(\mathbf{r}'_\perp, 0) \cdot \nabla_\perp G(R) \right) \right] d^2 \mathbf{r}'_\perp \quad (19.8.2)$$

where here $G(R) = e^{-jk_R R}/4\pi R$ with $R = |\mathbf{r} - \mathbf{r}'|$ and $z' = 0$, that is, $R = \sqrt{|\mathbf{r}_\perp - \mathbf{r}'_\perp|^2 + z^2}$. Because $E_\perp(\mathbf{r}'_\perp, 0)$ does not depend on \mathbf{r} , it is straightforward to verify using some vector identities that,

$$\hat{z} (\nabla_\perp G \cdot E_\perp) - E_\perp \frac{\partial G}{\partial z} = \nabla \times (\hat{z} \times E_\perp G) \quad (19.8.3)$$

This gives rise to *Smythe's formulas* for the electric and magnetic fields, for $z \geq 0$,

$$\begin{aligned} E(\mathbf{r}_\perp, z) &= 2 \nabla \times \int_{-\infty}^{\infty} \hat{z} \times E_\perp(\mathbf{r}'_\perp, 0) G(R) d^2 \mathbf{r}'_\perp \\ H(\mathbf{r}_\perp, z) &= \frac{2j}{\eta k} \nabla \times \left(\nabla \times \int_{-\infty}^{\infty} \hat{z} \times E_\perp(\mathbf{r}'_\perp, 0) G(R) d^2 \mathbf{r}'_\perp \right) \end{aligned} \quad \text{(Smythe)} \quad (19.8.4)$$

with $G(R) = e^{-jk_R R}/4\pi R$, and $R = \sqrt{|\mathbf{r}_\perp - \mathbf{r}'_\perp|^2 + z^2}$. In a similar fashion, we obtain the Smythe formulas for the alternative representation of Eq. (19.5.10), which can also be obtained by applying a duality transformation to (19.8.4),

$$\begin{aligned} H(\mathbf{r}_\perp, z) &= 2 \nabla \times \int_{-\infty}^{\infty} \hat{z} \times H_\perp(\mathbf{r}'_\perp, 0) G(R) d^2 \mathbf{r}'_\perp \\ E(\mathbf{r}_\perp, z) &= \frac{2\eta}{jk} \nabla \times \left(\nabla \times \int_{-\infty}^{\infty} \hat{z} \times H_\perp(\mathbf{r}'_\perp, 0) G(R) d^2 \mathbf{r}'_\perp \right) \end{aligned} \quad (19.8.5)$$

Perhaps a faster way of deriving Eqs. (19.8.4) is as follows. Working in the wavenumber domain and using the constraint, $\mathbf{k} \cdot \hat{E} = k_z \hat{E}_z + \mathbf{k}_\perp \cdot \hat{E}_\perp = 0$, and some vector identities, we obtain,

$$\mathbf{k} \times (\hat{z} \times \hat{E}_\perp) = \mathbf{k} \times (\hat{z} \times \hat{E}) = (\mathbf{k} \cdot \hat{E}) \hat{z} - (\mathbf{k} \cdot \hat{z}) \hat{E} = -\hat{E} k_z \Rightarrow \hat{E}(\mathbf{k}_\perp) = -\frac{\mathbf{k} \times (\hat{z} \times \hat{E}_\perp(\mathbf{k}_\perp))}{k_z}$$

Recalling that, $\hat{G}(\mathbf{k}_\perp, z) = e^{-jk_z z}/(2jk_z)$, is the 2-D Fourier transform of the Green's function $G(r) = e^{-jk_r r}/(4\pi r)$, for $z \geq 0$, we can write the propagation filter in the form,

$$\hat{h}(\mathbf{k}_\perp, z) = e^{-jk_z z} = 2jk_z \cdot \left[\frac{e^{-jk_z z}}{2jk_z} \right] = 2jk_z \cdot \hat{G}(\mathbf{k}_\perp, z) \quad (19.8.6)$$

Then, the Fourier transform of the propagated field becomes,

$$\hat{E}(\mathbf{k}_\perp, z) = \hat{E}(\mathbf{k}_\perp) e^{-jk_z z} = \hat{E}(\mathbf{k}_\perp) \cdot 2jk_z \cdot \hat{G}(\mathbf{k}_\perp, z) = -\frac{\mathbf{k} \times (\hat{\mathbf{z}} \times \hat{E}_\perp(\mathbf{k}_\perp))}{k_z} \cdot 2jk_z \cdot \hat{G}(\mathbf{k}_\perp, z)$$

or,

$$\hat{E}(\mathbf{k}_\perp, z) = -2jk \times (\hat{\mathbf{z}} \times \hat{E}_\perp(\mathbf{k}_\perp)) \cdot \hat{G}(\mathbf{k}_\perp, z) \tag{19.8.7}$$

Eq. (19.8.4) follows immediately from this by taking inverse Fourier transforms of both sides and replacing $-jk$ by ∇ .

Connection to Franz Formulas

The Smythe formulas can be also derived more directly by using the Franz formulas (18.10.13) and making use of the extinction theorem as we did in Sec. 19.1 in the discussion of the Rayleigh-Sommerfeld formula.

Assuming $z > 0$, and applying (18.10.13) to the closed surface $S + S_\infty$ of Fig. 19.1.1, and dropping the S_∞ term, it follows that the left-hand side of (18.10.13) will be zero if the point \mathbf{r} is not in the right half-space. In particular, it will be zero when evaluated at the reflected point $\mathbf{r}_- = \mathbf{r}_\perp - \hat{\mathbf{z}}z$ in the left half-space. To simplify the notation, we define the transverse electric and magnetic vector potentials:[†]

$$\begin{aligned} \mathbf{F}(\mathbf{r}) &= 2 \int_{-\infty}^{\infty} [\hat{\mathbf{z}} \times \mathbf{E}_\perp(\mathbf{r}'_\perp, 0)] G(R) d^2\mathbf{r}'_\perp \\ \mathbf{A}(\mathbf{r}) &= 2 \int_{-\infty}^{\infty} [\hat{\mathbf{z}} \times \mathbf{H}_\perp(\mathbf{r}'_\perp, 0)] G(R) d^2\mathbf{r}'_\perp \end{aligned} \tag{19.8.8}$$

where we took S to be the xy plane with the unit vector $\hat{\mathbf{n}} = \hat{\mathbf{z}}$, and $G(R) = e^{-jkR}/4\pi R$, and $R = \sqrt{|\mathbf{r}_\perp - \mathbf{r}'_\perp|^2 + z^2}$. Then, the Franz formulas, Eqs. (18.10.13) and (18.10.14), can be written as follows, after setting $\omega\mu = k\eta$ and $\omega\epsilon = k/\eta$,

$$\begin{aligned} \mathbf{E}(\mathbf{r}) &= \frac{1}{2} \frac{\eta}{jk} \nabla \times (\nabla \times \mathbf{A}) + \frac{1}{2} \nabla \times \mathbf{F} \\ \mathbf{H}(\mathbf{r}) &= \frac{1}{2} \frac{-1}{jk\eta} \nabla \times (\nabla \times \mathbf{F}) + \frac{1}{2} \nabla \times \mathbf{A} \end{aligned} \tag{19.8.9}$$

Noting that \mathbf{F}, \mathbf{A} are transverse and using some vector identities and the decomposition $\nabla = \nabla_\perp + \hat{\mathbf{z}}\partial_z$, we may rewrite the above in a form that explicitly separates the transverse and longitudinal parts, so that if \mathbf{r} is in the right half-space:

$$\begin{aligned} \mathbf{E}(\mathbf{r}) &= \underbrace{\frac{1}{2} \frac{\eta}{jk} [\nabla_\perp (\nabla_\perp \cdot \mathbf{A}) - \nabla^2 \mathbf{A}]}_{\text{transverse}} + \underbrace{\frac{1}{2} \hat{\mathbf{z}} \times \partial_z \mathbf{F} + \frac{1}{2} \frac{\eta}{jk} [\hat{\mathbf{z}} \partial_z (\nabla_\perp \cdot \mathbf{A})]}_{\text{longitudinal}} + \frac{1}{2} \nabla_\perp \times \mathbf{F} \\ \mathbf{H}(\mathbf{r}) &= \underbrace{\frac{1}{2} \frac{-1}{jk\eta} [\nabla_\perp (\nabla_\perp \cdot \mathbf{F}) - \nabla^2 \mathbf{F}]}_{\text{transverse}} + \underbrace{\frac{1}{2} \hat{\mathbf{z}} \times \partial_z \mathbf{A} + \frac{1}{2} \frac{-1}{jk\eta} [\hat{\mathbf{z}} \partial_z (\nabla_\perp \cdot \mathbf{F})]}_{\text{longitudinal}} + \frac{1}{2} \nabla_\perp \times \mathbf{A} \end{aligned} \tag{19.8.10}$$

[†]In the notation of Eq. (18.10.12), we have $\mathbf{F} = -2\mathbf{A}_{ms}/\epsilon$ and $\mathbf{A} = 2\mathbf{A}_s/\mu$.

where we used the identity,

$$\nabla \times (\nabla \times \mathbf{A}) = \nabla (\nabla \cdot \mathbf{A}) - \nabla^2 \mathbf{A} = \underbrace{\nabla_\perp (\nabla_\perp \cdot \mathbf{A}) - \nabla^2 \mathbf{A}}_{\text{transverse}} + \underbrace{\hat{\mathbf{z}} \partial_z (\nabla_\perp \cdot \mathbf{A})}_{\text{longitudinal}}$$

If \mathbf{r} is chosen to be the reflected point \mathbf{r}_- in the left half-space, then $G_- = G$ and the vectors \mathbf{F}, \mathbf{A} remain the same, but the gradient with respect to \mathbf{r}_- is now $\nabla_- = \nabla_\perp - \hat{\mathbf{z}}\partial_z$, arising from the replacement $z \rightarrow -z$. Thus, replacing $\partial_z \rightarrow -\partial_z$ in (19.8.10) and setting the result to zero, we have:

$$\begin{aligned} 0 &= \underbrace{\frac{1}{2} \frac{\eta}{jk} [\nabla_\perp (\nabla_\perp \cdot \mathbf{A}) - \nabla^2 \mathbf{A}]}_{\text{transverse}} - \underbrace{\frac{1}{2} \hat{\mathbf{z}} \times \partial_z \mathbf{F} + \frac{1}{2} \frac{\eta}{jk} [-\hat{\mathbf{z}} \partial_z (\nabla_\perp \cdot \mathbf{A})]}_{\text{longitudinal}} + \frac{1}{2} \nabla_\perp \times \mathbf{F} \\ 0 &= \underbrace{\frac{1}{2} \frac{-1}{jk\eta} [\nabla_\perp (\nabla_\perp \cdot \mathbf{F}) - \nabla^2 \mathbf{F}]}_{\text{transverse}} - \underbrace{\frac{1}{2} \hat{\mathbf{z}} \times \partial_z \mathbf{A} + \frac{1}{2} \frac{-1}{jk\eta} [-\hat{\mathbf{z}} \partial_z (\nabla_\perp \cdot \mathbf{F})]}_{\text{longitudinal}} + \frac{1}{2} \nabla_\perp \times \mathbf{A} \end{aligned} \tag{19.8.11}$$

Separating (19.8.11) into its transverse and longitudinal parts, we have:

$$\begin{aligned} \frac{\eta}{jk} [\nabla_\perp (\nabla_\perp \cdot \mathbf{A}) - \nabla^2 \mathbf{A}] &= \hat{\mathbf{z}} \times \partial_z \mathbf{F}, & \frac{1}{2} \frac{\eta}{jk} [\hat{\mathbf{z}} \partial_z (\nabla_\perp \cdot \mathbf{A})] &= \nabla_\perp \times \mathbf{F} \\ \frac{-1}{jk\eta} [\nabla_\perp (\nabla_\perp \cdot \mathbf{F}) - \nabla^2 \mathbf{F}] &= \hat{\mathbf{z}} \times \partial_z \mathbf{A}, & \frac{-1}{jk\eta} [\hat{\mathbf{z}} \partial_z (\nabla_\perp \cdot \mathbf{F})] &= \nabla_\perp \times \mathbf{A} \end{aligned} \tag{19.8.12}$$

Using these conditions into Eq. (19.8.10), we obtain the doubling of terms:

$$\begin{aligned} \mathbf{E}(\mathbf{r}) &= \nabla_\perp \times \mathbf{F} + \hat{\mathbf{z}} \times \partial_z \mathbf{F} = \nabla \times \mathbf{F} \\ \mathbf{H}(\mathbf{r}) &= \frac{-1}{jk\eta} [\nabla_\perp (\nabla_\perp \cdot \mathbf{F}) - \nabla^2 \mathbf{F} + \hat{\mathbf{z}} \partial_z (\nabla_\perp \cdot \mathbf{F})] = \frac{-1}{jk\eta} \nabla \times (\nabla \times \mathbf{F}) \end{aligned} \tag{19.8.13}$$

which are the same as Eqs. (19.8.4). Alternatively, we may express the diffracted fields in terms of the values of the magnetic field at the xy surface:

$$\mathbf{E}(\mathbf{r}) = \frac{\eta}{jk} [\nabla_\perp (\nabla_\perp \cdot \mathbf{A}) - \nabla^2 \mathbf{A} + \hat{\mathbf{z}} \partial_z (\nabla_\perp \cdot \mathbf{A})] = \frac{\eta}{jk} \nabla \times (\nabla \times \mathbf{A})$$

$$\mathbf{H}(\mathbf{r}) = \nabla_\perp \times \mathbf{A} + \hat{\mathbf{z}} \times \partial_z \mathbf{A} = \nabla \times \mathbf{A}$$

which are the same as (19.8.5).

By applying the operation $(k^2 + \nabla^2)$ to the definitions (19.8.8), and using the Green's function property, $(k^2 + \nabla^2)G(\mathbf{r} - \mathbf{r}') = -\delta^{(2)}(\mathbf{r}_\perp - \mathbf{r}'_\perp)\delta(z - z')$, applied at $z' = 0$, we find that \mathbf{F}, \mathbf{A} satisfy the Helmholtz equations,

$$\begin{aligned} \nabla^2 \mathbf{F} + k^2 \mathbf{F} &= -2[\hat{\mathbf{z}} \times \mathbf{E}_\perp(\mathbf{r}_\perp, 0)]\delta(z) \\ \nabla^2 \mathbf{A} + k^2 \mathbf{A} &= -2[\hat{\mathbf{z}} \times \mathbf{H}_\perp(\mathbf{r}_\perp, 0)]\delta(z) \end{aligned} \tag{19.8.15}$$

According to the field-equivalence principle, the effective surface currents defined in Eq. (18.10.8) are, $\mathbf{J}_s = \hat{\mathbf{z}} \times \mathbf{H}_\perp$ and $\mathbf{J}_{ms} = -\hat{\mathbf{z}} \times \mathbf{E}_\perp$, with the corresponding volume

currents, $J_s \delta(z)$ and $J_{ms} \delta(z)$. We note that Eqs. (19.8.15) are the Helmholtz equations (18.2.5) satisfied by the effective surface magnetic and electric vector potentials A_s, A_{ms} , driven by these volume currents as sources, that is,

$$\begin{aligned}\nabla^2 A + k^2 A &= -\mu J_s \delta(z) \\ \nabla^2 A_m + k^2 A_m &= -\epsilon J_{ms} \delta(z)\end{aligned}$$

where as we noted earlier, we have the identifications, $F = -2A_{ms}/\epsilon$ and $A = 2A_s/\mu$.

Summary

Because $z > 0$, both F and A satisfy the homogeneous Helmholtz equation, so that $\nabla \times (\nabla \times F) = \nabla(\nabla \cdot F) - \nabla^2 F = \nabla(\nabla \cdot F) + k^2 F$, and similarly for A . Thus, the expressions for the EM fields, may be summarized as follows, in terms of F ,

$$\begin{aligned}E &= \nabla \times F \\ -jk\eta H &= \nabla \times (\nabla \times F) = k^2 F + \nabla(\nabla \cdot F)\end{aligned}\quad (19.8.16)$$

or, separating transverse and longitudinal parts,

$$\begin{aligned}E_\perp &= \hat{z} \times \partial_z F \\ \hat{z} E_z &= \nabla_\perp \times F \\ -jk\eta H_\perp &= k^2 F + \nabla_\perp(\nabla_\perp \cdot F) \\ -jk\eta \hat{z} H_z &= \hat{z} \partial_z(\nabla_\perp \cdot F)\end{aligned}\quad (19.8.17)$$

and, writing them component-wise,

$$\begin{aligned}E_x &= -\partial_z F_y \\ E_y &= \partial_z F_x \\ E_z &= \partial_x F_y - \partial_y F_x \\ -jk\eta H_x &= k^2 F_x + \partial_x(\partial_x F_x + \partial_y F_y) \\ -jk\eta H_y &= k^2 F_y + \partial_y(\partial_x F_x + \partial_y F_y) \\ -jk\eta H_z &= \partial_z(\partial_x F_x + \partial_y F_y)\end{aligned}\quad (19.8.18)$$

where the components F_x, F_y are given by the definitions (19.8.8),

$$\begin{aligned}F_x(\mathbf{r}_\perp, z) &= 2 \int_{-\infty}^{\infty} E_y(\mathbf{r}'_\perp, 0) G(R) d^2 \mathbf{r}'_\perp \\ F_y(\mathbf{r}_\perp, z) &= -2 \int_{-\infty}^{\infty} E_x(\mathbf{r}'_\perp, 0) G(R) d^2 \mathbf{r}'_\perp \\ R &= \sqrt{|\mathbf{r}_\perp - \mathbf{r}'_\perp|^2 + z^2}\end{aligned}\quad (19.8.19)$$

Another set of useful relationships follows from the transverse part of Faraday's law, that is, $-jk\eta \mathbf{H}_\perp = \nabla_\perp E_z \times \hat{z} + \hat{z} \times \partial_z E_\perp$, or, $\hat{z} \times \partial_z E_\perp = -jk\eta \mathbf{H}_\perp - \nabla_\perp \times (\hat{z} E_z)$, and written in terms of F , after using the identity, $\nabla_\perp \times (\nabla_\perp \times F) = \nabla_\perp(\nabla_\perp \cdot F) - \nabla_\perp^2 F$,

$$\hat{z} \times \partial_z E_\perp = -jk\eta \mathbf{H}_\perp - \nabla_\perp \times (\hat{z} E_z) = k^2 F + \nabla_\perp(\nabla_\perp \cdot F) - \nabla_\perp \times (\nabla_\perp \times F), \quad \text{or,}$$

$$(k^2 + \nabla_\perp^2) F = \hat{z} \times \partial_z E_\perp = -jk\eta \mathbf{H}_\perp - \nabla_\perp E_z \times \hat{z}\quad (19.8.20)$$

$$\begin{aligned}(k^2 + \nabla_\perp^2) F_x &= -\partial_z E_y \\ (k^2 + \nabla_\perp^2) F_y &= \partial_z E_x\end{aligned}\quad (19.8.21)$$

where $\nabla_\perp^2 = \partial_x^2 + \partial_y^2$. An analogous set of relationships is obtained in terms of the magnetic vector potential A by applying a duality transformation to the above, that is, $E \rightarrow \mathbf{H}, \mathbf{H} \rightarrow -E, \eta \rightarrow \eta^{-1}$, and $F \rightarrow A$,

$$\begin{aligned}\mathbf{H} &= \nabla \times A \\ jk\eta^{-1} \mathbf{E} &= \nabla \times (\nabla \times A) = k^2 A + \nabla(\nabla \cdot A)\end{aligned}\quad (19.8.22)$$

or, separating transverse and longitudinal parts,

$$\begin{aligned}\mathbf{H}_\perp &= \hat{z} \times \partial_z A \\ \hat{z} H_z &= \nabla_\perp \times A \\ jk\eta^{-1} E_\perp &= k^2 A + \nabla_\perp(\nabla_\perp \cdot A) \\ jk\eta^{-1} \hat{z} E_z &= \hat{z} \partial_z(\nabla_\perp \cdot A)\end{aligned}\quad (19.8.23)$$

and, component-wise,

$$\begin{aligned}H_x &= -\partial_z A_y \\ H_y &= \partial_z A_x \\ H_z &= \partial_x A_y - \partial_y A_x \\ jk\eta^{-1} E_x &= k^2 A_x + \partial_x(\partial_x A_x + \partial_y A_y) \\ jk\eta^{-1} E_y &= k^2 A_y + \partial_y(\partial_x A_x + \partial_y A_y) \\ jk\eta^{-1} E_z &= \partial_z(\partial_x A_x + \partial_y A_y)\end{aligned}\quad (19.8.24)$$

with A_x, A_y given by the definitions (19.8.8),

$$\begin{aligned}A_x(\mathbf{r}_\perp, z) &= 2 \int_{-\infty}^{\infty} H_y(\mathbf{r}'_\perp, 0) G(R) d^2 \mathbf{r}'_\perp \\ A_y(\mathbf{r}_\perp, z) &= -2 \int_{-\infty}^{\infty} H_x(\mathbf{r}'_\perp, 0) G(R) d^2 \mathbf{r}'_\perp \\ R &= \sqrt{|\mathbf{r}_\perp - \mathbf{r}'_\perp|^2 + z^2}\end{aligned}\quad (19.8.25)$$

and, moreover,

$$(k^2 + \nabla_{\perp}^2) \mathbf{A} = \hat{\mathbf{z}} \times \partial_z \mathbf{H}_{\perp} = jk\eta^{-1} \mathbf{E}_{\perp} - \nabla_{\perp} H_z \times \hat{\mathbf{z}} \quad (19.8.26)$$

$$\begin{aligned} (k^2 + \nabla_{\perp}^2) A_x &= -\partial_z H_y \\ (k^2 + \nabla_{\perp}^2) A_y &= \partial_z H_x \end{aligned} \quad (19.8.27)$$

with (19.8.26) following from the transverse part of Ampère's law,

$$jk\eta^{-1} \mathbf{E}_{\perp} = \nabla_{\perp} \times (\hat{\mathbf{z}} H_z) + \hat{\mathbf{z}} \times \partial_z \mathbf{H}_{\perp} \Rightarrow \hat{\mathbf{z}} \times \partial_z \mathbf{H}_{\perp} = jk\eta^{-1} \mathbf{E}_{\perp} - \nabla_{\perp} \times (\hat{\mathbf{z}} H_z)$$

Equations (19.8.16)–(19.8.27) apply for $z > 0$. As we discussed in Sec. 19.1, for arbitrary $z \geq 0$ the fields might be different from the two sides of the $z = 0$ interface. In such cases, the definitions (19.8.8) of the electric and magnetic vector potentials must be modified to allow possibly different limiting values of the transverse fields at $z = 0^{\pm}$,

$$\begin{aligned} \mathbf{F}_{\pm}(\mathbf{r}_{\perp}, z) &= 2 \int_{-\infty}^{\infty} [\hat{\mathbf{z}} \times \mathbf{E}_{\perp}(\mathbf{r}'_{\perp}, 0^{\pm})] G(R) d^2 \mathbf{r}'_{\perp} \\ \mathbf{A}_{\pm}(\mathbf{r}_{\perp}, z) &= 2 \int_{-\infty}^{\infty} [\hat{\mathbf{z}} \times \mathbf{H}_{\perp}(\mathbf{r}'_{\perp}, 0^{\pm})] G(R) d^2 \mathbf{r}'_{\perp} \end{aligned} \quad (19.8.28)$$

Then, the Smythe formulas become, for $z \geq 0$,

$$\begin{aligned} \mathbf{E}_{\perp} &= \pm \hat{\mathbf{z}} \times \partial_z \mathbf{F}_{\pm} \\ \hat{\mathbf{z}} E_z &= \pm \nabla_{\perp} \times \mathbf{F}_{\pm} \\ -jk\eta \mathbf{H}_{\perp} &= \pm [k^2 \mathbf{F}_{\pm} + \nabla_{\perp} (\nabla_{\perp} \cdot \mathbf{F}_{\pm})] \\ -jk\eta \hat{\mathbf{z}} H_z &= \pm \hat{\mathbf{z}} \partial_z (\nabla_{\perp} \cdot \mathbf{F}_{\pm}) \end{aligned} \quad (19.8.29)$$

and,

$$\begin{aligned} \mathbf{H}_{\perp} &= \pm \hat{\mathbf{z}} \times \partial_z \mathbf{A}_{\pm} \\ \hat{\mathbf{z}} H_z &= \pm \nabla_{\perp} \times \mathbf{A}_{\pm} \\ jk\eta^{-1} \mathbf{E}_{\perp} &= \pm [k^2 \mathbf{A}_{\pm} + \nabla_{\perp} (\nabla_{\perp} \cdot \mathbf{A}_{\pm})] \\ jk\eta^{-1} \hat{\mathbf{z}} E_z &= \pm \hat{\mathbf{z}} \partial_z (\nabla_{\perp} \cdot \mathbf{A}_{\pm}) \end{aligned} \quad (19.8.30)$$

Let us explore these a bit further. If we assume that \mathbf{E}_{\perp} is continuous across the plane $z = 0$ (as would be the case for the *scattered fields* from planar conducting screens), that is, $\mathbf{E}_{\perp}(\mathbf{r}'_{\perp}, -0) = \mathbf{E}_{\perp}(\mathbf{r}'_{\perp}, +0)$, then, $\mathbf{F}_{+} = \mathbf{F}_{-}$, and \mathbf{F} becomes an even function of z , and Eq. (19.8.29) reads in this case,

$$\begin{aligned} \mathbf{E}_{\perp} &= \pm \hat{\mathbf{z}} \times \partial_z \mathbf{F} \\ \hat{\mathbf{z}} E_z &= \pm \nabla_{\perp} \times \mathbf{F} \\ -jk\eta \mathbf{H}_{\perp} &= \pm [k^2 \mathbf{F} + \nabla_{\perp} (\nabla_{\perp} \cdot \mathbf{F})] \\ -jk\eta \hat{\mathbf{z}} H_z &= \pm \hat{\mathbf{z}} \partial_z (\nabla_{\perp} \cdot \mathbf{F}) \end{aligned} \quad \text{for } z \geq 0 \quad (19.8.31)$$

Since the z -derivative of an even function is odd in z , it follows from Eq. (19.8.31) that $\mathbf{E}_{\perp}(\mathbf{r}_{\perp}, z)$ will be even in z , whereas $E_z(\mathbf{r}_{\perp}, z)$ will be odd, and similarly, $\mathbf{H}_{\perp}(\mathbf{r}_{\perp}, z)$ will be odd, while $H_z(\mathbf{r}_{\perp}, z)$ will be even.

But if \mathbf{H}_{\perp} is odd, then, $\mathbf{H}_{\perp}(\mathbf{r}'_{\perp}, -0) = -\mathbf{H}_{\perp}(\mathbf{r}'_{\perp}, +0)$, which implies that $\mathbf{A}_{-} = -\mathbf{A}_{+}$, and \mathbf{A} will be an odd function of z . Denoting \mathbf{A}_{+} simply by \mathbf{A} , we have $\mathbf{A}_{\pm} = \pm \mathbf{A}$, so that the \pm signs cancel out in Eq. (19.8.30), which can then be written as follows,

$$\begin{aligned} \mathbf{H}_{\perp} &= \hat{\mathbf{z}} \times \partial_z \mathbf{A} \\ \hat{\mathbf{z}} H_z &= \nabla_{\perp} \times \mathbf{A} \\ jk\eta^{-1} \mathbf{E}_{\perp} &= k^2 \mathbf{A} + \nabla_{\perp} (\nabla_{\perp} \cdot \mathbf{A}) \\ jk\eta^{-1} \hat{\mathbf{z}} E_z &= \hat{\mathbf{z}} \partial_z (\nabla_{\perp} \cdot \mathbf{A}) \end{aligned} \quad \text{for all } z \quad (19.8.32)$$

The derivation of Eqs. (19.8.31) and (19.8.32) was based on the assumption that the \mathbf{E}, \mathbf{H} fields satisfied the homogeneous Helmholtz equations and the Sommerfeld radiation condition in both half-spaces, $z \geq 0$. But if there are sources of fields in $z < 0$, but not in $z > 0$, then only the $z > 0$ part of these equations would hold.

The type of fields for which (19.8.31)–(19.8.32) hold for both half-spaces are those that are generated by sources lying on the $z = 0$ plane, such as the *scattered fields* from planar conducting screens that are generated by the induced currents on the conductors.

The implications of Eq. (19.8.31) and (19.8.32) for apertures in conducting screens is discussed next.

19.9 Apertures in Conducting Screens

Consider an electromagnetic field $\mathbf{E}^i, \mathbf{H}^i$ incident from $z < 0$ onto an infinitely thin perfectly conducting planar screen M in which an aperture A has been cut, as shown in Fig. 19.9.1. The metallic part M and the aperture A make up the whole $z = 0$ plane. In practice, a finite thickness and finite conductivity must be assumed for the conducting screen. However, this idealized version has served as a prototype for this sort of diffraction problem.

The total fields consist of the incident fields $\mathbf{E}^i, \mathbf{H}^i$ plus the scattered fields, say, $\mathbf{E}^s, \mathbf{H}^s$, generated by the induced surface currents on the conducting part, and radiated into the two half-spaces, $z \geq 0$,

$$\begin{aligned} \mathbf{E} &= \mathbf{E}^i + \mathbf{E}^s \\ \mathbf{H} &= \mathbf{H}^i + \mathbf{H}^s \end{aligned} \quad (19.9.1)$$

The fields must satisfy the boundary conditions that the total tangential electric field and total normal magnetic field be zero on the metallic part M , that is,

$$\begin{aligned} \hat{\mathbf{z}} \times \mathbf{E} &= \hat{\mathbf{z}} \times (\mathbf{E}^i + \mathbf{E}^s) = 0 \\ \hat{\mathbf{z}} \cdot \mathbf{H} &= \hat{\mathbf{z}} \cdot (\mathbf{H}^i + \mathbf{H}^s) = 0 \end{aligned} \quad \text{on } M \quad (19.9.2)$$

In addition, for the particular planar geometry under consideration, the scattered fields satisfy the following symmetry properties with respect to the $z = 0$ plane,

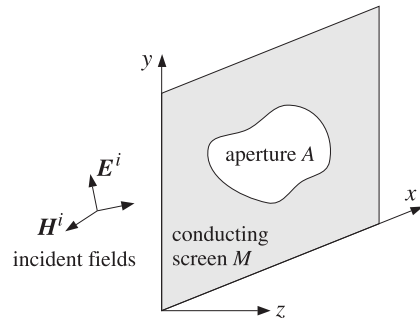


Fig. 19.9.1 Aperture in planar conducting screen.

$$\begin{matrix} E_x^s, E_y^s, H_z^s \text{ are even in } z \\ H_x^s, H_y^s, E_z^s \text{ are odd in } z \end{matrix} \quad (19.9.3)$$

Such conditions have been used invariably in all treatments of diffraction and scattering from such ideal planar conducting screens. They can be justified [41] by noting that the induced surface currents, causing the scattered fields, are constrained to flow on the infinitely thin conducting plane at $z = 0$ and have no z -component which would break the symmetry. The surface currents are free to radiate equally on both sides of the screen. See Ref. [1310] for a recent review of these symmetry properties.

The oddness of H_x^s, E_z^s together with their continuity across the aperture A implies that they must vanish on A . On the other hand, they must be discontinuous on the metallic part M . Thus, we have,

$$\begin{matrix} \hat{z} \times \mathbf{H}^s = 0 \\ \hat{z} \cdot \mathbf{E}^s = 0 \end{matrix} \quad \text{on } A \quad (19.9.4)$$

These imply that, on the aperture A , the corresponding components of the total field must remain equal to those of the incident fields, that is,

$$\begin{matrix} \hat{z} \times \mathbf{H} = \hat{z} \times \mathbf{H}^i \\ \hat{z} \cdot \mathbf{E} = \hat{z} \cdot \mathbf{E}^i \end{matrix} \quad \text{on } A \quad (19.9.5)$$

Because the scattered fields E^s, H^s satisfy the homogeneous Helmholtz equations on both sides $z \geq 0$ and the symmetry properties (19.9.3), it follows that Eqs. (19.8.31) and (19.8.32) will be applicable, that is, we have for $z \geq 0$,

$$\begin{matrix} \mathbf{E}^s = \pm \nabla \times \mathbf{F}^s \\ -jk\eta \mathbf{H}^s = \pm [k^2 \mathbf{F}^s + \nabla(\nabla_{\perp} \cdot \mathbf{F}^s)] \end{matrix} \quad \begin{matrix} \mathbf{H}^s = \nabla \times \mathbf{A}^s \\ jk\eta^{-1} \mathbf{E}^s = k^2 \mathbf{A}^s + \nabla(\nabla_{\perp} \cdot \mathbf{A}^s) \end{matrix} \quad (19.9.6)$$

where,

$$\begin{matrix} \mathbf{F}^s(\mathbf{r}_{\perp}, z) = 2 \int_{-\infty}^{\infty} [\hat{z} \times \mathbf{E}_{\perp}^s(\mathbf{r}'_{\perp}, 0)] G(R) d^2 \mathbf{r}'_{\perp} \\ \mathbf{A}^s(\mathbf{r}_{\perp}, z) = 2 \int_{-\infty}^{\infty} [\hat{z} \times \mathbf{H}_{\perp}^s(\mathbf{r}'_{\perp}, 0^+)] G(R) d^2 \mathbf{r}'_{\perp} \end{matrix} \quad R = \sqrt{|\mathbf{r}_{\perp} - \mathbf{r}'_{\perp}|^2 + z^2} \quad (19.9.7)$$

The left set is usually more convenient for dealing with small apertures in large screens, whereas the right set is more convenient for scattering from small planar conducting screens. Let us work with the left set first. Because $E_{\perp}^s = E_{\perp} - E_{\perp}^i$, we may split F^s into the sum,

$$\begin{matrix} \mathbf{F}^s = 2 \int_{-\infty}^{\infty} [\hat{z} \times (\mathbf{E}_{\perp} - \mathbf{E}_{\perp}^i)] G(R) d^2 \mathbf{r}'_{\perp} = \mathbf{F} - \mathbf{F}^i \\ \mathbf{F}(\mathbf{r}_{\perp}, z) = 2 \int_{-\infty}^{\infty} [\hat{z} \times \mathbf{E}_{\perp}(\mathbf{r}'_{\perp}, 0)] G(R) d^2 \mathbf{r}'_{\perp} \\ \mathbf{F}^i(\mathbf{r}_{\perp}, z) = 2 \int_{-\infty}^{\infty} [\hat{z} \times \mathbf{E}_{\perp}^i(\mathbf{r}'_{\perp}, 0)] G(R) d^2 \mathbf{r}'_{\perp} \end{matrix} \quad (19.9.8)$$

The integrations in (19.9.8) are over the entire $A+M$ plane at $z = 0$. However, the boundary conditions (19.9.2) require that $\hat{z} \times \mathbf{E}_{\perp} = 0$ on the conducting surface M , therefore, we may restrict the integration for the F -term to be over the aperture A only,

$$\mathbf{F}(\mathbf{r}_{\perp}, z) = 2 \int_A [\hat{z} \times \mathbf{E}_{\perp}(\mathbf{r}'_{\perp}, 0)] G(R) d^2 \mathbf{r}'_{\perp} \quad (19.9.9)$$

Replacing $F^s = F - F^i$ in Eq. (19.9.6) we obtain,

$$\begin{matrix} \mathbf{E} - \mathbf{E}^i = \mathbf{E}^s = \pm \nabla \times (\mathbf{F} - \mathbf{F}^i) \Rightarrow \mathbf{E} = \mathbf{E}^i \mp \nabla \times \mathbf{F}^i \pm \nabla \times \mathbf{F}, \text{ or,} \\ \mathbf{E} = \mathbf{E}^i \mp \mathbf{E}^r \pm \nabla \times \mathbf{F}, \text{ for } z \geq 0 \end{matrix} \quad (19.9.10)$$

where we defined $\mathbf{E}^r = \nabla \times \mathbf{F}^i$ for all $z \geq 0$. For $z > 0$, \mathbf{E}^r is equal to the incident field, $\mathbf{E}^r = \mathbf{E}^i$. Indeed, because we assumed that the sources generating the incident fields E^i, H^i are in the left half-space $z < 0$ and that there are no such sources in $z > 0$, it follows that \mathbf{E}^i would also satisfy (19.8.31), that is, $\mathbf{E}^i = \nabla \times \mathbf{F}^i$, but only for $z > 0$.

For $z < 0$, the field \mathbf{E}^r is the field that would be reflected from the conducting screen if that screen filled the entire $z = 0$ plane, as is depicted in Fig. 19.9.2.

This is most clearly seen by using the plane-wave spectrum representation for \mathbf{E}^i . The convolutional equation (19.9.8) defining \mathbf{F}^i can be written in the wavenumber domain in the following form, for all z ,

$$\begin{matrix} \mathbf{F}^i(\mathbf{r}_{\perp}, z) = 2 \int_{-\infty}^{\infty} [\hat{z} \times \mathbf{E}_{\perp}^i(\mathbf{r}'_{\perp}, 0)] G(R) d^2 \mathbf{r}'_{\perp} \\ = 2 \int_{-\infty}^{\infty} [\hat{z} \times \hat{\mathbf{E}}_{\perp}^i(\mathbf{k}_{\perp})] e^{-jk_z \cdot \mathbf{r}_{\perp}} \frac{e^{-jk_z |z|}}{2jk_z} \frac{d^2 \mathbf{k}_{\perp}}{(2\pi)^2} \end{matrix}$$

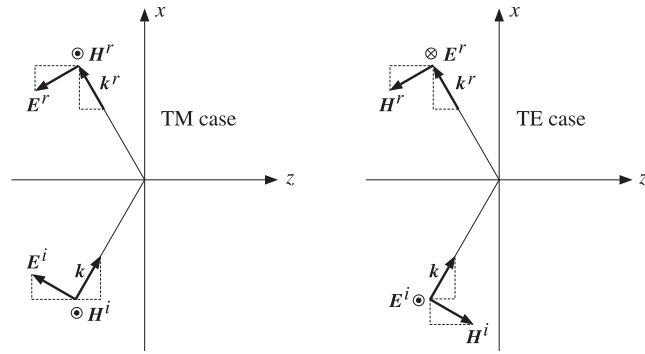


Fig. 19.9.2 Plane-wave components of incident and reflected waves.

where we used the Weyl representation for $G(R)$ given by Eq. (D.9) of Appendix D, which is valid for all $z \geq 0$. Replacing $|z| = \pm z$ when $z \geq 0$, we obtain the plane-wave spectrum representation of the field $E^r = \nabla \times F^i$,

$$\begin{aligned} E^r(\mathbf{r}_\perp, z) &= (\nabla_\perp + \hat{\mathbf{z}}\partial_z) \times \int_{-\infty}^{\infty} [\hat{\mathbf{z}} \times \hat{E}_\perp^i(\mathbf{k}_\perp)] e^{-jk_\perp \cdot \mathbf{r}_\perp} \frac{e^{\mp jk_z z}}{jk_z} \frac{d^2 \mathbf{k}_\perp}{(2\pi)^2} \\ &= - \int_{-\infty}^{\infty} \frac{(\mathbf{k}_\perp \pm \hat{\mathbf{z}}k_z) \times [\hat{\mathbf{z}} \times \hat{E}_\perp^i(\mathbf{k}_\perp)]}{k_z} e^{-jk_\perp \cdot \mathbf{r}_\perp} \frac{e^{\mp jk_z z}}{(2\pi)^2} d^2 \mathbf{k}_\perp \end{aligned}$$

where the gradient, $(\nabla_\perp + \hat{\mathbf{z}}\partial_z)$, was replaced by, $-j(\mathbf{k}_\perp \pm \hat{\mathbf{z}}k_z)$, when brought inside the integral. Using, $\mathbf{k}_\perp \cdot \hat{E}_\perp^i + k_z \hat{E}_z^i = 0$, and some vector identities, we obtain the 2-D Fourier transform of $E^r(\mathbf{r}_\perp, z)$,

$$\hat{E}^r(\mathbf{k}_\perp) = - \frac{(\mathbf{k}_\perp \pm \hat{\mathbf{z}}k_z) \times [\hat{\mathbf{z}} \times \hat{E}_\perp^i(\mathbf{k}_\perp)]}{k_z} = \pm \hat{E}_\perp^i + \hat{\mathbf{z}} \hat{E}_z^i$$

which shows that $E^r = -\hat{E}_\perp^i + \hat{\mathbf{z}} \hat{E}_z^i$, if $z < 0$, which is the reflected field, and $E^r = \hat{E}_\perp^i$ if $z > 0$. The reflected wavenumber $\mathbf{k}^r = \mathbf{k}_\perp - \hat{\mathbf{z}}k_z$ is depicted in Fig. 19.9.2. In conclusion, the total field of Eq. (19.9.10) is given by $E = E^i - E^r + \nabla \times F = \nabla \times F$, if $z > 0$, and by $E = E^i + E^r - \nabla \times F$, if $z < 0$,

$$E = \begin{cases} \nabla \times F, & \text{for } z > 0 \\ E^i + E^r - \nabla \times F, & \text{for } z < 0 \end{cases} \quad (19.9.11)$$

Defining the reflected magnetic field through, $-jk\eta H^r = \nabla \times E^r = \nabla \times (\nabla \times F^i)$, we again note that $H^r = H^i$ if $z > 0$. Thus, from (19.9.6) we find the total magnetic field,

$$H = \begin{cases} -\frac{1}{jk\eta} [k^2 F + \nabla(\nabla_\perp \cdot F)], & \text{for } z > 0 \\ H^i + H^r + \frac{1}{jk\eta} [k^2 F + \nabla(\nabla_\perp \cdot F)], & \text{for } z < 0 \end{cases} \quad (19.9.12)$$

The calculation of F from Eq. (19.9.9) requires knowledge of the transverse electric field components, $E_\perp(\mathbf{r}'_\perp, 0)$, on the aperture A , that is, for $\mathbf{r}'_\perp \in A$. These can be obtained, in principle, by enforcing the conditions (19.9.5). From Eqs. (19.9.11) and (19.9.12), we have $-jk\eta H_\perp = k^2 F + \nabla_\perp(\nabla_\perp \cdot F)$ and $E_z = \hat{\mathbf{z}} \cdot \nabla_\perp \times F$ for $z \geq 0$. Restricting these on A , and applying the conditions $H_\perp = H_\perp^i$ and $E_z = E_z^i$, we obtain the following integral equations for the unknowns $E_\perp(\mathbf{r}'_\perp, 0)$,

$$\boxed{\begin{aligned} k^2 F^0 + \nabla_\perp(\nabla_\perp \cdot F^0) &= -jk\eta H_\perp^i \\ \hat{\mathbf{z}} \cdot \nabla_\perp \times F^0 &= E_z^i \end{aligned}} \quad \text{on } A \quad (19.9.13)$$

where F^0 denotes the restriction of F on A , that is, with $R_0 = |\mathbf{r}_\perp - \mathbf{r}'_\perp|$, and $\mathbf{r}_\perp \in A$,

$$F^0(\mathbf{r}_\perp) = 2 \int_A [\hat{\mathbf{z}} \times E_\perp(\mathbf{r}'_\perp, 0)] G(R_0) d^2 \mathbf{r}'_\perp \quad (19.9.14)$$

Eqs. (19.9.13) read component-wise,

$$\boxed{\begin{aligned} k^2 F_x^0 + \partial_x(\partial_x F_x^0 + \partial_y F_y^0) &= -jk\eta H_x^i \\ k^2 F_y^0 + \partial_y(\partial_x F_x^0 + \partial_y F_y^0) &= -jk\eta H_y^i \\ \partial_x F_y^0 - \partial_y F_x^0 &= E_z^i \end{aligned}} \quad \text{on } A \quad (19.9.15)$$

An alternative set of integral equations is obtained from Eq. (19.8.20) by noting that on A , we have, $\hat{\mathbf{z}} \times \partial_z E_\perp = -jk\eta H_\perp - \nabla_\perp E_z \times \hat{\mathbf{z}} = -jk\eta H_\perp^i - \nabla_\perp E_z^i \times \hat{\mathbf{z}} = \hat{\mathbf{z}} \times \partial_z E_\perp^i$. Thus, Eqs. (19.9.13) can be replaced by,

$$\boxed{\begin{aligned} (k^2 + \nabla_\perp^2) F^0 &= \hat{\mathbf{z}} \times \partial_z E_\perp^i \\ \hat{\mathbf{z}} \cdot \nabla_\perp \times F^0 &= E_z^i \end{aligned}} \quad \text{on } A \quad (19.9.16)$$

In principle, Eqs. (19.9.9)–(19.9.16) provide a complete solution to the diffraction problem by an aperture, with all the boundary conditions properly taken into account.

By comparison, the *Kirchhoff approximation* consists of making the following approximation in the calculation of F in (19.9.9),

$$\begin{aligned} \hat{\mathbf{z}} \times E &= \hat{\mathbf{z}} \times E^i, & \text{on } A \\ \hat{\mathbf{z}} \times E &= 0, & \text{on } M \end{aligned} \quad (19.9.17)$$

This amounts to replacing F by F^i in (19.9.11) and (19.9.12) and, moreover, F^i is approximated by restricting its integration only to the aperture A . Thus, we have with $R = \sqrt{|\mathbf{r}_\perp - \mathbf{r}'_\perp|^2 + z^2}$, and $z \geq 0$,

$$\boxed{\begin{aligned} F^i &= 2 \int_A [\hat{\mathbf{z}} \times E_\perp^i(\mathbf{r}'_\perp, 0)] G(R) d^2 \mathbf{r}'_\perp \\ E &= \nabla \times F^i \\ -jk\eta H &= k^2 F^i + \nabla(\nabla_\perp \cdot F^i) \end{aligned}} \quad \text{(Kirchhoff approximation)} \quad (19.9.18)$$

The purpose of the integral equations (19.9.13) was to determine the correct boundary values of the transverse electric field, $\hat{\mathbf{z}} \times \mathbf{E}$, in the aperture A . The alternative procedure based on the magnetic potential A^s in Eq. (19.9.6) determines instead the correct values of the scattered transverse magnetic field, $\hat{\mathbf{z}} \times \mathbf{H}^s$, on the conducting surface M . Because $\hat{\mathbf{z}} \times \mathbf{H}^s = 0$ on the aperture A , the integral in the defining equation (19.9.7) for A^s can be restricted to be over the conductor M only, that is, with $R = \sqrt{|\mathbf{r}_\perp - \mathbf{r}'_\perp|^2 + z^2}$,

$$A^s(\mathbf{r}_\perp, z) = 2 \int_M [\hat{\mathbf{z}} \times \mathbf{H}_\perp^s(\mathbf{r}'_\perp, 0^+)] G(R) d^2\mathbf{r}'_\perp \quad (19.9.19)$$

The total fields are obtained from Eq. (19.9.6), for all $z \geq 0$,

$$\begin{aligned} \mathbf{H} &= \mathbf{H}^i + \mathbf{H}^s = \mathbf{H}^i + \nabla \times A^s \\ \mathbf{E} &= \mathbf{E}^i + \mathbf{E}^s = \mathbf{E}^i + \frac{\eta}{jk} [k^2 A^s + \nabla(\nabla_\perp \cdot A^s)] \end{aligned} \quad (19.9.20)$$

The boundary conditions (19.9.2) on the conductor M can be restated as,

$$\begin{aligned} \hat{\mathbf{z}} \times \mathbf{E}^s &= -\hat{\mathbf{z}} \times \mathbf{E}^i \\ \hat{\mathbf{z}} \cdot \mathbf{H}^s &= -\hat{\mathbf{z}} \cdot \mathbf{H}^i \end{aligned} \Rightarrow \begin{aligned} \mathbf{E}_\perp^s &= -\mathbf{E}_\perp^i \\ H_z^s &= -H_z^i \end{aligned} \quad \text{on } M \quad (19.9.21)$$

Restricting Eqs. (19.9.20) to the conductor surface M and using (19.9.21), we obtain the following integral equations for the unknowns $\hat{\mathbf{z}} \times \mathbf{H}_\perp^s$ on M ,

$$\begin{aligned} k^2 A^0 + \nabla_\perp(\nabla_\perp \cdot A^0) &= -jk\eta^{-1} \mathbf{E}_\perp^i \\ \hat{\mathbf{z}} \cdot \nabla_\perp \times A^0 &= -H_z^i \end{aligned} \quad \text{on } M \quad (19.9.22)$$

where A^0 denotes the restriction of A^s on M , that is, with $R_0 = |\mathbf{r}_\perp - \mathbf{r}'_\perp|$, and $\mathbf{r}_\perp \in M$,

$$A^0(\mathbf{r}_\perp) = 2 \int_M [\hat{\mathbf{z}} \times \mathbf{H}_\perp^s(\mathbf{r}'_\perp, 0^+)] G(R_0) d^2\mathbf{r}'_\perp \quad (19.9.23)$$

Component-wise, Eqs. (19.9.22) are,

$$\begin{aligned} k^2 A_x^0 + \partial_x(\partial_x A_x^0 + \partial_y A_y^0) &= -jk\eta^{-1} E_x^i \\ k^2 A_y^0 + \partial_y(\partial_x A_x^0 + \partial_y A_y^0) &= -jk\eta^{-1} E_y^i \\ \partial_x A_y^0 - \partial_y A_x^0 &= -H_z^i \end{aligned} \quad \text{on } M \quad (19.9.24)$$

An equivalent system of integral equations may be obtained by combining (19.9.22) with Maxwell's equations for \mathbf{E}^i on M , that is,

$$\begin{aligned} k^2 A^0 + \nabla_\perp(\nabla_\perp \cdot A^0) &= -jk\eta^{-1} \mathbf{E}_\perp^i = -\hat{\mathbf{z}} \times \partial_z \mathbf{H}_\perp^i - \nabla_\perp \times (\hat{\mathbf{z}} H_z^i) \\ &= -\hat{\mathbf{z}} \times \partial_z \mathbf{H}_\perp^i + \nabla_\perp \times (\nabla_\perp \times A^0) = -\hat{\mathbf{z}} \times \partial_z \mathbf{H}_\perp^i + \nabla_\perp(\nabla_\perp \cdot A^0) - \nabla_\perp^2 A^0 \end{aligned}$$

which leads to,

$$\begin{aligned} (k^2 + \nabla_\perp^2) A^0 &= -\hat{\mathbf{z}} \times \partial_z \mathbf{H}_\perp^i \\ \hat{\mathbf{z}} \cdot \nabla_\perp \times A^0 &= -H_z^i \end{aligned} \quad \text{on } M \quad (19.9.25)$$

Eqs. (19.9.19)–(19.9.25) provide an alternative procedure for solving the diffraction problem. Because it involves integral equations over the metal surface M , the procedure is convenient for dealing with scattering from small flat conducting objects over which the integrations are more manageable. By contrast, the procedure based on Eqs. (19.9.9)–(19.9.16) involves integral equations over the aperture A , and therefore, it is more appropriate for small apertures.

In the next two sections, we discuss two examples illustrating the above procedures. In Sec. 19.10, we revisit Sommerfeld's exact solution of the half-plane problem and derive it using the formalism of Eqs. (19.9.19)–(19.9.25). In Sec. 19.11, we discuss the Rayleigh-Bethe-Bouwkamp approximate solution of diffraction by small holes using the formalism of Eqs. (19.9.9)–(19.9.16).

With the exception of the Sommerfeld half-space problem and some of its relatives, the integral equations (19.9.13) or (19.9.22) can only be solved numerically. An incomplete set references on the original formulation of such integral equations, on their numerical solution, including Wiener-Hopf factorization methods, and on some applications is [1312–1372].

19.10 Sommerfeld's Half-Plane Problem Revisited

The Sommerfeld half-plane problem was discussed in Sec. 18.15. Here, we reconsider it by solving the integral equations (19.9.22) exactly using the plane-wave spectrum representation and Wiener-Hopf factorization methods.

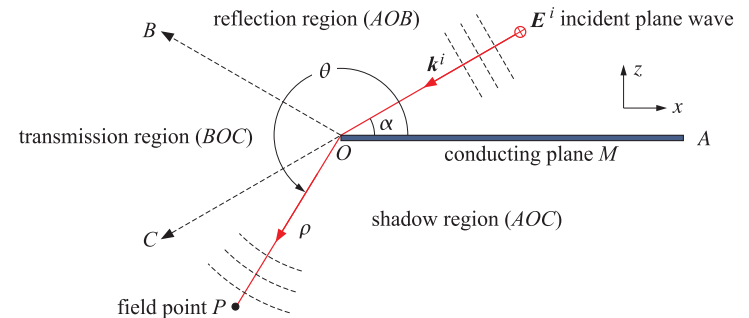


Fig. 19.10.1 Plane wave incident on conducting half-plane.

We discuss only the TE case, and to facilitate the comparison with Sec. 18.15, we make only minor changes in notation, interchanging y and z . The geometry is depicted in Fig. 19.10.1, where the conducting half-plane occupies the right-half ($x \geq 0$) of the xy plane.

A TE plane wave is incident from $z > 0$ onto the conducting plane at an angle α with respect to the x -axis, and we will assume that $0 \leq \alpha \leq 90^\circ$,

$$\begin{aligned} E^i &= \hat{y} E_y^i(x, z) = \hat{y} E_0 \exp(jk_x^i x + jk_z^i z) \\ k\eta H^i &= (\hat{x} k_z^i - \hat{z} k_x^i) E_0 \exp(jk_x^i x + jk_z^i z) \\ k_x^i &= k \cos \alpha, \quad k_z^i = k \sin \alpha \end{aligned} \tag{19.10.1}$$

Introducing polar coordinates, $x = \rho \cos \theta, z = \rho \sin \theta$, as shown in Fig. 19.10.1, the Sommerfeld solution from Sec. 18.15 is given by,

$$E_y = -E_0 \left[e^{jk\rho \cos \theta_r} D(v_r) - e^{jk\rho \cos \theta_i} D(v_i) \right] \tag{19.10.2}$$

where

$$\begin{aligned} \theta_i &= \theta - \alpha, \quad v_i = \sqrt{\frac{4k\rho}{\pi}} \cos \frac{\theta_i}{2} \\ \theta_r &= \theta + \alpha, \quad v_r = \sqrt{\frac{4k\rho}{\pi}} \cos \frac{\theta_r}{2} \end{aligned} \tag{19.10.3}$$

and $D(v)$ is the Fresnel diffraction coefficient, given in terms of the Fresnel integral $\mathcal{F}(v)$ of Appendix F,

$$D(v) = \frac{1}{1-j} \left[\frac{1-j}{2} + \mathcal{F}(v) \right] = \frac{1}{1-j} \int_{-\infty}^v e^{-j\pi u^2/2} du \tag{19.10.4}$$

The magnetic field is determined in terms of E_y from, $jk\eta \mathbf{H} = -\nabla \times \mathbf{E}$,

$$\begin{aligned} jk\eta H_x &= \frac{\partial E_y}{\partial z} = \sin \theta \frac{\partial E_y}{\partial \rho} + \cos \theta \frac{1}{\rho} \frac{\partial E_y}{\partial \theta} \\ -jk\eta H_z &= \frac{\partial E_y}{\partial x} = \cos \theta \frac{\partial E_y}{\partial \rho} - \sin \theta \frac{1}{\rho} \frac{\partial E_y}{\partial \theta} \end{aligned} \tag{19.10.5}$$

Using (19.10.2), we find,

$$\eta H_x = E_0 \sin \alpha \left[e^{jk\rho \cos \theta_r} D(v_r) + e^{jk\rho \cos \theta_i} D(v_i) \right] + E_0 F(\rho) \cos \frac{\theta}{2} \sin \frac{\alpha}{2} \tag{19.10.6}$$

$$\begin{aligned} \eta H_z &= E_0 \cos \alpha \left[e^{jk\rho \cos \theta_r} D(v_r) - e^{jk\rho \cos \theta_i} D(v_i) \right] + E_0 F(\rho) \sin \frac{\theta}{2} \sin \frac{\alpha}{2} \\ F(\rho) &= \sqrt{\frac{2}{\pi k\rho}} e^{-jk\rho - j\frac{\pi}{4}} \end{aligned} \tag{19.10.7}$$

The corresponding scattered fields are, $E^s = \mathbf{E} - E^i, \mathbf{H}^s = \mathbf{H} - \mathbf{H}^i$. Noting that $k_x^i x + k_z^i z = k\rho \cos \theta_i$, and using the identity, $D(-v) = 1 - D(v)$, we find,

$$\begin{aligned} E_y^s &= -E_0 \left[e^{jk\rho \cos \theta_r} D(v_r) + e^{jk\rho \cos \theta_i} D(-v_i) \right] \\ \eta H_x^s &= E_0 \sin \alpha \left[e^{jk\rho \cos \theta_r} D(v_r) - e^{jk\rho \cos \theta_i} D(-v_i) \right] + E_0 F(\rho) \cos \frac{\theta}{2} \sin \frac{\alpha}{2} \\ \eta H_z^s &= E_0 \cos \alpha \left[e^{jk\rho \cos \theta_r} D(v_r) + e^{jk\rho \cos \theta_i} D(-v_i) \right] + E_0 F(\rho) \sin \frac{\theta}{2} \sin \frac{\alpha}{2} \end{aligned} \tag{19.10.8}$$

We may verify explicitly the symmetry properties (19.9.3) and boundary conditions (19.9.21). The replacement $z \rightarrow -z$ amounts to the following substitutions,

$$\begin{aligned} \theta &\rightarrow 2\pi - \theta, & \cos \frac{\theta}{2} &\rightarrow -\cos \frac{\theta}{2}, & \sin \frac{\theta}{2} &\rightarrow \sin \frac{\theta}{2} \\ \theta_i &\rightarrow 2\pi - \theta_r, & v_i &\rightarrow -v_r, & \cos \theta_i &\rightarrow \cos \theta_r \\ \theta_r &\rightarrow 2\pi - \theta_i, & v_r &\rightarrow -v_i, & \cos \theta_r &\rightarrow \cos \theta_i \end{aligned} \tag{19.10.9}$$

It follows then by inspection of Eqs. (19.10.8) that E_y^s, H_z^s are even in z , and H_x^s is odd. Similarly, we can verify that on the conducting surface, $\theta = 0$ or $\theta = 2\pi$, we have $E_y^s = -E_y^i$ and $H_z^s = -H_z^i$. We note also that H_x^s vanishes on the aperture, that is, at $z = 0$ and $x < 0$, or, $\theta = \pi$.

Next, we carry out the procedure based on the integral equations (19.9.22). We assume that there is no dependence on the y coordinate and that the only non-zero field components are E_y, H_x, H_z . It follows that,

$$\hat{z} \times \mathbf{H}_\perp^s = \hat{z} \times \hat{x} H_x^s = \hat{y} H_x^s$$

and therefore, the vector potential $A^s(x, z)$ defined in (19.9.19) will have only a y -component, say, $A_y^s(x, z)$, given by,

$$A_y^s(x, z) = 2 \int_0^\infty H_x^s(x', 0) G(R) dx' dy', \quad R = \sqrt{(x-x')^2 + (y-y')^2 + z^2}$$

where the integration is only over the metal part, $x \geq 0$, and $H_x^s(x', 0)$ denotes the value of the scattered field $H_x^s(x', z')$ on the transmitted side, $z' = 0^-$.

Integrating out the y dependence using Eq. (19.4.1), we may rewrite A_y^s in terms of the 2-D Green's function, $G_2(x, z) = -\frac{j}{4} H_0^{(2)}(k\sqrt{x^2 + z^2})$,

$$A_y^s(x, z) = 2 \int_0^\infty H_x^s(x', 0) G_2(x-x', z) dx' \tag{19.10.10}$$

$$A_y^s(x, 0) = 2 \int_0^\infty H_x^s(x', 0) G_2(x-x', 0) dx'$$

The integral equation (19.9.22) has only a y -component, and because there is no y -dependence (i.e., all y -derivatives are zero), it reads simply,

$$k^2 A_y(x, 0) = -jk\eta^{-1} E_y^i(x, 0), \quad \text{for } x \geq 0$$

which can be rearranged as, $jk\eta A_y^s(x, 0) = E_y^i(x, 0)$, and more explicitly,

$$2jk\eta \int_0^\infty H_x^s(x', 0) G_2(x-x', 0) dx' = E_0 e^{jk_x^i x} \quad \text{for } x \geq 0 \tag{19.10.11}$$

Because of the restriction, $x \geq 0$, this is an convolutional integral equation of the Wiener-Hopf type and cannot be solved by simply taking Fourier transforms of both sides—it can be solved by spectral factorization methods.

The second of Eqs. (19.9.22) is automatically satisfied by virtue of Maxwell's equations for E^i, H^i . We have, $\partial_x E_y^i(x, 0) = jk_x^i E_y^i(x, 0) = -jk\eta H_z^i(x, 0)$, which implies that, $\partial_x A_y^s(x, 0) = -H_z^i(x, 0)$, as required by (19.9.22).

Once the $H_x^s(x, 0)$ is found, it determines $A_y^s(x, z)$ for all z . Then, the scattered and total electric fields can be found for all x, z from (19.9.20), remembering that $\partial_y = 0$,

$$E_y^s(x, z) = -jk\eta A_y^s(x, z) \tag{19.10.12}$$

$$E_y(x, z) = E_y^i(x, z) + E_y^s(x, z) = E_0 e^{jk_x x + jk_z z} - jk\eta A_y^s(x, z)$$

The integral equation condition (19.10.11) is equivalent to the vanishing of the tangential E -field on the conducting surface, that is, $E_y(x, 0)$ is a *left-sided* function, satisfying, $E_y(x, 0) = 0$, for $x \geq 0$.

The function $H_x^s(x', 0)$ is *right-sided* because it must vanish on the aperture side, $x' < 0$. Thus, the integration in (19.10.10) can be extended to the entire real-axis, and we may use the plane-wave spectrum representation (19.4.3) of G_2 to write A_y^s as a Fourier integral, involving the as yet unknown Fourier transform $\hat{H}_x^s(k_x)$ of $H_x^s(x', 0)$,

$$A_y^s(x, z) = 2 \int_{-\infty}^{\infty} H_x^s(x', 0) G_2(x - x', z) dx' = 2 \int_{-\infty}^{\infty} \frac{\hat{H}_x^s(k_x)}{2jk_z} e^{-jk_x x - jk_z |z|} \frac{dk_x}{2\pi}$$

$$A_y^s(x, z) = \int_{-\infty}^{\infty} \hat{A}_y^s(k_x) e^{-jk_x x - jk_z |z|} \frac{dk_x}{2\pi}$$

$$A_y^s(x, 0) = \int_{-\infty}^{\infty} \hat{A}_y^s(k_x) e^{-jk_x x} \frac{dk_x}{2\pi} \tag{19.10.13}$$

$$\hat{A}_y^s(k_x) = \frac{\hat{H}_x^s(k_x)}{jk_z}$$

Setting $z = 0$ in (19.10.12) and taking Fourier transforms of both sides, and using (19.10.13), we have,

$$E_y(x, 0) = E_y^i(x, 0) - jk\eta A_y^s(x, 0) \tag{19.10.14}$$

$$\hat{E}_y(k_x) = \hat{E}_y^i(k_x) - k\eta \frac{\hat{H}_x^s(k_x)}{k_z}$$

The Fourier transform of the input plane wave is,

$$\hat{E}_y^i(k_x) = \int_{-\infty}^{\infty} E_0 e^{jk_x x} e^{jk_x^i x} dx = 2\pi E_0 \delta(k_x + k_x^i) \tag{19.10.15}$$

Our objective is to solve (19.10.14) for $\hat{H}_x^s(k_x)$. So far we know that $E_y(x, 0)$ is a left-sided function, but its Fourier transform $\hat{E}_y(k_x)$ is unknown, and we also know that $\hat{H}_x^s(k_x)$ is the Fourier transform of a right-sided function. This information is enough to solve (19.10.14).

Before delving into the solution, let us consider the analyticity properties of the Fourier transforms of right-sided and left-sided functions. Given a right-sided function $f(x)$, that is, one that has support only for $x \geq 0$ and vanishes for all $x < 0$, its Fourier transform and its inverse will be denoted by,

$$F_+(k_x) = \int_0^{\infty} f(x) e^{jk_x x} dx \Rightarrow f(x) = \int_{-\infty}^{\infty} F_+(k_x) e^{-jk_x x} \frac{dk_x}{2\pi} \tag{19.10.16}$$

Let us assume that $f(x)$ decays exponentially like $e^{-\epsilon x}$ for large positive x . Then, it is straightforward to see that $F_+(k_x)$ can be analytically continued in the complex k_x -plane to the region, $\text{Im}(k_x) > -\epsilon$. We will refer to this as the *upper-half plane* (UHP). We have for large $x > 0$,

$$f(x) e^{jk_x x} \rightarrow e^{-\epsilon x} e^{j[\text{Re}(k_x) + j\text{Im}(k_x)]x} = e^{j\text{Re}(k_x)x} e^{-[\text{Im}(k_x) + \epsilon]x}$$

which converges to zero if $\text{Im}(k_x) > -\epsilon$, rendering the integral $F_+(k_x)$ convergent. Conversely, the analyticity of $F_+(k_x)$ implies that $f(x)$ will be a right-sided function, so that, $f(x) = 0$ for $x < 0$. To see this, take $x < 0$ and replace the real-axis integration contour by a closed contour C consisting of the real axis and an infinite upper semi-circle,

$$f(x) = \int_{-\infty}^{\infty} F_+(k_x) e^{-jk_x x} \frac{dk_x}{2\pi} = \oint_C F_+(k_x) e^{-jk_x x} \frac{dk_x}{2\pi}$$

Since $F_+(k_x)$ is analytic in the upper-half plane, the above contour integral will be zero. The contribution of the infinite semi-circle is zero for $x < 0$. Indeed, let $k_x = R e^{j\beta}$ be a point on that upper circle, so that $0 < \beta < \pi$, then, since $\sin \beta \geq 0$ and $x < 0$,

$$e^{-jk_x x} = e^{-j(R \cos \beta + jR \sin \beta)x} = e^{-jRx \cos \beta} e^{-R|x| \sin \beta} \rightarrow 0, \text{ as } R \rightarrow \infty$$

Similarly, a *left-sided* function $f(x)$, i.e., one that vanishes for $x > 0$ and converges exponentially to zero like $e^{-\epsilon|x|}$ for $x < 0$, will have a Fourier transform that is regular in the *lower-half plane* (LHP), $\text{Im}(k_x) < \epsilon$,

$$F_-(k_x) = \int_0^{\infty} f(x) e^{jk_x x} dx \Rightarrow f(x) = \int_{-\infty}^{\infty} F_-(k_x) e^{-jk_x x} \frac{dk_x}{2\pi} \tag{19.10.17}$$

More generally, the Fourier transform of a double-sided function that decays exponentially like $e^{-\epsilon|x|}$, can be split into the sum of its right-sided/UHP part and its left-sided/LHP part,

$$F(k_x) = \int_{-\infty}^{\infty} f(x) e^{jk_x x} dx = \underbrace{\int_0^{\infty} f(x) e^{jk_x x} dx}_{\text{upper}} + \underbrace{\int_{-\infty}^0 f(x) e^{jk_x x} dx}_{\text{lower}} = F_+(k_x) + F_-(k_x) \tag{19.10.18}$$

where $F(k_x)$ will now be analytic in the strip, $-\epsilon < \text{Im}(k_x) < \epsilon$. The integration contour of the inverse Fourier transform can be taken to be any line parallel to the real-axis as long as it lies in that strip, for example, with, $-\epsilon < a < \epsilon$, we have,

$$f(x) = \int_{-\infty + ja}^{+\infty + ja} F(k_x) e^{-jk_x x} \frac{dk_x}{2\pi} \tag{19.10.19}$$

The assumed exponential decay may be justified on physical grounds by allowing a small amount of loss in the propagation medium, which effectively means that the wavenumber k will acquire a small negative imaginary part, that is, replacing, $k \rightarrow k - j\epsilon$.

The wavenumber $k_z = \sqrt{k^2 - k_x^2}$ is defined in terms of the evanescent square-root for real-valued k_x . But for complex k_x , it must be defined by the square root branch such that $k_z = k$ when $k_x = 0$. When a small loss is introduced, we have, $k_z = \sqrt{(k - j\epsilon)^2 - k_x^2}$.

The factors in k_z have the following upper/lower half-plane analyticity properties and provide an example of *spectral factorization*,

$$k_z = \sqrt{(k - j\epsilon)^2 - k_x^2} = \underbrace{\sqrt{k - j\epsilon + k_x}}_{\text{lower-half plane}} \cdot \underbrace{\sqrt{k - j\epsilon - k_x}}_{\text{upper-half plane}} \quad (19.10.20)$$

We now turn to the solution of (19.10.14). Since $H_x^s(x, 0)$ is right-sided its Fourier transform, $\hat{H}_x^s(k_x)$ will be analytic in the upper-half plane, and since $E_y(x, 0)$ is left-sided, its Fourier transform, $\hat{E}_y(k_x)$, will be analytic in the lower-half plane. Thus, assuming for a moment a more general incident field, the various terms in (19.10.14) will have the following analyticity properties,

$$\underbrace{\hat{E}_y(k_x)}_{\text{lower}} = \underbrace{\hat{E}_y^i(k_x)}_{\text{strip}} - k\eta \underbrace{\frac{\hat{H}_x^s(k_x)}{k_z}}_{\text{strip}} \quad (19.10.21)$$

Replacing k_z by the factorization (19.10.20), $k_z = \sqrt{k - k_x} \sqrt{k + k_x}$, and multiplying both sides by the LHP factor $\sqrt{k + k_x}$, we have,

$$\underbrace{\sqrt{k + k_x} \hat{E}_y(k_x)}_{\text{lower}} = \underbrace{\sqrt{k + k_x} \hat{E}_y^i(k_x)}_{\text{strip}} - k\eta \underbrace{\frac{\hat{H}_x^s(k_x)}{\sqrt{k - k_x}}}_{\text{upper}}$$

Splitting the term, $\sqrt{k + k_x} \hat{E}_y^i(k_x)$ into its UHP and LHP parts as in (19.10.18), and moving the LHP part to the left side, we obtain,

$$\underbrace{\sqrt{k + k_x} \hat{E}_y(k_x)}_{\text{lower}} - \underbrace{\left[\sqrt{k + k_x} \hat{E}_y^i(k_x) \right]_{-}}_{\text{lower}} = \underbrace{\left[\sqrt{k + k_x} \hat{E}_y^i(k_x) \right]_{+}}_{\text{upper}} - k\eta \underbrace{\frac{\hat{H}_x^s(k_x)}{\sqrt{k - k_x}}}_{\text{upper}} \quad (19.10.22)$$

This difference is simultaneously analytic in the upper and lower half planes, that is, in the entire complex plane, and one may argue that it must be identically zero. See [1316,1367] for a more precise justification, and [1371] for a more physical explanation based on the edge behavior of the fields as $x \rightarrow 0$ at $z = 0$. Thus, we obtain,

$$\begin{aligned} k\eta \frac{\hat{H}_x^s(k_x)}{\sqrt{k - k_x}} - \left[\sqrt{k + k_x} \hat{E}_y^i(k_x) \right]_{+} &= 0 \\ \sqrt{k + k_x} \hat{E}_y(k_x) - \left[\sqrt{k + k_x} \hat{E}_y^i(k_x) \right]_{-} &= 0 \end{aligned}$$

The solution for $\hat{H}_x^s(k_x)$, is then,

$$\boxed{k\eta \hat{H}_x^s(k_x) = \sqrt{k - k_x} \left[\sqrt{k + k_x} \hat{E}_y^i(k_x) \right]_{+}} \quad (19.10.23)$$

The solution for $\hat{E}_y(k_x)$ is given by (19.10.21) with the found $\hat{H}_x^s(k_x)$. If we were to ignore the right-sidedness instruction $[]_{+}$, the solution would be, $k\eta \hat{H}_x^s(k_x) = \sqrt{k - k_x} \sqrt{k + k_x} \hat{E}_y^i(k_x) =$

$k_z \hat{E}_y^i(k_x)$, and would correspond to the solution of the integral equation (19.10.11) if that were valid for all x , not just $x > 0$.

For the particular incident plane wave case, we have,

$$\sqrt{k + k_x} \hat{E}_y^i(k_x) = 2\pi E_0 \sqrt{k + k_x} \delta(k_x + k_x^i) = 2\pi E_0 \sqrt{k - k_x^i} \delta(k_x + k_x^i)$$

where we replaced $k_x = -k_x^i$ inside the square root as forced by the delta function. Inverting this Fourier transform and resumming its right-sided part, we obtain,

$$\left[\sqrt{k + k_x} \hat{E}_y^i(k_x) \right]_{+} = E_0 \sqrt{k - k_x^i} \int_0^{\infty} e^{j(k_x + k_x^i)x} dx = -\frac{E_0 \sqrt{k - k_x^i}}{j(k_x + k_x^i)} \quad (19.10.24)$$

In performing this integral, we replaced, $k - k - j\epsilon$, so that $k_x^i = k \cos \alpha$ also acquires a small imaginary part, being replaced by $(k - j\epsilon) \cos \alpha = k \cos \alpha - j\epsilon \cos \alpha$, where, $\epsilon \cos \alpha = \epsilon \cos \alpha$. Here, $\epsilon \cos \alpha > 0$, since we assumed $0 \leq \alpha \leq \pi/2$. It follows that with $x > 0$, the exponential in (19.10.24) will converge to zero for, $\text{Im}(k_x) > \epsilon \cos \alpha$,

$$e^{j(k_x + k_x^i)x} = e^{j[\text{Re}(k_x) + k \cos \alpha]x} e^{-[\text{Im}(k_x) - \epsilon \cos \alpha]x} \rightarrow 0, \quad \text{as } x \rightarrow \infty$$

Inserting (19.10.24) into (19.10.23), we find,

$$\boxed{k\eta \hat{H}_x^s(k_x) = -\frac{E_0 \sqrt{k - k_x^i} \sqrt{k - k_x}}{j(k_x + k_x^i)}} \quad \text{for } \text{Im}(k_x) > \epsilon \cos \alpha \quad (19.10.25)$$

Recalling (19.10.13) and dividing by jk_z , this also gives the Fourier transform, $\hat{A}_y^s(k_x)$, of the vector potential $A_y^s(x, 0)$. Because $1/k_z$ is analytic in the strip, $-\epsilon < \text{Im}(k_x) < \epsilon$, the resulting Fourier transform will be analytic in the intersection of the two regions $-\epsilon < \text{Im}(k_x) < \epsilon$ and $\text{Im}(k_x) > \epsilon \cos \alpha$, that is, $\epsilon \cos \alpha < \text{Im}(k_x) < \epsilon$,

$$k\eta \hat{A}_y^s(k_x) = \frac{k\eta \hat{H}_x^s(k_x)}{jk_z} = \frac{k\eta \hat{H}_x^s(k_x)}{j\sqrt{k - k_x} \sqrt{k + k_x}} = \frac{E_0 \sqrt{k - k_x^i}}{\sqrt{k + k_x} (k_x + k_x^i)}$$

Thus, the Fourier transform of the scattered field $E_y^s(x, 0)$ will be,

$$\boxed{\hat{E}_y^s(k_x) = -jk\eta \hat{A}_y^s(k_x) = \frac{E_0 \sqrt{k - k_x^i}}{j\sqrt{k + k_x} (k_x + k_x^i)}} \quad \text{for } \epsilon \cos \alpha < \text{Im}(k_x) < \epsilon \quad (19.10.26)$$

From the plane-wave spectrum representation, the Fourier transform of $E_y^s(x, z)$ will be, $\hat{E}_y^s(k_x) e^{-jk_z|z|}$. Therefore, $E_y^s(x, z)$ will be given by the corresponding inverse Fourier transform, whose integration contour can be any horizontal line that lies in the analyticity strip, $\epsilon \cos \alpha < \text{Im}(k_x) < \epsilon$,

$$\boxed{E_y^s(x, z) = \frac{1}{2\pi j} \int_{C_a} \frac{E_0 \sqrt{k - k_x^i}}{\sqrt{k + k_x} (k_x + k_x^i)} e^{-jk_x x - jk_z |z|} dk_x} \quad (19.10.27)$$

where C_a is the horizontal line running from $(-\infty + ja)$ to $(+\infty + ja)$, where $\epsilon_\alpha < a < \epsilon$, as depicted by the red line in Fig. 19.10.2. It follows that total electric field will be, $E_y(x, z) = E_y^i(x, z) + E_y^s(x, z)$, or,

$$E_y(x, z) = E_0 e^{jk_x^i x + jk_z^i z} + \frac{1}{2\pi j} \int_{C_a} \frac{E_0 \sqrt{k - k_x^i}}{\sqrt{k + k_x} (k_x + k_x^i)} e^{-jk_x x - jk_z |z|} dk_x \quad (19.10.28)$$

We note that C_a runs below the branch point at $k_x = -k + j\epsilon$, and above the pole at $k_x = -k_x^i + j\epsilon_\alpha$, and above the branch point at $k_x = k - j\epsilon$. In the limit $\epsilon \rightarrow 0^+$, the contour becomes the horizontal k_x axis, but dented as shown in the bottom half of Fig. 19.10.2.

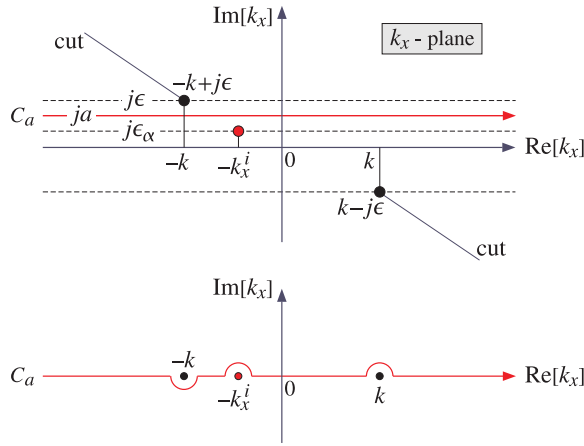


Fig. 19.10.2 Integration contour C_a on k_x -plane, and its limit as $\epsilon \rightarrow 0^+$.

Eqs. (19.10.27) and (19.10.28) provide an exact solution to the Sommerfeld half-plane problem. We discuss next how this solution can be transformed into the form of Eq. (19.10.2) or (19.10.8).

As shown in Fig. 19.10.3, the observation angle θ traces three possible regions: reflection, transmission, and shadow. For each value of θ , the contour C_a will be deformed into the following contour on the k_x -plane, defined parametrically for, $-\infty < t < \infty$,

$$k_x = k \cos(\theta + jt) = k \cos \theta \cosh t - jk \sin \theta \sinh t \quad (19.10.29)$$

This represents a hyperbola on the k_x -plane because as follows from (19.10.29),

$$\left(\frac{\text{Re}(k_x)}{k \cos \theta}\right)^2 - \left(\frac{\text{Im}(k_x)}{k \sin \theta}\right)^2 = 1$$

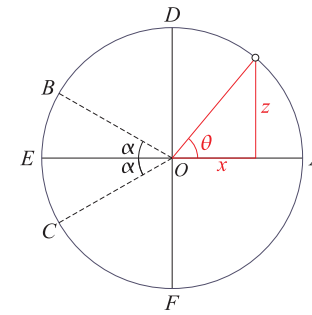


Fig. 19.10.3 Reflection (AB), transmission (BC), and shadow (CA) regions.

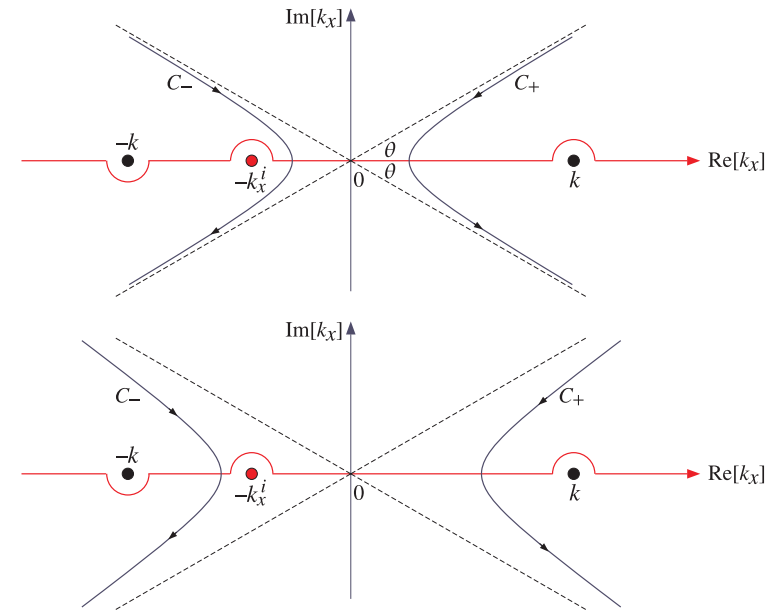


Fig. 19.10.4 Transformed contours for the cases, $|\theta - \pi| > \alpha$ (top), and, $|\theta - \pi| < \alpha$ (bottom).

The asymptotes of the hyperbola are the two straight lines with slopes $\pm \tan \theta$, as determined by the limits,

$$\frac{\text{Im}(k_x)}{\text{Re}(k_x)} = \tan \theta \tanh t \rightarrow \pm \tan \theta, \quad \text{as } t \rightarrow \pm \infty$$

The apex of the hyperbola is at the point, $k_x = k \cos \theta$, corresponding to $t = 0$. Depending on the sign of $\cos \theta$, the hyperbola actually has two branches denoted by C_\pm and depicted in Fig. 19.10.4, corresponding to the two cases, $\cos \theta \gtrless 0$, or, equivalently

to the two angle ranges (FAD) and (DEF) of Fig. 19.10.3,

$$-\frac{3\pi}{2} \leq \theta \leq \frac{\pi}{2} \quad \text{and} \quad \frac{\pi}{2} \leq \theta \leq \frac{3\pi}{2}$$

In particular, we note that over the shadow region, $\pi - \alpha \leq \theta \leq \pi + \alpha$, the value of $\cos \theta$ is negative but has magnitude, $|\cos \theta| > \cos \alpha$, and therefore, the apex of the C_- hyperbola lies to the left of the pole at $k_x = -k_x^i$, whereas for the other values of θ in the (DEF) range, it lies to the right of the pole.

To transform the integral (19.10.27), we form a closed contour consisting of the C_a axis, one of the hyperbolic contours C_{\pm} , and upper and lower arcs at infinite radial distances. The contribution of such arcs can be argued to be zero provided one closes C_+ as shown in Fig. 19.10.5, and C_- as in Fig. 19.10.6.

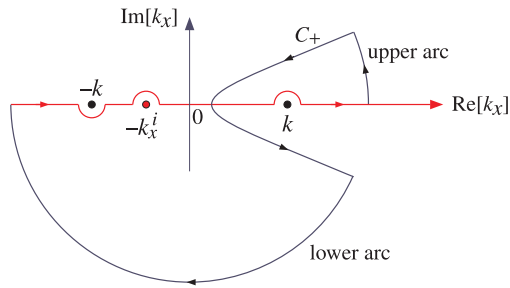


Fig. 19.10.5 Right contour C_+ for the cases, $\frac{\pi}{2} \leq |\theta - \pi| \leq \pi$.

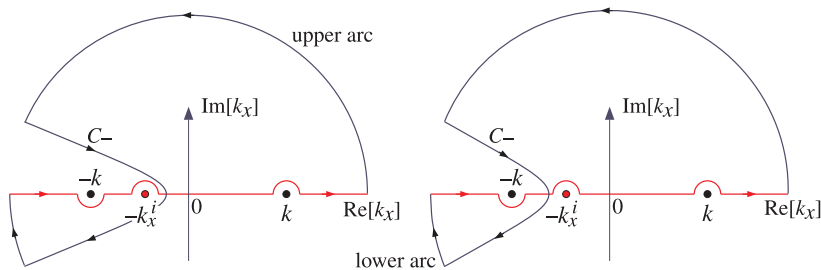


Fig. 19.10.6 Left contour C_- for, $\alpha \leq |\theta - \pi| < \frac{\pi}{2}$ (left), and, $|\theta - \pi| \leq \alpha$ (right).

The integral (19.10.27) can then be calculated as,

$$E_y^s = \frac{1}{2\pi j} \int_{C_a} = \frac{1}{2\pi j} \oint_{C_a+C_{\pm}+\text{arcs}} - \frac{1}{2\pi j} \int_{C_{\pm}} = -R + I \quad (19.10.30)$$

where I represents the integral over C_{\pm} (it is the same for either branch),

$$I = -\frac{1}{2\pi j} \int_{C_{\pm}} \frac{E_0 \sqrt{k - k_x^i}}{\sqrt{k + k_x} (k_x + k_x^i)} e^{-jk_x x - jk_z |z|} dk_x \quad (19.10.31)$$

and R represents the contribution of the closed contour, that is, $-R$ is the residue of the pole at $k_x = -k_x^i$, if the pole is enclosed[†], while R is zero if the pole is not enclosed. That residue, if it is non-zero, is calculated very simply as,

$$R = \frac{E_0 \sqrt{k - k_x^i}}{\sqrt{k + k_x}} e^{-jk_x x - jk_z |z|} \Big|_{k_x = -k_x^i} = E_0 e^{jk_x^i x - jk_z^i |z|} \quad (19.10.32)$$

Let us introduce the simplified notation, for the incident and reflected fields,

$$E^i = E_0 e^{jk_x x + jk_z z} = E_0 e^{jk\rho \cos \theta_i} \quad (19.10.33)$$

$$E^r = E_0 e^{jk_x x - jk_z z} = E_0 e^{jk\rho \cos \theta_r}$$

In this notation, R takes on the following values in the three angle ranges,

$$R = \begin{cases} E^r, & \text{reflection, } 0 \leq \theta \leq \pi - \alpha \\ 0, & \text{transmission, } \pi - \alpha \leq \theta \leq \pi + \alpha \\ E^i, & \text{shadow, } \pi + \alpha \leq \theta \leq 2\pi \end{cases} \quad (19.10.34)$$

Moreover, E_y^s of (19.10.8) can be expressed more simply as,

$$E_y^s = - [E^r D(v_r) + E^i D(-v_i)] \quad (19.10.35)$$

In the evaluation of the contour integral I , we must decide how to define k_z in the exponential. Since, $k_z^2 = k^2 - k_x^2$ and $k_x = k \cos(\theta + jt)$, we have, $k_z = \pm k \sin(\theta + jt)$. The proper sign of the square root must be decided by analytic continuation so that $k_z = k$ when $k_x = 0$. When $z > 0$, or, $0 \leq \theta \leq \pi$, we must choose $k_z = k \sin(\theta + jt)$, because k_x vanishes when $\theta = \pi/2$ and $t = 0$. On the other hand, when $z < 0$, or, $\pi \leq \theta \leq 2\pi$, we must choose $k_z = -k \sin(\theta + jt)$, because now k_x vanishes when $\theta = 3\pi/2$ and $t = 0$. In summary, we must choose, $k_z = \text{sign}(z) \cdot k \sin(\theta + jt)$. Then, regardless of the sign of z , the exponent becomes,

$$k_x x + k_z |z| = k \cos(\theta + jt) \rho \cos \theta + k \sin(\theta + jt) \rho \sin \theta = k\rho \cosh t$$

where we replaced, $\text{sign}(z) \cdot |z| = z$, and used cylindrical coordinates for x, z . The various factors in the integrand of I can be replaced now by,

$$dk_x = -jk \sin(\theta + jt) dt = -2jk \sin\left(\frac{\theta + jt}{2}\right) \cos\left(\frac{\theta + jt}{2}\right) dt$$

$$e^{-jk_x x - jk_z |z|} = e^{-jk\rho \cosh t}$$

$$\sqrt{k - k_x^i} = \sqrt{2k} \sin \frac{\alpha}{2}$$

$$\sqrt{k + k_x} = \sqrt{k + k \cos(\theta + jt)} = \sqrt{2k} \cos\left(\frac{\theta + jt}{2}\right)$$

$$k_x + k_x^i = k [\cosh(\theta + jt) + \cos \alpha]$$

[†]minus sign because the contour runs clockwise

The integral I in (19.10.31) is transformed then into,

$$I = \frac{E_0}{\pi} \int_{-\infty}^{\infty} \frac{\sin \frac{\alpha}{2} \sin \left(\frac{\theta + jt}{2} \right)}{\cosh(\theta + jt) + \cos \alpha} e^{-jk\rho \cosh t} dt \quad (19.10.36)$$

Using some trigonometric identities, and the definitions $\theta_i = \theta - \alpha$ and $\theta_r = \theta + \alpha$, we rewrite I as,

$$\begin{aligned} I &= \frac{E_0}{4\pi} \int_{-\infty}^{\infty} \frac{\cos \left(\frac{\theta_i + jt}{2} \right) - \cos \left(\frac{\theta_r + jt}{2} \right)}{\cos \left(\frac{\theta_i + jt}{2} \right) \cdot \cos \left(\frac{\theta_r + jt}{2} \right)} e^{-jk\rho \cosh t} dt \\ &= \frac{E_0}{4\pi} \int_{-\infty}^{\infty} \left[\frac{1}{\cos \left(\frac{\theta_r + jt}{2} \right)} - \frac{1}{\cos \left(\frac{\theta_i + jt}{2} \right)} \right] e^{-jk\rho \cosh t} dt \\ &= \frac{E_0}{4\pi} \int_0^{\infty} \left[\frac{1}{\cos \left(\frac{\theta_r + jt}{2} \right)} + \frac{1}{\cos \left(\frac{\theta_r - jt}{2} \right)} - \frac{1}{\cos \left(\frac{\theta_i + jt}{2} \right)} - \frac{1}{\cos \left(\frac{\theta_i - jt}{2} \right)} \right] e^{-jk\rho \cosh t} dt \end{aligned}$$

where in the last equation we split the integration range into $-\infty < t < 0$ and $0 < t < \infty$. Recombining the terms and using some more trigonometric identities, we may cast I in the form,

$$I = \frac{E_0}{\pi} \int_0^{\infty} \left[\frac{\cos \frac{\theta_r}{2} \cosh \frac{t}{2}}{\cos \theta_r + \cosh t} - \frac{\cos \frac{\theta_i}{2} \cosh \frac{t}{2}}{\cos \theta_i + \cosh t} \right] e^{-jk\rho \cosh t} dt \quad (19.10.37)$$

Using the integral of Eq. (F.25) of Appendix F, we may express I in terms of the Fresnel diffraction coefficient $D(v)$,

$$I = E_0 \operatorname{sign}(v_r) e^{jk\rho \cos \theta_r} D(-|v_r|) - E_0 \operatorname{sign}(v_i) e^{jk\rho \cos \theta_i} D(-|v_i|)$$

where v_r, v_i were defined in Eq. (19.10.3). Thus, we finally have for E_y^s ,

$$E_y^s = -R + I = -R + \operatorname{sign}(v_r) E^r D(-|v_r|) - \operatorname{sign}(v_i) E^i D(-|v_i|) \quad (19.10.38)$$

We can now verify that E_y^s agrees with the Sommerfeld expression, (19.10.35). Indeed, over the reflection region, we have $v_i > 0$, $v_r > 0$, and $R = E^r$, so that,

$$E_y^s = -E^r + E^r D(-v_r) - E^i D(-v_i) = - \left[E^r D(v_r) + E^i D(-v_i) \right]$$

where we used $D(v_r) = 1 - D(-v_r)$. Over the transmission region, we have $R = 0$, $v_i > 0$, $v_r < 0$, so that,

$$E_y^s = -E^r D(v_r) - E^i D(-v_i) = - \left[E^r D(v_r) + E^i D(-v_i) \right]$$

where we replaced, $-|v_r| = v_r$. Finally, in the shadow region, we have $R = E^i$, $v_i < 0$, $v_r < 0$, and we obtain, replacing, $1 - D(v_i) = D(-v_i)$,

$$E_y^s = -E^i - E^r D(v_r) + E^i D(v_i) = - \left[E^r D(v_r) + E^i D(-v_i) \right]$$

Finally, we discuss dropping the contributions of the infinite arcs. Along such arcs, we set $k_x = Re^{j\beta}$ with large radius R . The limits of β are determined by the asymptotes of the hyperbolae, which lie at angles $\pm\theta$ or $\pi \pm \theta$ with respect to the k_x -axis.

Then, one must show that the exponential $\exp(-jk_x x - jk_z |z|)$ will converge to zero in the limit $R \rightarrow \infty$. This will be guaranteed if the exponent, $-j(k_x x + k_z |z|)$, has negative real part along each arc. To verify this, we must consider six different cases corresponding to the angle ranges AD, DB, BE, EC, CF, FA shown in Fig. 19.10.3.

For large k_x , the wavenumber $k_z = \sqrt{k^2 - k_x^2}$ can be approximated by $k_z = \mp jk_x$, where we must choose $k_z = -jk_x$ for the upper-half plane arcs, and $k_z = jk_x$ for the lower-half plane ones. Below we summarize all possible cases. In each case, the limits on β, θ imply that the required real part will be negative.

1. AD range: $0 \leq \theta \leq \frac{\pi}{2}$, $z \geq 0$, using C_+ , Fig. 19.10.5.

$$\begin{aligned} \text{upper arc: } k_x &= Re^{j\beta}, \quad 0 \leq \beta \leq \theta, \quad k_z = -jk_x \\ \operatorname{Re}[-j(k_x x + k_z |z|)] &= R\rho \sin(\beta - \theta) < 0 \end{aligned}$$

$$\begin{aligned} \text{lower arc: } k_x &= Re^{j\beta}, \quad \pi \leq \beta \leq 2\pi - \theta, \quad k_z = jk_x \\ \operatorname{Re}[-j(k_x x + k_z |z|)] &= R\rho \sin(\beta + \theta) < 0 \end{aligned}$$

2. DB range: $\frac{\pi}{2} \leq \theta \leq \pi - \alpha$, $z \geq 0$, using C_- , Fig. 19.10.6 right.

$$\begin{aligned} \text{upper arc: } k_x &= Re^{j\beta}, \quad 0 \leq \beta \leq \theta, \quad k_z = -jk_x \\ \operatorname{Re}[-j(k_x x + k_z |z|)] &= R\rho \sin(\beta - \theta) < 0 \end{aligned}$$

$$\begin{aligned} \text{lower arc: } k_x &= Re^{j\beta}, \quad \pi \leq \beta \leq 2\pi - \theta, \quad k_z = jk_x \\ \operatorname{Re}[-j(k_x x + k_z |z|)] &= R\rho \sin(\beta + \theta) < 0 \end{aligned}$$

3. BE range: $\pi - \alpha \leq \theta \leq \pi$, $z \geq 0$, using C_- , Fig. 19.10.6 left.

$$\begin{aligned} \text{upper arc: } k_x &= Re^{j\beta}, \quad 0 \leq \beta \leq \theta, \quad k_z = -jk_x \\ \operatorname{Re}[-j(k_x x + k_z |z|)] &= R\rho \sin(\beta - \theta) < 0 \end{aligned}$$

$$\begin{aligned} \text{lower arc: } k_x &= Re^{j\beta}, \quad \pi \leq \beta \leq 2\pi - \theta, \quad k_z = jk_x \\ \operatorname{Re}[-j(k_x x + k_z |z|)] &= R\rho \sin(\beta + \theta) < 0 \end{aligned}$$

4. EC range: $\pi \leq \theta \leq \pi + \alpha$, $z \leq 0$, using C_- , Fig. 19.10.6 left.

$$\begin{aligned} \text{upper arc: } k_x &= Re^{j\beta}, \quad 0 \leq \beta \leq 2\pi - \theta, \quad k_z = -jk_x \\ \operatorname{Re}[-j(k_x x + k_z |z|)] &= R\rho \sin(\beta + \theta) < 0 \end{aligned}$$

$$\begin{aligned} \text{lower arc: } k_x &= Re^{j\beta}, \quad \pi \leq \beta \leq \theta, \quad k_z = jk_x \\ \operatorname{Re}[-j(k_x x + k_z |z|)] &= R\rho \sin(\beta - \theta) < 0 \end{aligned}$$

5. *CF* range: $\pi + \alpha \leq \theta \leq \frac{3\pi}{2}$, $z \leq 0$, using C_- , Fig. 19.10.6 right.

upper arc: $k_x = Re^{j\beta}$, $0 \leq \beta \leq 2\pi - \theta$, $k_z = -jk_x$
 $Re[-j(k_x x + k_z |z|)] = R\rho \sin(\beta + \theta) < 0$

lower arc: $k_x = Re^{j\beta}$, $\pi \leq \beta \leq \theta$, $k_z = jk_x$
 $Re[-j(k_x x + k_z |z|)] = R\rho \sin(\beta - \theta) < 0$

6. *FA* range: $\frac{3\pi}{2} \leq \theta \leq 2\pi$, $z \leq 0$, using C_+ , Fig. 19.10.5.

upper arc: $k_x = Re^{j\beta}$, $0 \leq \beta \leq 2\pi - \theta$, $k_z = -jk_x$
 $Re[-j(k_x x + k_z |z|)] = R\rho \sin(\beta + \theta) < 0$

lower arc: $k_x = Re^{j\beta}$, $\pi \leq \beta \leq \theta$, $k_z = jk_x$
 $Re[-j(k_x x + k_z |z|)] = R\rho \sin(\beta - \theta) < 0$

19.11 Diffraction by Small Holes – Bethe-Bouwkamp Model

The problem of diffraction by an electrically small, subwavelength, circular hole in a planar conducting screen has received a lot of attention because of its relevance in near-field applications [534], such as scanning near-field optical microscopy (SNOM or NSOM), as well as in electromagnetic compatibility, field penetration, and interference applications. Even though the conducting screen is assumed to be infinitely-thin, perfectly conducting, and of infinite extent, this idealized problem has served as a useful paradigm for small-aperture problems because of its simple analytical solution.

It was originally solved by Rayleigh [1312] for the special case of a normally incident plane wave, then solved again by Bethe [1314] for arbitrary incident fields, and then corrected by Bouwkamp [1322-1324] for incident plane waves. Meixner and Andrejewski solved it exactly using spheroidal functions [1320]. References [1312-1372] discuss this and other aperture problems; see also the following references [1373-1397] on the phenomenon of *extraordinary transmission* by subwavelength apertures, which is not explained by the simple Bethe-Bouwkamp model (see however, [1357].)

Rayleigh’s approach, which has been followed by all later treatments, was to expand the solution in power series in the variable ka , where $k = 2\pi/\lambda$ is the free-space wavenumber and a the hole radius, and keep only the lowest, first-order, terms in ka . References [1334-1336] carry out such series expansion procedures in detail.

The terms “electrically small” and “subwavelength” refer to the condition, $ka \ll 1$, or equivalently, $a \ll \lambda$, and can be thought of as a low-frequency approximation. In the opposite, high-frequency-large-aperture, regime characterized by, $ka \gg 1$, or, $a \gg \lambda$, the usual Kirchhoff approximation becomes applicable.

In the next two sections, we derive the Bethe-Bouwkamp model by using Copson’s method [1317,1318] to solve the integral equations (19.9.13) for the aperture tangential electric field, and show that under certain conditions[†] the solution is actually valid for

[†]namely, that on the aperture, the transverse derivatives, ∇_{\perp} , of the incident fields are of order k .

more general incident fields than just plane waves. We clarify the Bouwkamp correction and explain why it is necessary for the near-fields and why it does not affect the far-zone fields which are correctly derived from the Bethe solution. We determine the transmission characteristics of the small aperture and compare them with those of the Kirchhoff approximation. Then, following the recent methods of Michalski and Mosig [1364], we derive the plane-wave spectrum representation of the solution and use it to calculate the diffracted fields to the right of the aperture, deriving closed-form expressions for both the near and the far fields, and providing MATLAB functions for numerically calculating the fields at any distance.

The geometry of the problem is illustrated in Fig. 19.11.1 below. The metallic screen M is the xy -plane at $z = 0$, with the circular aperture A of radius a centered at the origin. The incident fields E^i, H^i are assumed to be incident from the left half-space, $z < 0$, and can have arbitrary orientation.

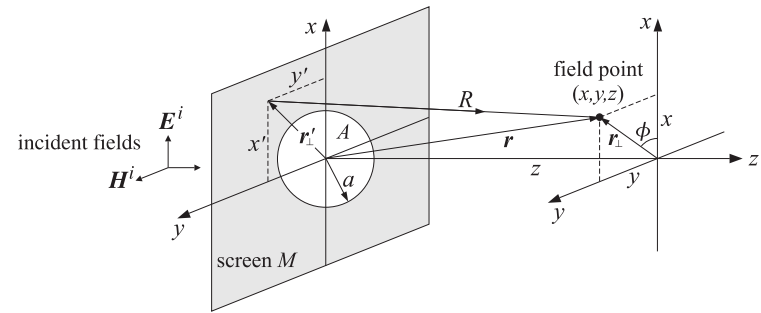


Fig. 19.11.1 Circular aperture at $z = 0$, incident fields from $z < 0$, field point at $z \geq 0$.

We will use cylindrical coordinates defined by[†]

$$\begin{aligned} \rho &= |\mathbf{r}_{\perp}| = \sqrt{x^2 + y^2} & \Leftrightarrow & \quad x = \rho \cos \phi \\ \phi &= \text{atan2}(y, x) & & \quad y = \rho \sin \phi \end{aligned} \tag{19.11.1}$$

with unit transverse vector, $\hat{\mathbf{r}}_{\perp} = \mathbf{r}_{\perp} / |\mathbf{r}_{\perp}| = \mathbf{r}_{\perp} / \rho$,

$$\begin{aligned} \mathbf{r}_{\perp} &= \hat{\mathbf{x}}x + \hat{\mathbf{y}}y = \hat{\mathbf{x}}\rho \cos \phi + \hat{\mathbf{y}}\rho \sin \phi = \rho \hat{\mathbf{r}}_{\perp} \\ \hat{\mathbf{r}}_{\perp} &= \hat{\mathbf{x}} \cos \phi + \hat{\mathbf{y}} \sin \phi \end{aligned} \tag{19.11.2}$$

We recall from Sec. 19.9 that the diffracted fields to the right of the aperture are given by Smythe’s formulas, for $z \geq 0$,

$$\begin{aligned} \mathbf{E} &= \nabla \times \mathbf{F} \\ -jk\eta \mathbf{H} &= k^2 \mathbf{F} + \nabla(\nabla_{\perp} \cdot \mathbf{F}) \end{aligned} \tag{19.11.3}$$

[†]atan2(y, x) is the four-quadrant arc tangent, atan(y/x), and is a built-in function in MATLAB.

with the electric vector potential, $F(\mathbf{r}_\perp, z)$, given in terms of the effective surface magnetic current, $2\hat{\mathbf{z}} \times \mathbf{E}_\perp(\mathbf{r}'_\perp, 0)$, where, $R = \sqrt{|\mathbf{r}_\perp - \mathbf{r}'_\perp|^2 + z^2}$,

$$F(\mathbf{r}_\perp, z) = 2 \int_A [\hat{\mathbf{z}} \times \mathbf{E}_\perp(\mathbf{r}'_\perp, 0)] G(R) d^2\mathbf{r}'_\perp = \hat{\mathbf{z}} \times \int_A \mathbf{E}_\perp(\mathbf{r}'_\perp, 0) \frac{e^{-jkR}}{2\pi R} d^2\mathbf{r}'_\perp \quad (19.11.4)$$

The aperture tangential electric field, $\mathbf{E}_\perp(\mathbf{r}'_\perp, 0)$, is determined by the integral equations,

$$\boxed{\begin{aligned} k^2 F^0 + \nabla_\perp(\nabla_\perp \cdot F^0) &= -jk\eta \mathbf{H}_\perp^i \\ \hat{\mathbf{z}} \cdot \nabla_\perp \times F^0 &= E_z^i \end{aligned}} \quad \text{on } A \quad (19.11.5)$$

where $F^0(\mathbf{r}_\perp)$ denotes the restriction of $F(\mathbf{r}_\perp, z)$ on A , that is, at $z = 0$,

$$F^0(\mathbf{r}_\perp) = F(\mathbf{r}_\perp, 0) = \hat{\mathbf{z}} \times \int_A \mathbf{E}_\perp(\mathbf{r}'_\perp, 0) \frac{e^{-jkR_0}}{2\pi R_0} d^2\mathbf{r}'_\perp \quad (19.11.6)$$

with $R_0 = |\mathbf{r}_\perp - \mathbf{r}'_\perp|$ and $\mathbf{r}_\perp \in A$. Component-wise, Eqs. (19.11.5) read,

$$\boxed{\begin{aligned} k^2 F_x^0 + \partial_x(\partial_x F_x^0 + \partial_y F_y^0) &= -jk\eta H_x^i \\ k^2 F_y^0 + \partial_y(\partial_x F_x^0 + \partial_y F_y^0) &= -jk\eta H_y^i \\ \partial_x F_y^0 - \partial_y F_x^0 &= E_z^i \end{aligned}} \quad \text{on } A \quad (19.11.7)$$

The Bethe-Bouwkamp solution for $\mathbf{E}_\perp(\mathbf{r}_\perp, 0)$ is obtained by solving the integral equations (19.11.7) to first-order in ka . For points on the aperture ($\rho \leq a$), it is given by,

$$\mathbf{E}_\perp(\mathbf{r}_\perp, 0) = A \underbrace{\frac{\mathbf{r}_\perp}{\Delta(\rho)}}_{\text{Bethe}} + \underbrace{\mathbf{B} \Delta(\rho) + \mathbf{C} \Delta(\rho) - \frac{(\mathbf{C} \cdot \mathbf{r}_\perp) \mathbf{r}_\perp}{\Delta(\rho)}}_{\text{Bouwkamp}}, \quad \text{for } \rho \leq a \quad (19.11.8)$$

where, $\Delta(\rho) = \sqrt{a^2 - \rho^2}$, and the scalar A , and transverse vectors \mathbf{B}, \mathbf{C} , are constants defined in terms of the incident field as follows,

$$\boxed{\begin{aligned} A &= \frac{2}{\pi} E_z^i \\ \mathbf{B} &= \frac{4}{\pi} jk\eta \mathbf{H}_\perp^i \times \hat{\mathbf{z}} \\ \mathbf{C} &= -\frac{4}{3\pi} [\nabla_\perp E_z^i + jk\eta \mathbf{H}_\perp^i \times \hat{\mathbf{z}}] \end{aligned}} \Rightarrow \begin{aligned} B_x &= \frac{4}{\pi} jk\eta H_y^i \\ B_y &= -\frac{4}{\pi} jk\eta H_x^i \\ C_x &= -\frac{4}{3\pi} [\partial_x E_z^i + jk\eta H_y^i] \\ C_y &= -\frac{4}{3\pi} [\partial_y E_z^i - jk\eta H_x^i] \end{aligned} \quad (19.11.9)$$

where, $H_x^i, E_z^i, \nabla_\perp E_z^i$, are the incident field values at the aperture center, $(x, y) = (0, 0)$. The first two terms in (19.11.8) represent the original Bethe result, and the \mathbf{C} -terms, the Bouwkamp correction. Eq. (19.11.8) is valid only for $\rho \leq a$. On the conducting part M , the transverse fields must vanish, that is, $\mathbf{E}_\perp(\mathbf{r}_\perp, 0) = 0$, for $\rho > a$, as required by the boundary conditions.

Noting that $\nabla_\perp \Delta = -\mathbf{r}_\perp / \Delta$ and $\nabla_\perp(\mathbf{C} \cdot \mathbf{r}_\perp) = \mathbf{C}$, the Bouwkamp correction can be written as a complete transverse gradient—and this is the reason, as we see below, why that term does not contribute to the far-zone fields [1324,1329],

$$\mathbf{E}_\perp(\mathbf{r}_\perp, 0) = A \underbrace{\frac{\mathbf{r}_\perp}{\Delta(\rho)}}_{\text{Bethe}} + \underbrace{\mathbf{B} \Delta(\rho) + \nabla_\perp[(\mathbf{C} \cdot \mathbf{r}_\perp) \Delta(\rho)]}_{\text{Bouwkamp}}, \quad \text{for } \rho \leq a \quad (19.11.10)$$

The expression (19.11.8) meets the additional regularity condition that the azimuthal component (i.e., the ϕ -component) of \mathbf{E}_\perp vanish at the edge of the aperture, that is, at $\rho = a$. Indeed, resolving \mathbf{E}_\perp into its radial and azimuthal components, we may write, $\mathbf{E}_\perp = \hat{\rho} E_\rho + \hat{\phi} E_\phi$, where $\hat{\rho} = \hat{\mathbf{r}}_\perp$. It follows that, $\hat{\mathbf{r}}_\perp \times \mathbf{E}_\perp = \hat{\mathbf{z}} E_\phi$, and since $\hat{\mathbf{r}}_\perp \times \mathbf{r}_\perp = 0$, we have from (19.11.8),

$$\hat{\mathbf{z}} E_\phi = \hat{\mathbf{r}}_\perp \times \mathbf{E}_\perp = \hat{\mathbf{r}}_\perp \times (\mathbf{B} + \mathbf{C}) \Delta(\rho) = \hat{\mathbf{r}}_\perp \times (\mathbf{B} + \mathbf{C}) \sqrt{a^2 - \rho^2}$$

which vanishes at $\rho = a$.

To derive (19.11.8) we follow Copson's procedure [1317,1318] of assuming the functional form of Eq. (19.11.8) and then fixing the coefficients $A, \mathbf{B}, \mathbf{C}$ in order to satisfy the integral equation (19.11.5). Working with the quantity $F^0 \times \hat{\mathbf{z}}$, we may write (19.11.6) in the simpler form,

$$F^0(\mathbf{r}_\perp) \times \hat{\mathbf{z}} = \int_A \mathbf{E}_\perp(\mathbf{r}'_\perp, 0) \frac{e^{-jkR_0}}{2\pi R_0} d^2\mathbf{r}'_\perp, \quad R_0 = |\mathbf{r}_\perp - \mathbf{r}'_\perp| \quad (19.11.11)$$

Next, we carry out the Rayleigh procedure of expanding in powers of k and keeping only first-order terms. To this order, we have,

$$\frac{e^{-jkR_0}}{R_0} \approx \frac{1 - jkR_0}{R_0} = \frac{1}{R_0} - jk$$

where we note that the quantity kR_0 is of order ka because $R_0 = |\mathbf{r}_\perp - \mathbf{r}'_\perp|$ remains less than $2a$ since both $\mathbf{r}_\perp, \mathbf{r}'_\perp$ lie in A . If we also expand the desired solution \mathbf{E}_\perp to order k , that is, as a sum of terms of the form, $\mathbf{E}_\perp = \mathbf{E}_\perp^{(0)} + k \mathbf{E}_\perp^{(1)} + O(k^2)$, then, to first-order in k , Eq. (19.11.11) becomes,

$$F^0(\mathbf{r}_\perp) \times \hat{\mathbf{z}} = \int_A \frac{\mathbf{E}_\perp^{(0)}(\mathbf{r}'_\perp, 0) + k \mathbf{E}_\perp^{(1)}(\mathbf{r}'_\perp, 0)}{2\pi R_0} d^2\mathbf{r}'_\perp - \int_A \frac{jk \mathbf{E}_\perp^{(0)}(\mathbf{r}'_\perp, 0)}{2\pi} d^2\mathbf{r}'_\perp$$

But the last term is simply a constant that can be ignored because it will have no effect on the integral equations (19.11.7). Indeed, the term $k^2 F^0$ in (19.11.7) can be dropped because it is of order k^2 , and since F^0 is differentiated in the rest of the terms, the above constant will have no effect. Thus, the first-order expression for F^0 is,

$$F^0(\mathbf{r}_\perp) \times \hat{\mathbf{z}} = \int_A \frac{\mathbf{E}_\perp(\mathbf{r}'_\perp, 0)}{2\pi R_0} d^2\mathbf{r}'_\perp, \quad R_0 = |\mathbf{r}_\perp - \mathbf{r}'_\perp| \quad (19.11.12)$$

The corresponding approximate integral equations to be solved, become,

$$\begin{aligned} \partial_x(\partial_x F_x^0 + \partial_y F_y^0) &= -jk\eta H_x^i \\ \partial_y(\partial_x F_x^0 + \partial_y F_y^0) &= -jk\eta H_y^i \\ \partial_x F_y^0 - \partial_y F_x^0 &= E_z^i \end{aligned} \quad (19.11.13)$$

Inserting (19.11.8) into (19.11.12), we obtain,

$$\mathbf{F}^0(\mathbf{r}_\perp) \times \hat{\mathbf{z}} = \int_A \left[A \frac{\mathbf{r}'_\perp}{\Delta(\rho')} + B \Delta(\rho') + C \Delta(\rho') - \frac{(\mathbf{C} \cdot \mathbf{r}'_\perp) \mathbf{r}'_\perp}{\Delta(\rho')} \right] \frac{d^2 \mathbf{r}'_\perp}{2\pi R_0}$$

The indicated integrals can be done exactly; see for example, Refs. [1317] and [1334],

$$\begin{aligned} \int_A \Delta(\rho') \frac{d^2 \mathbf{r}'_\perp}{2\pi R_0} &= \frac{\pi}{4} \left(a^2 - \frac{1}{2} \rho^2 \right) \\ \int_A \frac{\mathbf{r}'_\perp}{\Delta(\rho')} \frac{d^2 \mathbf{r}'_\perp}{2\pi R_0} &= \frac{\pi}{4} \mathbf{r}_\perp \\ \int_A \left[C \Delta(\rho') - \frac{(\mathbf{C} \cdot \mathbf{r}'_\perp) \mathbf{r}'_\perp}{\Delta(\rho')} \right] \frac{d^2 \mathbf{r}'_\perp}{2\pi R_0} &= \frac{\pi}{32} (4a^2 - 3\rho^2) C - \frac{3\pi}{16} (\mathbf{C} \cdot \mathbf{r}_\perp) \mathbf{r}_\perp \end{aligned} \quad (19.11.14)$$

Ignoring the constant terms in (19.11.14) for the same reasons as mentioned above, we obtain the order- k approximation to \mathbf{F}^0 , for $\mathbf{r}_\perp \in A$,

$$\mathbf{F}^0(\mathbf{r}_\perp) \times \hat{\mathbf{z}} = \frac{\pi}{4} A \mathbf{r}_\perp - \frac{\pi}{32} (4B + 3C) \rho^2 - \frac{3\pi}{16} (\mathbf{C} \cdot \mathbf{r}_\perp) \mathbf{r}_\perp \quad (19.11.15)$$

and since, $\mathbf{F}^0(\mathbf{r}_\perp) \times \hat{\mathbf{z}} = \hat{\mathbf{x}} F_y^0 - \hat{\mathbf{y}} F_x^0$, we have component-wise,

$$\begin{aligned} F_x^0 &= -\frac{\pi}{4} A y + \frac{\pi}{32} (4B_y + 3C_y) \rho^2 + \frac{3\pi}{16} (C_x x + C_y y) y \\ F_y^0 &= \frac{\pi}{4} A x - \frac{\pi}{32} (4B_x + 3C_x) \rho^2 - \frac{3\pi}{16} (C_x x + C_y y) x \end{aligned} \quad (19.11.16)$$

Remembering that, $\rho^2 = x^2 + y^2$, we obtain the derivatives,

$$\partial_x F_x^0 + \partial_y F_y^0 = \frac{\pi}{4} (x B_y - y B_x) \quad (19.11.17)$$

$$\begin{aligned} \partial_x (\partial_x F_x^0 + \partial_y F_y^0) &= \frac{\pi}{4} B_y \\ \partial_y (\partial_x F_x^0 + \partial_y F_y^0) &= -\frac{\pi}{4} B_x \end{aligned} \quad (19.11.18)$$

$$\partial_x F_y^0 - \partial_y F_x^0 = \frac{\pi}{2} A - \frac{\pi}{4} [x(B_x + 3C_x) + y(B_y + 3C_y)]$$

The incident fields in the right-hand side of Eq. (19.11.13), being evaluated on A , are also functions of \mathbf{r}_\perp . Because the aperture is small, Bethe assumed that they vary little over A and replaced them with their values at the origin $(x, y) = (0, 0)$. But as a small improvement, we may expand them in Taylor series about the origin, so that the integral equations (19.11.13) become for $\mathbf{r}_\perp \in A$,

$$\begin{aligned} \partial_x (\partial_x F_x^0 + \partial_y F_y^0) &= -jk\eta H_x^i(\mathbf{r}_\perp) = -jk\eta [H_x^i(0) + \mathbf{r}_\perp \cdot \nabla_\perp H_x^i(0)] \\ \partial_y (\partial_x F_x^0 + \partial_y F_y^0) &= -jk\eta H_y^i(\mathbf{r}_\perp) = -jk\eta [H_y^i(0) + \mathbf{r}_\perp \cdot \nabla_\perp H_y^i(0)] \\ \partial_x F_y^0 - \partial_y F_x^0 &= E_z^i(\mathbf{r}_\perp) = E_z^i(0) + \mathbf{r}_\perp \cdot \nabla_\perp E_z^i(0) \end{aligned} \quad (19.11.19)$$

If we now make the reasonable assumption that the transverse derivatives ∇_\perp of the fields are of order k ,[†] then the gradient terms in the H_\perp^i equations can be dropped because they are being multiplied by jk , making them of order k^2 . On the other hand, the gradient terms must be kept in the E_z^i equation in order to have a consistent expansion to first-order in k .[†] It follows then that the integral equations must be approximated to first-order in k as follows, for $(x, y) \in A$,

$$\begin{aligned} \partial_x (\partial_x F_x^0 + \partial_y F_y^0) &= -jk\eta H_x^i(0) \\ \partial_y (\partial_x F_x^0 + \partial_y F_y^0) &= -jk\eta H_y^i(0) \\ \partial_x F_y^0 - \partial_y F_x^0 &= E_z^i(0) + x \partial_x E_z^i(0) + y \partial_y E_z^i(0) \end{aligned} \quad (19.11.20)$$

In order to satisfy the integral equations, the right-hand sides of Eqs. (19.11.18) and (19.11.20) must match for all $(x, y) \in A$, resulting in the following conditions on the A, B, C constants, the solutions of which are precisely Eqs. (19.11.9),

$$\begin{aligned} \frac{\pi}{4} B_y &= -jk\eta H_x^i(0), & \frac{\pi}{4} (B_x + 3C_x) &= -\partial_x E_z^i(0) \\ -\frac{\pi}{4} B_x &= -jk\eta H_y^i(0), & \frac{\pi}{4} (B_y + 3C_y) &= -\partial_y E_z^i(0) \\ \frac{\pi}{2} A &= E_z^i(0) \end{aligned}$$

Far-Field Approximation

Next, we discuss the far-zone radiation field approximation. Once the aperture fields E_\perp are known, one can in principle, calculate the vector potential for any point to the right of the aperture,

$$\mathbf{F}(\mathbf{r}) = 2 \hat{\mathbf{z}} \times \int_A E_\perp(\mathbf{r}', 0) G(R) d^2 \mathbf{r}', \quad R = |\mathbf{r} - \mathbf{r}'| = \sqrt{|\mathbf{r}_\perp - \mathbf{r}'_\perp|^2 + z^2} \quad (19.11.21)$$

At large distances from the aperture, one would normally make the usual radiation-field approximations,

$$\begin{aligned} R &= |\mathbf{r} - \mathbf{r}'| = \sqrt{r^2 + r'^2 - 2\mathbf{r} \cdot \mathbf{r}'} \approx r - \frac{\mathbf{r} \cdot \mathbf{r}'}{r} = r - \hat{\mathbf{r}} \cdot \mathbf{r}' \\ G(R) &= \frac{e^{-jkR}}{4\pi R} \approx \frac{e^{-jk(r - \hat{\mathbf{r}} \cdot \mathbf{r}')}}{4\pi r} = \frac{e^{-jkr}}{4\pi r} e^{jk \cdot \mathbf{r}'} = G(r) e^{jk \cdot \mathbf{r}'}, \quad \mathbf{k} = k \hat{\mathbf{r}} \end{aligned}$$

As in Sec. 19.6, the resulting \mathbf{F} can be expressed in terms of the 2-D Fourier transform $\hat{E}_\perp(\mathbf{k}_\perp)$ of the aperture fields $E_\perp(\mathbf{r}_\perp, 0)$ evaluated at the wavenumber, $\mathbf{k} = k \hat{\mathbf{r}}$,

$$\mathbf{F}(\mathbf{r}) = 2 \hat{\mathbf{z}} \times \hat{E}_\perp(\mathbf{k}_\perp) \Big|_{\mathbf{k} = k \hat{\mathbf{r}}} \cdot G(r) \quad (19.11.22)$$

[†]For plane waves, this assumption is valid. More generally, it may be justified from Maxwell's equations, which suggest that the spatial derivatives are of order k , that is, $\nabla \times E^i = -jk\eta H^i$ and $\nabla \times \eta H^i = jkE^i$.

[†]Bethe had originally omitted these terms, but were later added by Bouwkamp.

and replacing, $\nabla \rightarrow -jk = -jk\hat{r}$, we obtain, the radiation field,

$$\mathbf{E}_{\text{rad}} = \nabla \times \mathbf{F} = -jk\hat{r} \times [\hat{\mathbf{z}} \times \hat{\mathbf{E}}_{\perp}(\mathbf{k}_{\perp})] \Big|_{k=k\hat{r}} \cdot G(r) \quad (19.11.23)$$

which is equivalent to Eq. (19.6.1) obtained from the stationary-phase method. We carry out this approach later on. Here we work directly in the space domain. Since the aperture is small and kr' is of order ka , one could make the further approximation, $e^{jk\cdot r'} \approx (1 + j\mathbf{k} \cdot \mathbf{r}')$, and replace,

$$G(R) \approx G(r) e^{jk\cdot r'} \approx G(r) (1 + j\mathbf{k} \cdot \mathbf{r}') \quad (19.11.24)$$

into (19.11.21),

$$\mathbf{F}(r) = 2\hat{\mathbf{z}} \times \int_A \mathbf{E}_{\perp}(\mathbf{r}', 0) (1 + j\mathbf{k} \cdot \mathbf{r}') d^2\mathbf{r}' G(r) \quad (19.11.25)$$

The indicated integrations with respect to \mathbf{r}' can be done exactly. However, a slightly better approximation can be obtained by expanding the entire $G(R)$ in Taylor series around the origin, that is,

$$G(R) = G(\mathbf{r} - \mathbf{r}') \approx G(r) - \mathbf{r}' \cdot \nabla G(r) \quad (19.11.26)$$

where $\nabla G(r)$ is the gradient with respect to \mathbf{r} ,

$$G(r) = \frac{e^{-jkr}}{4\pi r}, \quad \nabla G(r) = -\hat{r} \left(jk + \frac{1}{r} \right) \frac{e^{-jkr}}{4\pi r} = -\hat{r} \left(jk + \frac{1}{r} \right) G(r) \quad (19.11.27)$$

Using (19.11.26) into (19.11.21), and noting that $\mathbf{r}' = \mathbf{r}'_{\perp}$, we obtain,

$$\mathbf{F}(r) = 2\hat{\mathbf{z}} \times \int_A \mathbf{E}_{\perp}(\mathbf{r}'_{\perp}, 0) [G(r) - \mathbf{r}'_{\perp} \cdot \nabla_{\perp} G(r)] d^2\mathbf{r}'_{\perp} \quad (19.11.28)$$

This becomes equivalent to (19.11.21) when $kr \gg 1$. In that limit, the jk term wins over the $1/r$ term in (19.11.27) and we have, $\nabla G(r) \approx -jk\hat{r}G(r) = -jkG(r)$. Inserting (19.11.8) into (19.11.28), we must calculate the integrals,

$$\begin{aligned} & \int_A \mathbf{E}_{\perp}(\mathbf{r}'_{\perp}, 0) [G(r) - \mathbf{r}'_{\perp} \cdot \nabla_{\perp} G(r)] d^2\mathbf{r}'_{\perp} = \\ & = \int_A \left[A \frac{\mathbf{r}'_{\perp}}{\Delta(\rho')} + \mathbf{B} \Delta(\rho') + \mathbf{C} \Delta(\rho') - \frac{(\mathbf{C} \cdot \mathbf{r}'_{\perp}) \mathbf{r}'_{\perp}}{\Delta(\rho')} \right] [G(r) - \mathbf{r}'_{\perp} \cdot \nabla_{\perp} G(r)] d^2\mathbf{r}'_{\perp} \\ & = \int_A \left[A \frac{\mathbf{r}'_{\perp}}{\Delta(\rho')} + \mathbf{B} \Delta(\rho') + \nabla_{\perp} [(C \cdot \mathbf{r}'_{\perp}) \Delta(\rho')] \right] G(r) d^2\mathbf{r}'_{\perp} - \\ & - \int_A \left[A \frac{\mathbf{r}'_{\perp}}{\Delta(\rho')} + \mathbf{B} \Delta(\rho') + \mathbf{C} \Delta(\rho') - \frac{(\mathbf{C} \cdot \mathbf{r}'_{\perp}) \mathbf{r}'_{\perp}}{\Delta(\rho')} \right] [\mathbf{r}'_{\perp} \cdot \nabla_{\perp} G(r)] d^2\mathbf{r}'_{\perp} \end{aligned}$$

where in the first set of terms multiplying $G(r)$, we replaced the Bouwkamp correction terms by their equivalent expression as a gradient given in (19.11.10). The integral of that term vanishes; indeed, using Eq. (C.45) of Appendix C, which is a consequence of the 2-D divergence theorem, we have,

$$\int_A \nabla_{\perp} [(C \cdot \mathbf{r}_{\perp}) \Delta(\rho)] d^2\mathbf{r}_{\perp} = \oint_C [(C \cdot \mathbf{r}_{\perp}) \Delta(\rho)] \hat{\mathbf{n}} dl = 0$$

where the contour C is the periphery ($\rho = a$) of the aperture, where $\Delta(\rho)$ vanishes, and also for this contour, $\hat{\mathbf{n}}$ is the unit vector in the radial direction \mathbf{r}_{\perp} .

Of the remaining terms in the above integrals, those that involve an odd number of powers of \mathbf{r}'_{\perp} are zero because of the symmetry of the integration range. Only two terms finally survive, which can be integrated exactly,

$$\begin{aligned} & \int_A \mathbf{E}_{\perp}(\mathbf{r}'_{\perp}, 0) [G(r) - \mathbf{r}'_{\perp} \cdot \nabla_{\perp} G(r)] d^2\mathbf{r}'_{\perp} = \\ & = \int_A \left[\mathbf{B} \Delta(\rho') G(r) - A \frac{\mathbf{r}'_{\perp}}{\Delta(\rho')} \mathbf{r}'_{\perp} \cdot \nabla_{\perp} G(r) \right] d^2\mathbf{r}'_{\perp} = \frac{2\pi a^3}{3} [\mathbf{B} G(r) - A \nabla_{\perp} G(r)] \end{aligned}$$

These follow from the integrals,

$$\int_A \Delta(\rho') d^2\mathbf{r}'_{\perp} = \frac{2\pi a^3}{3}, \quad \int_A \frac{x'_{\alpha} x'_{\beta}}{\Delta(\rho')} d^2\mathbf{r}'_{\perp} = \frac{2\pi a^3}{3} \delta_{\alpha\beta}, \quad \alpha, \beta = 1, 2$$

Thus, the far-field approximation to the vector potential (19.11.28) is,

$$\mathbf{F}_{\text{far}}(r) = \frac{4\pi a^3}{3} [\hat{\mathbf{z}} \times \mathbf{B} G(r) - A \hat{\mathbf{z}} \times \nabla_{\perp} G(r)] \quad (19.11.29)$$

Noting that $\hat{\mathbf{z}} \times \nabla_{\perp} G(r) = \hat{\mathbf{z}} \times \nabla G(r)$, and replacing \mathbf{B}, A in terms of the incident fields, we obtain,

$$\mathbf{F}_{\text{far}}(r) = \frac{8a^3}{3} [2jk\eta \mathbf{H}_{\perp}^i G(r) - E_z^i \hat{\mathbf{z}} \times \nabla G(r)] \quad (19.11.30)$$

This is recognized as the vector potential for the sum of an electric and a magnetic dipole. Indeed, we recall from Sec. 15.5, Eqs. (15.5.4) and (15.5.8), that two electric and magnetic dipoles, \mathbf{p}, \mathbf{m} , would have a combined vector potential,

$$\mathbf{F} = \nabla G(r) \times \mathbf{P} - jkG(r) \mathbf{M}, \quad \mathbf{P} = \frac{1}{c} \mathbf{p}, \quad \mathbf{M} = \eta \mathbf{m} \quad (19.11.31)$$

Comparing this with (19.11.30) we conclude that, in the far zone, the small circular hole acts as a combination of magnetic and electric dipoles given by,

$$\mathbf{M} = -\frac{16a^3}{3} \eta \mathbf{H}_{\perp}^i, \quad \mathbf{P} = \frac{8a^3}{3} E_z^i \hat{\mathbf{z}} \quad (19.11.32)$$

or component-wise,

$$M_x = -\frac{16a^3}{3} \eta H_x^i, \quad M_y = -\frac{16a^3}{3} \eta H_y^i, \quad P_z = \frac{8a^3}{3} E_z^i \quad (19.11.33)$$

The corresponding far-field electric and magnetic fields are then given by Eqs. (19.11.3), which can be written in the dual form of Eqs. (15.5.5) and (15.5.9),

$$\begin{aligned} \mathbf{E}_{\text{far}} &= \nabla \times [\nabla G(r) \times \mathbf{P} - jkG(r) \mathbf{M}] \\ \eta \mathbf{H}_{\text{far}} &= \nabla \times [\nabla G(r) \times \mathbf{M} + jkG(r) \mathbf{P}] \end{aligned} \quad (19.11.34)$$

For numerical evaluation, it is more convenient to rewrite (19.11.34) in the form,

$$\begin{aligned} \mathbf{E}_{\text{far}} &= \left[k^2 \mathbf{P} + (\mathbf{P} \cdot \nabla) \nabla \right] G - jk \nabla G \times \mathbf{M} \\ \eta \mathbf{H}_{\text{far}} &= \left[k^2 \mathbf{M} + (\mathbf{M} \cdot \nabla) \nabla \right] G + jk \nabla G \times \mathbf{P} \end{aligned} \quad (19.11.35)$$

Radiation Pattern, Radiated Power, Transmission Coefficient

The far-field expressions (19.11.32) simplify considerably in the radiation zone, that is, for $kr \gg 1$. Replacing, $\nabla \rightarrow -jk\hat{\mathbf{r}}$, with $\mathbf{k} = k\hat{\mathbf{r}}$, we obtain,

$$\begin{aligned} \mathbf{E}_{\text{rad}} &= k^2 \left[\hat{\mathbf{r}} \times (\mathbf{P} \times \hat{\mathbf{r}}) + \mathbf{M} \times \hat{\mathbf{r}} \right] \frac{e^{-jkr}}{4\pi r} \\ \eta \mathbf{H}_{\text{rad}} &= k^2 \left[\hat{\mathbf{r}} \times (\mathbf{M} \times \hat{\mathbf{r}}) - \mathbf{P} \times \hat{\mathbf{r}} \right] \frac{e^{-jkr}}{4\pi r} \end{aligned} \quad (\text{radiation fields}) \quad (19.11.36)$$

and similarly, in this limit, the vector potential (19.11.29) becomes in the radiation zone,

$$\mathbf{F}_{\text{rad}}(\mathbf{r}) = \frac{4\pi a^3}{3} \hat{\mathbf{z}} \times [\mathbf{B} + j\mathbf{k}_{\perp} A] G(r) \quad (19.11.37)$$

Comparing this with Eq. (19.11.22), we may identify the 2-D Fourier transform of $\mathbf{E}_{\perp}(\mathbf{r}_{\perp}, 0)$ evaluated at $\mathbf{k} = k\hat{\mathbf{r}}$,

$$\hat{\mathbf{E}}_{\perp}(\mathbf{k}_{\perp}) = \frac{2\pi a^3}{3} [\mathbf{B} + j\mathbf{k}_{\perp} A] \quad (19.11.38)$$

This will be verified below based on the exact expression (19.12.13) of $\hat{\mathbf{E}}_{\perp}(\mathbf{k}_{\perp})$.

To clarify the terms “far” versus “radiation” fields, we note that because we assumed that $ka \ll 1$, or, $a \ll 1/k$, we may distinguish two far-distance ranges:

- (i) the far zone, $a \ll r \ll 1/k$
- (ii) the radiation zone, $1/k \ll r$

with the former evolving into the latter roughly when $r = 1/k$. The radiation fields go down like $1/r$, but the far-zone ones have also a $1/r^2$ dependence which dominates for smaller r , but eventually disappears. Example 19.12.1 demonstrates this behavior.

As expected, the radiation fields satisfy, $\eta \mathbf{H}_{\text{rad}} = \hat{\mathbf{r}} \times \mathbf{E}_{\text{rad}}$, and do not have a radial component. In spherical coordinates, we have, $\hat{\mathbf{r}} \times (\mathbf{P} \times \hat{\mathbf{r}}) = \hat{\boldsymbol{\theta}} P_{\theta} + \hat{\boldsymbol{\phi}} P_{\phi}$, and, $\mathbf{P} \times \hat{\mathbf{r}} = \hat{\boldsymbol{\theta}} P_{\phi} - \hat{\boldsymbol{\phi}} P_{\theta}$, and similarly for \mathbf{M} , and therefore, Eqs. (19.11.36) read,

$$\begin{aligned} \mathbf{E}_{\text{rad}} &= k^2 \left[\hat{\boldsymbol{\theta}} (P_{\theta} + M_{\phi}) - \hat{\boldsymbol{\phi}} M_{\theta} \right] G(r) \\ \eta \mathbf{H}_{\text{rad}} &= k^2 \left[\hat{\boldsymbol{\phi}} (P_{\theta} + M_{\phi}) + \hat{\boldsymbol{\theta}} M_{\theta} \right] G(r) \end{aligned} \quad (\text{radiation fields}) \quad (19.11.39)$$

where we note that $P_{\phi} = (\hat{\boldsymbol{\phi}} \cdot \hat{\mathbf{z}}) P_z = 0$. Expressed in terms of the cartesian components (19.11.33), the spherical components are as follows,

$$\begin{aligned} P_{\theta} + M_{\phi} &= -\sin \theta P_z - \sin \phi M_x + \cos \phi M_y \\ M_{\theta} &= (\cos \phi M_x + \sin \phi M_y) \cos \theta \end{aligned}$$

and since, $E_{\theta} = k^2 (P_{\theta} + M_{\phi}) G$ and $E_{\phi} = -k^2 M_{\theta} G$,

$$\begin{aligned} E_{\theta} &= \eta H_{\phi} = \frac{4a^3 k^2}{3\pi} \left(\eta H_x^i \sin \phi - \eta H_y^i \cos \phi - \frac{1}{2} E_z^i \sin \theta \right) \frac{e^{-jkr}}{r} \\ E_{\phi} &= -\eta H_{\theta} = \frac{4a^3 k^2}{3\pi} (\eta H_x^i \cos \phi + \eta H_y^i \sin \phi) \cos \theta \frac{e^{-jkr}}{r} \end{aligned} \quad (19.11.40)$$

The time-averaged Poynting vector has only a radial component given by,

$$\begin{aligned} \mathcal{P}_r &= \frac{1}{2} \text{Re}[\hat{\mathbf{r}} \cdot \mathbf{E}_{\text{rad}} \times \mathbf{H}_{\text{rad}}^*] = \frac{1}{2\eta} \left[|E_{\theta}|^2 + |E_{\phi}|^2 \right] \\ &= \frac{8a^6 k^4}{9\pi^2 \eta r^2} \left[|\eta H_x^i \sin \phi - \eta H_y^i \cos \phi - \frac{1}{2} E_z^i \sin \theta|^2 + |\eta H_x^i \cos \phi + \eta H_y^i \sin \phi|^2 \cos^2 \theta \right] \end{aligned} \quad (19.11.41)$$

The corresponding radiation intensity will be,

$$\begin{aligned} \frac{dP}{d\Omega} &= r^2 \mathcal{P}_r = \frac{8a^6 k^4}{9\pi^2 \eta} \left[|\eta H_x^i \sin \phi - \eta H_y^i \cos \phi - \frac{1}{2} E_z^i \sin \theta|^2 + \right. \\ &\quad \left. + |\eta H_x^i \cos \phi + \eta H_y^i \sin \phi|^2 \cos^2 \theta \right] \end{aligned} \quad (19.11.42)$$

It has a fairly complicated dependence on θ, ϕ . For example, a TM plane wave with xz as the plane of incidence would have $H_y^i \neq 0$, but $H_x^i = E_z^i = 0$, resulting in,

$$\frac{dP}{d\Omega} = \frac{8a^6 k^4}{9\pi^2 \eta} (\cos^2 \phi + \sin^2 \phi \cos^2 \theta) |\eta H_y^i|^2 \quad (19.11.43)$$

The radiated power is obtained by integrating (19.11.42) over all solid angles, $d\Omega = \sin \theta d\theta d\phi$, in the right hemisphere,

$$P_{\text{rad}} = \int_0^{\pi/2} \int_0^{2\pi} \frac{dP}{d\Omega} \sin \theta d\theta d\phi$$

resulting in,

$$P_{\text{rad}} = \frac{64(ka)^4}{27\pi^2} \cdot \pi a^2 \cdot \frac{1}{2\eta} \left[|\eta \mathbf{H}_{\perp}^i|^2 + \frac{1}{4} |E_z^i|^2 \right] \quad (19.11.44)$$

Let us compare this with the predictions of the Kirchhoff approximation, which was defined in Eq. (19.9.18), that is, with $R = \sqrt{|\mathbf{r}_{\perp} - \mathbf{r}'_{\perp}|^2 + z^2}$, and $z \geq 0$,

$$\begin{aligned} \mathbf{F}^i &= 2 \int_A [\hat{\mathbf{z}} \times \mathbf{E}_{\perp}^i(\mathbf{r}'_{\perp}, 0)] G(R) d^2 \mathbf{r}'_{\perp} \\ \mathbf{E} &= \nabla \times \mathbf{F}^i \\ -jk\eta \mathbf{H} &= k^2 \mathbf{F}^i + \nabla (\nabla_{\perp} \cdot \mathbf{F}^i) \end{aligned} \quad (19.11.45)$$

In the radiation zone, we replace $G(R) \approx G(r) e^{jk \cdot r'}$, and $\nabla \rightarrow -jk = -jk\hat{\mathbf{x}}$, and obtain,

$$\begin{aligned}\hat{\mathbf{E}}_{\perp}^i &= \int_A \mathbf{E}_{\perp}^i(\mathbf{r}'_{\perp}, 0) e^{jk_{\perp} \cdot \mathbf{r}'_{\perp}} d^2 \mathbf{r}'_{\perp} \\ \mathbf{F}_{\text{rad}}^i &= 2 \hat{\mathbf{z}} \times \hat{\mathbf{E}}_{\perp}^i G(r) \\ \mathbf{E}_{\text{rad}} &= -2jk \hat{\mathbf{r}} \times \mathbf{F}_{\text{rad}}^i = -2jk \hat{\mathbf{r}} \times (\hat{\mathbf{z}} \times \hat{\mathbf{E}}_{\perp}^i) G(r) \\ \eta \mathbf{H}_{\text{rad}} &= \hat{\mathbf{r}} \times \mathbf{E}_{\text{rad}}\end{aligned}\quad (19.11.46)$$

and in spherical coordinates,

$$\begin{aligned}E_{\theta} &= \eta H_{\phi} = 2jk (\hat{E}_x^i \cos \phi + \hat{E}_y^i \sin \phi) \frac{e^{-jkr}}{4\pi r} \\ E_{\phi} &= -\eta H_{\theta} = 2jk \cos \theta (\hat{E}_y^i \cos \phi - \hat{E}_x^i \sin \phi) \frac{e^{-jkr}}{4\pi r}\end{aligned}\quad (19.11.47)$$

Since the aperture is small, we may expand $\mathbf{E}_{\perp}^i(\mathbf{r}'_{\perp}, 0)$ and the exponential $e^{jk \cdot r'}$ in Taylor series about the origin and keep up to first-order terms in ka , obtaining the approximation to the Fourier integral,

$$\begin{aligned}\hat{\mathbf{E}}_{\perp}^i &= \int_A \mathbf{E}_{\perp}^i(\mathbf{r}'_{\perp}, 0) e^{jk_{\perp} \cdot \mathbf{r}'_{\perp}} d^2 \mathbf{r}'_{\perp} \approx \int_A \left[\mathbf{E}_{\perp}^i(0) + (\mathbf{r}'_{\perp} \cdot \nabla_{\perp}) \mathbf{E}_{\perp}^i(0) \right] [1 + j\mathbf{k}_{\perp} \cdot \mathbf{r}'_{\perp}] d^2 \mathbf{r}'_{\perp} \\ &= \int_A \left[\mathbf{E}_{\perp}^i(0) + (\mathbf{r}'_{\perp} \cdot \nabla_{\perp}) \mathbf{E}_{\perp}^i(0) (j\mathbf{k}_{\perp} \cdot \mathbf{r}'_{\perp}) \right] d^2 \mathbf{r}'_{\perp}\end{aligned}$$

where the linear terms in \mathbf{r}'_{\perp} were dropped because they do not contribute to the integral by symmetry, and the remaining terms may be integrated to give,

$$\hat{\mathbf{E}}_{\perp}^i = \pi a^2 \left[\mathbf{E}_{\perp}^i(0) + \frac{j}{4} (\mathbf{k}_{\perp} \cdot \nabla_{\perp}) \mathbf{E}_{\perp}^i(0) \right] \quad (19.11.48)$$

where the incident fields and their derivatives are evaluated at the origin $(x, y) = (0, 0)$. Since the derivatives are already assumed to be of order k , the second term in (19.11.49) is of order k^2 and can be ignored. Problem 19.2 considers the effect of this term. Thus, we will work with the approximation,

$$\hat{\mathbf{E}}_{\perp}^i = \pi a^2 \mathbf{E}_{\perp}^i(0) \Rightarrow \hat{E}_x^i = \pi a^2 E_x^i(0), \quad \hat{E}_y^i = \pi a^2 E_y^i(0) \quad (19.11.49)$$

As before, the radiated power is obtained by integrating the radiation intensity over all solid angles in the right hemisphere,

$$\begin{aligned}P_{\text{rad}} &= \int_0^{\pi/2} \int_0^{2\pi} \frac{dP}{d\Omega} \sin \theta d\theta d\phi = \\ &= \int_0^{\pi/2} \int_0^{2\pi} r^2 \frac{1}{2\eta} [|E_{\theta}|^2 + |E_{\phi}|^2] \sin \theta d\theta d\phi\end{aligned}\quad (19.11.50)$$

The angle integrations can be done explicitly, where \mathbf{E}_{\perp}^i stands for $\mathbf{E}_{\perp}^i(0)$,

$$P_{\text{rad}} = \frac{(ka)^2}{3} \cdot \pi a^2 \cdot \frac{1}{2\eta} |\mathbf{E}_{\perp}^i|^2 \quad (\text{Kirchhoff approximation}) \quad (19.11.51)$$

Comparing with (19.11.44), we note that the Bethe-Bouwkamp theory predicts a much smaller radiated power — by a factor of $(ka)^2$ — than ordinary Kirchhoff theory.

Two related concepts to the radiated power are the *transmission cross section* of the aperture, defined as the radiated power divided by the magnitude of the time-averaged Poynting vector of the incident fields, and the *transmission coefficient*, which is the transmission cross section normalized by the area of the aperture, that is,

$$|\mathcal{P}^i| = \left| \frac{1}{2} \text{Re}[\mathbf{E}^i \times \mathbf{H}^{i*}] \right| \quad (19.11.52)$$

$$\sigma = \frac{P_{\text{rad}}}{|\mathcal{P}^i|}, \quad \tau = \frac{\sigma}{\pi a^2} = \frac{P_{\text{rad}}}{|\mathcal{P}^i| \cdot \pi a^2} \quad (19.11.53)$$

Thus, for Eqs. (19.11.44) and (19.11.50), we have,

$$\begin{aligned}\tau &= \frac{64 (ka)^4}{27\pi^2} \cdot \frac{|\eta \mathbf{H}_{\perp}^i|^2 + \frac{1}{4} |E_z^i|^2}{|\eta \text{Re}[\mathbf{E}^i \times \mathbf{H}^{i*}]|} \quad (\text{Bethe-Bouwkamp}) \\ \tau &= \frac{(ka)^2}{3} \cdot \frac{|\mathbf{E}_{\perp}^i|^2}{|\eta \text{Re}[\mathbf{E}^i \times \mathbf{H}^{i*}]|} \quad (\text{Kirchhoff approximation})\end{aligned}\quad (19.11.54)$$

The second factors depend on the particulars of the incident fields. As an example, consider an incident plane wave decomposed into a sum of a TE part (i.e., the E_0 terms) and a TM part (the H_0 terms,) with TE/TM being defined with respect to the plane of incidence, which may be taken to be the xz plane without loss of generality,

$$\begin{aligned}\mathbf{E}^i &= \left[\hat{\mathbf{y}} E_0 + (\hat{\mathbf{x}} k_z^i - \hat{\mathbf{z}} k_x^i) \frac{\eta H_0}{k} \right] e^{-jk_x^i x - jk_z^i z} \\ \mathbf{H}^i &= \left[\hat{\mathbf{y}} H_0 - (\hat{\mathbf{x}} k_z^i - \hat{\mathbf{z}} k_x^i) \frac{E_0}{\eta k} \right] e^{-jk_x^i x - jk_z^i z} \\ \mathbf{k}^i &= \hat{\mathbf{x}} k_x^i + \hat{\mathbf{z}} k_z^i\end{aligned}\quad (19.11.55)$$

This may represent either a propagating plane wave or an evanescent one. For the propagating case, if θ_i is the angle of incidence with respect to the z -axis, then,

$$k_x^i = k \sin \theta_i, \quad k_z^i = k \cos \theta_i = \sqrt{k^2 - |k_x^i|^2} \quad (19.11.56)$$

For the evanescent case, we have $k_x^i \geq k$, and k_z^i is given by the evanescent square root,

$$k_x^i \geq k, \quad k_z^i = -j \sqrt{|k_x^i|^2 - k^2} \quad (19.11.57)$$

The plane wave satisfies, $\mathbf{k}^i \cdot \mathbf{E}^i = \mathbf{k}^i \cdot \mathbf{H}^i = 0$, and, $\eta \mathbf{k} \mathbf{H}^i = \mathbf{k}^i \times \mathbf{E}^i$. Since k_x^i is always real-valued, but k_z^i may be complex, we have, $\mathbf{k}^{i*} = \hat{\mathbf{x}} k_x^i + \hat{\mathbf{z}} k_z^{i*} = \mathbf{k}^i + \hat{\mathbf{z}} (k_z^{i*} - k_z^i)$, which implies, $\mathbf{k}^{i*} \cdot \mathbf{E}^i = \mathbf{k}^i \cdot \mathbf{E}^i + E_z^i (k_z^{i*} - k_z^i) = E_z^i (k_z^{i*} - k_z^i) = -(k_z^{i*} - k_z^i) \eta H_0 k_x^i / k$. Using these results, we obtain the time-averaged Poynting vector,

$$\begin{aligned}\mathcal{P}^i &= \frac{1}{2} \text{Re}[\mathbf{E}^i \times \mathbf{H}^{i*}] = \frac{1}{2k\eta} \text{Re}[\mathbf{E}^i \times (\mathbf{k}^{i*} \times \mathbf{E}^i)] = \\ &= \frac{1}{2k\eta} \text{Re} \left[\mathbf{k}^{i*} |\mathbf{E}^i|^2 - \mathbf{E}^{i*} (\mathbf{k}^{i*} \cdot \mathbf{E}^i) \right] = \frac{1}{2k\eta} \text{Re} \left[\mathbf{k}^{i*} |\mathbf{E}^i|^2 - \mathbf{E}^{i*} E_z^i (k_z^{i*} - k_z^i) \right]\end{aligned}$$

From this and the definitions (19.11.55), we obtain the x, y, z components of the Poynting vector \mathbf{P}^i , which are valid for both the propagating and the evanescent cases,

$$\begin{aligned} P_x &= \frac{1}{2\eta} \frac{k_x^i}{k} \left[|E_0|^2 + |\eta H_0|^2 \right] \\ P_y &= \frac{1}{2\eta} \frac{k_x^i}{k} \left[\frac{2 \operatorname{Im}(k_z^i)}{k} \operatorname{Im}[E_0 \eta H_0^*] \right] \\ P_z &= \frac{1}{2\eta} \frac{\operatorname{Re}(k_z^i)}{k} \left[|E_0|^2 + |\eta H_0|^2 \frac{|k_x^i|^2 + |k_z^i|^2}{k^2} \right] \end{aligned} \quad (19.11.58)$$

We note that, as expected, $P_z = 0$ in the evanescent case. The corresponding magnitudes, $|\mathbf{P}^i| = \sqrt{P_x^2 + P_y^2 + P_z^2}$, are in the two cases,

$$|\mathbf{P}^i| = \frac{1}{2\eta} \left[|E_0|^2 + |\eta H_0|^2 \right] \cdot K_i \quad (19.11.59)$$

where the factor K_i is defined as,

$$\begin{aligned} K_i &= 1 \quad (\text{propagating}) \\ K_i &= \frac{k_x^i}{k} \left[1 + \left(\frac{2 \operatorname{Im}(k_z^i) \operatorname{Im}[E_0 \eta H_0^*]}{k[|E_0|^2 + |\eta H_0|^2]} \right)^2 \right]^{1/2} \quad (\text{evanescent}) \end{aligned} \quad (19.11.60)$$

If the TE or TM fields are incident separately, or, if E_0, H_0 have the same phase, then, $K_i = k_x^i/k$ in the evanescent case. Similarly, we can express the quantity,

$$|\eta \mathbf{H}_\perp^i|^2 + \frac{1}{4} |E_z^i|^2 = \frac{|k_z^i|^2}{k^2} |E_0|^2 + \left(1 + \frac{1}{4} \frac{|k_x^i|^2}{k^2} \right) |\eta H_0|^2 \quad (19.11.61)$$

Thus, the radiated power and the transmission coefficient for the Bethe-Bouwkamp case can be written as,

$$P_{\text{rad}} = \frac{64(ka)^4}{27\pi^2} \cdot \pi a^2 \cdot \frac{1}{2\eta} \left[\frac{|k_z^i|^2}{k^2} |E_0|^2 + \left(1 + \frac{1}{4} \frac{|k_x^i|^2}{k^2} \right) |\eta H_0|^2 \right] \quad (19.11.62)$$

$$\tau = \frac{64(ka)^4}{27\pi^2} \cdot \frac{\frac{|k_z^i|^2}{k^2} |E_0|^2 + \left(1 + \frac{1}{4} \frac{|k_x^i|^2}{k^2} \right) |\eta H_0|^2}{K_i \left[|E_0|^2 + |\eta H_0|^2 \right]} \quad (19.11.63)$$

In particular, for the propagating case, we obtain Bethe's result,

$$\tau = \frac{64(ka)^4}{27\pi^2} \cdot \frac{\cos^2 \theta_i |E_0|^2 + \left(1 + \frac{1}{4} \sin^2 \theta_i \right) |\eta H_0|^2}{|E_0|^2 + |\eta H_0|^2} \quad (19.11.64)$$

Example 19.11.1: The phenomenon of extraordinary optical transmission [1373–1397] is not observed in the idealized Bethe-Bouwkamp case, but requires more complicated structures consisting of conductors of finite thickness or arrays of holes. One possible explanation of the phenomenon is that it is due to the coupling of evanescent surface plasmons to the

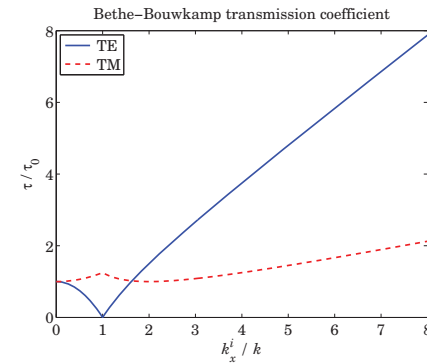
subwavelength holes. As a step in this direction, Petersson and Smith [1357] showed that the transmission coefficient of an evanescent plane wave in the Bethe-Bouwkamp model is much larger than for the case of ordinary propagating incident waves.

Here, we consider the same example of [1357], but our calculations correspond only to their lowest-order results. The example has $ka = \pi/100$, and for the TE case, we set $E_0 = 1, \eta H_0 = 0$, and for TM, $E_0 = 0, \eta H_0 = 1$. The following MATLAB code calculates τ from Eq. (19.11.63) over the range, $0 \leq k_x^i/k \leq 8$ and plots τ/τ_0 , in the figure below, where $\tau_0 = 64(ka)^4/(27\pi^2) = 2.3395 \times 10^{-7}$. The evanescent range corresponds to $k_x^i/k > 1$.

```
ka = pi/100;
kx = linspace(0,8,161);
kz = sqrt(1-kx.^2).*(kx<=1) - j*sqrt(kx.^2-1).*(kx>1);
Ki = (kx<=1) + kx.*(kx>1);
tau0 = 64*(ka)^4/27/pi^2;

tau_te = abs(kz).^2 ./ Ki;
tau_tm = (1 + kx.^2/4) ./ Ki;

plot(kx,tau_te,'b-', kx,tau_tm,'r--');
```



Example 19.11.2: Consider the Kirchhoff approximation of Eqs. (19.11.45)–(19.11.47) under the incident plane wave of Eq. (19.11.55). In this case, the 2-D spatial Fourier transform in Eq. (19.11.46) can be done exactly [1333] regardless of the size of the aperture. The incident field at the aperture is, with $k_x^i = k \sin \theta_i$, $k_z^i = k \cos \theta_i$,

$$E_\perp^i(\mathbf{r}'_\perp, 0) = \left(\hat{\mathbf{x}} \frac{k_z^i}{k} \eta H_0 + \hat{\mathbf{y}} E_0 \right) e^{-jk_x^i x'}$$

and its Fourier transform,

$$\hat{E}_\perp^i(k_x, k_y) = \int_A E_\perp^i(\mathbf{r}'_\perp, 0) e^{jk_x \cdot \mathbf{r}'_\perp} d^2 \mathbf{r}'_\perp = \left(\hat{\mathbf{x}} \frac{k_z^i}{k} \eta H_0 + \hat{\mathbf{y}} E_0 \right) \int_A e^{j(k_x - k_x^i)x' + k_y y'} dx' dy'$$

The integral over the circular aperture can be done exactly,

$$f(k_x, k_y) = \int_A e^{j(k_x - k_x^i)x' + k_y y'} dx' dy' = \pi a^2 \cdot \frac{2J_1(q_\perp a)}{q_\perp a} \quad (19.11.65)$$

where, $q_{\perp} = \sqrt{(k_x - k_x^i)^2 + k_y^2}$, and J_1 is the Bessel function of order-1. Thus, the Fourier transform components are,

$$\begin{aligned}\hat{E}_x^i(k_x, k_y) &= \frac{k_z^i}{k} \eta H_0 \cdot f(k_x, k_y) \\ \hat{E}_y^i(k_x, k_y) &= E_0 \cdot f(k_x, k_y)\end{aligned}\quad (19.11.66)$$

The radiation zone fields are obtained from (19.11.47),

$$\begin{aligned}E_{\theta} &= 2jk \left(\frac{k_z^i}{k} \eta H_0 \cos \phi + E_0 \sin \phi \right) \cdot \pi a^2 \cdot \frac{2J_1(q_{\perp} a)}{q_{\perp} a} \cdot \frac{e^{-jkr}}{4\pi r} \\ E_{\phi} &= 2jk \cos \theta \left(E_0 \cos \phi - \frac{k_z^i}{k} \eta H_0 \sin \phi \right) \cdot \pi a^2 \cdot \frac{2J_1(q_{\perp} a)}{q_{\perp} a} \cdot \frac{e^{-jkr}}{4\pi r}\end{aligned}\quad (19.11.67)$$

Since in spherical coordinates, $k_x = k \sin \theta \cos \phi$, $k_y = k \sin \theta \sin \phi$, we have,

$$\begin{aligned}q_{\perp} &= \sqrt{(k_x - k_x^i)^2 + k_y^2} = k \sqrt{(\sin \theta \cos \phi - \sin \theta_i \cos \phi)^2 + \sin^2 \theta \sin^2 \phi} \\ &= k \sqrt{\sin^2 \theta - 2 \sin \theta \sin \theta_i \cos \phi + \sin^2 \theta_i}\end{aligned}$$

If the \mathbf{r}' -dependence of the incident fields is ignored, that is, setting $k_x^i = 0$ in the exponent of Eq. (19.11.65), then, $q_{\perp} = k \sin \theta$, and one recovers the usual Airy pattern of a uniform circular aperture, as we discussed in Sec. 18.9. \square

19.12 Plane-Wave Spectrum – Bethe-Bouwkamp Model

We saw in Sections 19.5 and 19.8 that Smythe's diffraction formulas are equivalent to the plane-wave spectrum representation, for $z \geq 0$,

$$\begin{aligned}E(\mathbf{r}_{\perp}, z) &= \nabla \times \int_{-\infty}^{\infty} \hat{\mathbf{z}} \times E_{\perp}(\mathbf{r}'_{\perp}, 0) \frac{e^{-jkR}}{2\pi R} d^2 \mathbf{r}'_{\perp} \\ &= \int_{-\infty}^{\infty} \left[\hat{\mathbf{E}}_{\perp}(\mathbf{k}_{\perp}) + \hat{\mathbf{z}} \hat{E}_z(\mathbf{k}_{\perp}) \right] e^{-jk_{\perp} \cdot \mathbf{r}_{\perp}} e^{-jk_z z} \frac{d^2 \mathbf{k}_{\perp}}{(2\pi)^2}\end{aligned}\quad (19.12.1)$$

where, $R = \sqrt{|\mathbf{r}_{\perp} - \mathbf{r}'_{\perp}|^2 + z^2}$, and, $\mathbf{k} = \mathbf{k}_{\perp} + \hat{\mathbf{z}} k_z = \hat{\mathbf{x}} k_x + \hat{\mathbf{y}} k_y + \hat{\mathbf{z}} k_z$, with the z -component derived from the condition, $\mathbf{k} \cdot \hat{\mathbf{E}} = 0$,

$$\hat{E}_z(\mathbf{k}_{\perp}) = -\frac{\mathbf{k}_{\perp} \cdot \hat{\mathbf{E}}_{\perp}(\mathbf{k}_{\perp})}{k_z}\quad (19.12.2)$$

where $\hat{\mathbf{E}}_{\perp}(\mathbf{k}_{\perp})$ is the 2-D Fourier transform of the aperture transverse field $E_{\perp}(\mathbf{r}_{\perp}, 0)$,

$$\hat{\mathbf{E}}_{\perp}(\mathbf{k}_{\perp}) = \int_{-\infty}^{\infty} E_{\perp}(\mathbf{r}_{\perp}, 0) e^{jk_{\perp} \cdot \mathbf{r}_{\perp}} d^2 \mathbf{r}_{\perp}\quad (19.12.3)$$

Its inverse Fourier transform is,

$$E_{\perp}(\mathbf{r}_{\perp}, 0) = \int_{-\infty}^{\infty} \hat{\mathbf{E}}_{\perp}(\mathbf{k}_{\perp}) e^{-jk_{\perp} \cdot \mathbf{r}_{\perp}} \frac{d^2 \mathbf{k}_{\perp}}{(2\pi)^2}\quad (19.12.4)$$

Similarly, the magnetic field is given by,

$$\mathbf{H}(\mathbf{r}_{\perp}, z) = \int_{-\infty}^{\infty} \hat{\mathbf{H}}(\mathbf{k}_{\perp}) e^{-jk_{\perp} \cdot \mathbf{r}_{\perp}} e^{-jk_z z} \frac{d^2 \mathbf{k}_{\perp}}{(2\pi)^2}\quad (19.12.5)$$

where, the 2-D Fourier transform $\hat{\mathbf{H}}(\mathbf{k}_{\perp})$ is related to $\hat{\mathbf{E}}_{\perp}(\mathbf{k}_{\perp})$ by,

$$k \eta \hat{\mathbf{H}}(\mathbf{k}_{\perp}) = \mathbf{k} \times \hat{\mathbf{E}}(\mathbf{k}_{\perp}) = \mathbf{k} \times \left[\hat{\mathbf{E}}_{\perp}(\mathbf{k}_{\perp}) + \hat{\mathbf{z}} \hat{E}_z(\mathbf{k}_{\perp}) \right]\quad (19.12.6)$$

Since the Bethe-Bouwkamp field $E_{\perp}(\mathbf{r}_{\perp}, 0)$ is known explicitly, its 2-D Fourier transform $\hat{\mathbf{E}}_{\perp}(\mathbf{k}_{\perp})$ can be determined analytically [1350-1353, 1359, 1360]. The spatial integration in (19.12.3) can be restricted to the aperture A only since E_{\perp} vanishes on the conductor. Thus,

$$\hat{\mathbf{E}}_{\perp}(\mathbf{k}_{\perp}) = \int_A \left[A \frac{\mathbf{r}_{\perp}}{\Delta(\rho)} + B \Delta(\rho) + C \Delta(\rho) - \frac{(\mathbf{C} \cdot \mathbf{r}_{\perp}) \mathbf{r}_{\perp}}{\Delta(\rho)} \right] e^{jk_{\perp} \cdot \mathbf{r}_{\perp}} d^2 \mathbf{r}_{\perp}\quad (19.12.7)$$

Let us introduce cylindrical coordinates for the transverse wavenumber, $\mathbf{k}_{\perp} = \hat{\mathbf{x}} k_x + \hat{\mathbf{y}} k_y$,

$$\begin{aligned}k_{\rho} &= |\mathbf{k}_{\perp}| = \sqrt{k_x^2 + k_y^2} & k_x &= k_{\rho} \cos \psi \\ \psi &= \text{atan2}(k_y, k_x) & k_y &= k_{\rho} \sin \psi \\ \hat{\mathbf{k}}_{\perp} &= \frac{\mathbf{k}_{\perp}}{k_{\rho}} & \hat{\mathbf{k}}_{\perp} &= \hat{\mathbf{x}} \cos \psi + \hat{\mathbf{y}} \sin \psi\end{aligned}\quad (19.12.8)$$

The required 2-D Fourier transforms in Eq. (19.12.7) are all expressible in terms of the spherical Bessel functions, $j_1(k_{\rho} a)$, $j_2(k_{\rho} a)$, of orders 1 and 2, which are defined as follows (see also Appendix J),

$$\begin{aligned}j_0(z) &= \frac{\sin z}{z} \\ j_1(z) &= -j'_0(z) = \frac{\sin z - z \cos z}{z^2} \\ j_2(z) &= -z \left(\frac{j_1(z)}{z} \right)' = \frac{(3 - z^2) \sin z - 3z \cos z}{z^3}\end{aligned}\quad (19.12.9)$$

where the prime denotes differentiation. They are connected by the identity,

$$j_0(z) + j_2(z) = \frac{3j_1(z)}{z}\quad (19.12.10)$$

The Fourier transforms of the individual terms in (19.12.7) are as follows,

$$\begin{aligned}\int_A \frac{\mathbf{r}_{\perp}}{\Delta(\rho)} e^{jk_{\perp} \cdot \mathbf{r}_{\perp}} d^2 \mathbf{r}_{\perp} &= 2\pi a^2 \cdot \frac{j_1(\mathbf{k}_{\perp})}{k_{\rho}} j_1(k_{\rho} a) \\ \int_A \Delta(\rho) e^{jk_{\perp} \cdot \mathbf{r}_{\perp}} d^2 \mathbf{r}_{\perp} &= 2\pi a^2 \cdot \frac{j_1(k_{\rho} a)}{k_{\rho}} \\ \int_A \left[C \Delta(\rho) - \frac{(\mathbf{C} \cdot \mathbf{r}_{\perp}) \mathbf{r}_{\perp}}{\Delta(\rho)} \right] e^{jk_{\perp} \cdot \mathbf{r}_{\perp}} d^2 \mathbf{r}_{\perp} &= 2\pi a^3 \cdot \frac{\mathbf{k}_{\perp} (\mathbf{C} \cdot \mathbf{k}_{\perp})}{k_{\rho}^2} j_2(k_{\rho} a)\end{aligned}\quad (19.12.11)$$

All of these are obtained from the following basic transform and its differentiation with respect to k_x and k_y , (see Problem 19.4),

$$\int_A \frac{1}{\Delta(\rho)} e^{jk_{\perp} \cdot r_{\perp}} d^2 r_{\perp} = 2\pi a \cdot j_0(k_{\rho} a) \quad (19.12.12)$$

Indeed, using the cylindrical coordinate definitions in (19.11.1) and (19.12.8), we have, $\mathbf{k}_{\perp} \cdot \mathbf{r}_{\perp} = k_{\rho} \rho \cos(\phi - \psi)$, and

$$\begin{aligned} \int_A \frac{1}{\Delta(\rho)} e^{jk_{\perp} \cdot r_{\perp}} d^2 r_{\perp} &= \int_0^a \int_0^{2\pi} \frac{1}{\sqrt{a^2 - \rho^2}} e^{jk_{\rho} \rho \cos(\phi - \psi)} \rho d\rho d\phi = \\ &= \int_0^a \frac{J_0(k_{\rho} \rho)}{\sqrt{a^2 - \rho^2}} 2\pi \rho d\rho = 2\pi \cdot \frac{\sin(k_{\rho} a)}{k_{\rho}} = 2\pi a \cdot \frac{\sin(k_{\rho} a)}{k_{\rho} a} \end{aligned}$$

It follows now that the transform (19.12.7) of $E_{\perp}(\mathbf{r}_{\perp}, 0)$ is,

$$\hat{E}_{\perp}(\mathbf{k}_{\perp}) = 2\pi a^2 \cdot \frac{j\mathbf{k}_{\perp} A + B}{k_{\rho}} j_1(k_{\rho} a) + 2\pi a^3 \cdot \frac{\mathbf{k}_{\perp} (\mathbf{k}_{\perp} \cdot \mathbf{C})}{k_{\rho}^2} j_2(k_{\rho} a) \quad (19.12.13)$$

and to clarify the notation, we write (19.12.13) component-wise,

$$\begin{aligned} \hat{E}_x &= 2\pi a^2 \cdot \frac{j k_x A + B_x}{k_{\rho}} j_1(k_{\rho} a) + 2\pi a^3 \cdot \frac{k_x (k_x C_x + k_y C_y)}{k_{\rho}^2} j_2(k_{\rho} a) \\ \hat{E}_y &= 2\pi a^2 \cdot \frac{j k_y A + B_y}{k_{\rho}} j_1(k_{\rho} a) + 2\pi a^3 \cdot \frac{k_y (k_x C_x + k_y C_y)}{k_{\rho}^2} j_2(k_{\rho} a) \end{aligned} \quad (19.12.14)$$

The transforms of the remaining field components are expressible in terms of $\hat{E}_{\perp}(\mathbf{k}_{\perp})$,

$$\hat{E}_z = -\frac{\mathbf{k}_{\perp} \cdot \hat{E}_{\perp}}{k_z} = -2\pi a^2 \cdot \frac{j k_{\rho}^2 A + \mathbf{k}_{\perp} \cdot \mathbf{B}}{k_{\rho} k_z} j_1(k_{\rho} a) - 2\pi a^3 \cdot \frac{\mathbf{k}_{\perp} \cdot \mathbf{C}}{k_z} j_2(k_{\rho} a) \quad (19.12.15)$$

Resolving (19.12.6) into transverse and longitudinal parts, we have,

$$\eta \hat{H}_z = \frac{\hat{\mathbf{z}} \cdot (\mathbf{k}_{\perp} \times \hat{E}_{\perp})}{k} = -2\pi a^2 \cdot \frac{\hat{\mathbf{z}} \cdot (\mathbf{B} \times \mathbf{k}_{\perp})}{k k_{\rho}} j_1(k_{\rho} a) \quad (19.12.16)$$

$$\begin{aligned} \eta \hat{H}_{\perp} \times \hat{\mathbf{z}} &= \frac{k_z \hat{E}_{\perp} - \mathbf{k}_{\perp} \hat{E}_z}{k} = \frac{k_z^2 \hat{E}_{\perp} - \mathbf{k}_{\perp} k_z \hat{E}_z}{k k_z} = \frac{k_z^2 \hat{E}_{\perp} + \mathbf{k}_{\perp} (\mathbf{k}_{\perp} \cdot \hat{E}_{\perp})}{k k_z} \\ &= \frac{(k^2 - k_z^2) \hat{E}_{\perp} + \mathbf{k}_{\perp} (\mathbf{k}_{\perp} \cdot \hat{E}_{\perp})}{k k_z} = \frac{k \hat{E}_{\perp}}{k_z} - \frac{\mathbf{k}_{\perp} \times (\hat{E}_{\perp} \times \mathbf{k}_{\perp})}{k k_z}, \quad \text{or,} \end{aligned}$$

$$\begin{aligned} \eta \hat{H}_{\perp} \times \hat{\mathbf{z}} &= 2\pi k a^2 \cdot \frac{j \mathbf{k}_{\perp} A + B}{k_{\rho} k_z} j_1(k_{\rho} a) + 2\pi k a^3 \cdot \frac{\mathbf{k}_{\perp} (\mathbf{C} \cdot \mathbf{k}_{\perp})}{k_{\rho}^2 k_z} j_2(k_{\rho} a) \\ &\quad - 2\pi a^2 \cdot \frac{\mathbf{k}_{\perp} \times (\mathbf{B} \times \mathbf{k}_{\perp})}{k k_{\rho} k_z} j_1(k_{\rho} a) \end{aligned} \quad (19.12.17)$$

In deriving the radiation fields of Eqs. (19.11.36) and (19.11.37), we kept terms up to first order in ka . The same results can be obtained by taking the small- ka limit of Eq. (19.12.13). Indeed, using the Taylor series expansions for j_1, j_2 ,

$$j_1(z) \approx \frac{z}{3}, \quad j_2(z) \approx \frac{z^2}{15}, \quad \text{for small } z$$

we obtain the following approximation, where terms of order $(ka)^2$ are ignored,

$$\begin{aligned} \hat{E}_{\perp}(\mathbf{k}_{\perp}) &= 2\pi a^2 \cdot \frac{j \mathbf{k}_{\perp} A + B}{k_{\rho}} j_1(k_{\rho} a) + 2\pi a^3 \cdot \frac{(\mathbf{k}_{\perp} \cdot \mathbf{C}) \mathbf{k}_{\perp}}{k_{\rho}^2} j_2(k_{\rho} a) \\ &\approx \frac{2\pi a^3}{3} (j \mathbf{k}_{\perp} A + B) + \frac{2\pi a^5}{15} (\mathbf{k}_{\perp} \cdot \mathbf{C}) \mathbf{k}_{\perp} \approx \frac{2\pi a^3}{3} (j \mathbf{k}_{\perp} A + B) \end{aligned}$$

which agrees with Eq. (19.11.38). The radiation fields are then obtained from Eq. (19.6.1), which is equivalent to (19.11.36) and to (19.11.40),

$$E_{\text{rad}} = 2jk \cos \theta \hat{E}(\mathbf{k}_{\perp}) G(r) = 2jk \cos \theta \frac{2\pi a^3}{3} (j \mathbf{k}_{\perp} A + B) \frac{e^{-jkr}}{4\pi r} \quad (19.12.18)$$

Besides obtaining the radiation fields, the usefulness of the plane-wave spectrum representation lies in allowing the calculation of the fields at any distance $z \geq 0$ from the aperture by performing an inverse 2-D Fourier transform. The inverse transform for any field component is,

$$E(\mathbf{r}_{\perp}, z) = \int_{-\infty}^{\infty} \hat{E}(\mathbf{k}_{\perp}) e^{-jk_{\perp} \cdot \mathbf{r}_{\perp}} e^{-jk_z z} \frac{d^2 \mathbf{k}_{\perp}}{(2\pi)^2} \quad (19.12.19)$$

Using cylindrical coordinates for both \mathbf{r}_{\perp} and \mathbf{k}_{\perp} as defined in Eqs. (19.11.1) and (19.12.8), and noting that $dk_x dk_y = k_{\rho} dk_{\rho} d\psi$, and, $\mathbf{k}_{\perp} \cdot \mathbf{r}_{\perp} = k_{\rho} \rho \cos(\psi - \phi)$, and that k_z depends only on k_{ρ} , we may rewrite (19.12.19) in the form,

$$E(\rho, \phi, z) = \int_0^{\infty} \int_0^{2\pi} \hat{E}(k_{\rho}, \psi) e^{-jk_{\rho} \rho \cos(\psi - \phi)} e^{-jk_z z} \frac{k_{\rho} dk_{\rho} d\psi}{(2\pi)^2}$$

and express it as a two-step process of first integrating with respect to the angle ψ and then with respect to k_{ρ} ,

$$\begin{aligned} \tilde{E}(\rho, \phi, k_{\rho}) &= \int_0^{2\pi} \hat{E}(k_{\rho}, \psi) e^{-jk_{\rho} \rho \cos(\psi - \phi)} \frac{d\psi}{(2\pi)^2} \\ E(\rho, \phi, z) &= \int_0^{\infty} \tilde{E}(\rho, \phi, k_{\rho}) e^{-jk_z z} k_{\rho} dk_{\rho} \end{aligned} \quad (19.12.20)$$

$$\hat{E}(k_{\rho}, \psi) \rightarrow \int d\psi \rightarrow \tilde{E}(\rho, \phi, k_{\rho}) \rightarrow \int dk_{\rho} \rightarrow E(\rho, \phi, z)$$

The ψ -dependence is separated from the k_ρ -dependence in \hat{E}, \hat{H} . To see this, we may rewrite \hat{E}, \hat{H} in terms of the angular unit vector, $\hat{k}_\perp = \hat{x} \cos \psi + \hat{y} \sin \psi$,

$$\begin{aligned}\hat{E}_\perp &= 2\pi a^2 j \hat{k}_\perp A j_1 + 2\pi a^2 \mathbf{B} \frac{j_1}{jk_z} + 2\pi a^3 \hat{k}_\perp (\hat{k}_\perp \cdot \mathbf{C}) j_2 \\ \hat{E}_z &= 2\pi a^2 A \frac{k_\rho j_1}{jk_z} - 2\pi a^2 (j \hat{k}_\perp \cdot \mathbf{B}) \frac{j_1}{jk_z} - 2\pi a^3 (j \hat{k}_\perp \cdot \mathbf{C}) \frac{k_\rho j_2}{jk_z} \\ \eta \hat{H}_z &= 2\pi a^2 \cdot \frac{j \hat{k}_\perp \cdot (\mathbf{B} \times \hat{z})}{jk} j_1 \\ \eta \hat{H}_\perp \times \hat{z} &= 2\pi j k a^2 j \hat{k}_\perp A \frac{j_1}{jk_z} + 2\pi j k a^2 \mathbf{B} \frac{j_1}{jk_z k_\rho} + 2\pi j k a^3 \hat{k}_\perp (\hat{k}_\perp \cdot \mathbf{C}) \frac{j_2}{jk_z} \\ &\quad + 2\pi a^2 \frac{\hat{k}_\perp \times (\mathbf{B} \times \hat{k}_\perp)}{jk} \frac{k_\rho j_1}{jk_z}\end{aligned}\quad (19.12.21)$$

where for simplicity, j_1, j_2 stand for $j_1(k_\rho a), j_2(k_\rho a)$, and for a reason to become clear later, in some terms we have multiplied and divided by j so that k_z appears as, jk_z . The angular integrations over ψ can be done with the help of the following integrals resulting in the ordinary Bessel functions of orders 0,1,2,

$$\int_0^{2\pi} \frac{d\psi}{2\pi} e^{-jk_\rho \rho \cos(\psi-\phi)} \begin{bmatrix} 1 \\ j \hat{k}_\perp \\ \hat{k}_\perp (\mathbf{C} \cdot \hat{k}_\perp) \\ \hat{k}_\perp \times (\mathbf{B} \times \hat{k}_\perp) \end{bmatrix} = \begin{bmatrix} J_0 \\ \hat{r}_\perp J_1 \\ \frac{\mathbf{C}}{2} (J_0 + J_2) - \hat{r}_\perp (\mathbf{C} \cdot \hat{r}_\perp) J_2 \\ \frac{\mathbf{B}}{2} (J_0 - J_2) + \hat{r}_\perp (\mathbf{B} \cdot \hat{r}_\perp) J_2 \end{bmatrix}\quad (19.12.22)$$

where, $\hat{r}_\perp = \hat{x} \cos \phi + \hat{y} \sin \phi$, and J_0, J_1, J_2 stand for $J_0(k_\rho \rho), J_1(k_\rho \rho), J_2(k_\rho \rho)$. Equations (19.12.22) are consequences of the following relationship, for real z ,

$$\int_0^{2\pi} \frac{d\psi}{2\pi} e^{-jz \cos(\psi-\phi)} e^{\pm jn\psi} = (-j)^n J_n(z) e^{\pm jn\phi}\quad (19.12.23)$$

which is a consequence of the standard Fourier series expansion [1822],

$$e^{jz \cos \theta} = \sum_{n=0}^{\infty} j^n J_n(z) e^{jn\theta}\quad (19.12.24)$$

It follows that the angle integrations in Eqs. (19.12.21) will be,

$$\begin{aligned}\hat{E}_\perp &= a^2 \hat{r}_\perp A J_1 j_1 + a^2 \mathbf{B} \frac{J_0 j_1}{k_\rho} + a^3 \frac{\mathbf{C}}{2} (J_0 + J_2) j_2 - a^3 \hat{r}_\perp (\mathbf{C} \cdot \hat{r}_\perp) J_2 j_2 \\ \hat{E}_z &= a^2 A \frac{k_\rho J_0 j_1}{jk_z} - a^2 (\mathbf{B} \cdot \hat{r}_\perp) \frac{J_1 j_1}{jk_z} - a^3 (\mathbf{C} \cdot \hat{r}_\perp) \frac{k_\rho J_1 j_2}{jk_z} \\ \eta \hat{H}_z &= a^2 \cdot \frac{\hat{r}_\perp \cdot (\mathbf{B} \times \hat{z})}{jk} J_1 j_1 \\ \eta \hat{H}_\perp \times \hat{z} &= j k a^2 \hat{r}_\perp A \frac{J_1 j_1}{jk_z} + j k a^2 \mathbf{B} \frac{J_0 j_1}{jk_z k_\rho} \\ &\quad + j k a^3 \frac{\mathbf{C}}{2} \frac{(J_0 + J_2) j_2}{jk_z} - j k a^3 \hat{r}_\perp (\mathbf{C} \cdot \hat{r}_\perp) \frac{J_2 j_2}{jk_z} \\ &\quad + a^2 \frac{\mathbf{B}}{2jk} \frac{k_\rho (J_0 - J_2) j_1}{jk_z} + a^2 \frac{\hat{r}_\perp (\mathbf{B} \cdot \hat{r}_\perp)}{jk} \frac{k_\rho J_2 j_1}{jk_z}\end{aligned}\quad (19.12.25)$$

The ϕ -dependence resides in \hat{r}_\perp , while all the other factors are functions of k_ρ . The final step requires that all terms be multiplied by $k_\rho e^{-jk_z z}$ and integrated over k_ρ . Following Michalski and Mosig [1364], we introduce the following Hankel-transform integrals, multiplied by enough factors of a to make them dimensionless,

$$F_{nm}^{pq}(\rho, z) = a^{p-q+1} \int_0^\infty \frac{(k_\rho)^p}{(jk_z)^q} J_n(k_\rho \rho) j_m(k_\rho a) e^{-jk_z z} dk_\rho\quad (19.12.26)$$

With these definitions, the E -fields at the observation point (ρ, ϕ, z) are given by,

$$\begin{aligned}E_\perp(\rho, \phi, z) &= \hat{r}_\perp A F_{11}^{10} + a \mathbf{B} F_{01}^{00} + \frac{a \mathbf{C}}{2} (F_{02}^{10} + F_{22}^{10}) - a \hat{r}_\perp (\mathbf{C} \cdot \hat{r}_\perp) F_{22}^{10} \\ E_z(\rho, \phi, z) &= A F_{01}^{21} - a (\mathbf{B} \cdot \hat{r}_\perp) F_{11}^{11} - a (\mathbf{C} \cdot \hat{r}_\perp) F_{12}^{21}\end{aligned}\quad (19.12.27)$$

It proves convenient to use the identity (19.12.10) to express the quantities F_{02}^{10}, F_{12}^{21} , in terms of the following F 's,

$$\begin{aligned}F_{02}^{10} &= 3F_{01}^{00} - F_{00}^{10} \\ F_{12}^{21} &= 3F_{11}^{11} - F_{10}^{21}\end{aligned}\quad (19.12.28)$$

With these substitutions, the E -fields as well as the H -fields become,

$$\begin{aligned}E_\perp &= \hat{r}_\perp A F_{11}^{10} + a \mathbf{B} F_{01}^{00} + \frac{a \mathbf{C}}{2} (3F_{01}^{00} - F_{00}^{10} + F_{22}^{10}) - a \hat{r}_\perp (\mathbf{C} \cdot \hat{r}_\perp) F_{22}^{10} \\ E_z &= A F_{01}^{21} - a (\mathbf{B} \cdot \hat{r}_\perp) F_{11}^{11} - a (\mathbf{C} \cdot \hat{r}_\perp) (3F_{11}^{11} - F_{10}^{21}) \\ \eta H_z &= \frac{\hat{r}_\perp \cdot (\mathbf{B} \times \hat{z})}{jk} F_{11}^{10} \\ \eta H_\perp \times \hat{z} &= j k a \hat{r}_\perp A F_{11}^{11} + \frac{\mathbf{B}}{2jk} (F_{01}^{21} - F_{21}^{21}) + \frac{\hat{r}_\perp (\mathbf{B} \cdot \hat{r}_\perp)}{jk} F_{21}^{21} \\ &\quad + j k a^2 \mathbf{B} F_{01}^{01} + j k a^2 \frac{\mathbf{C}}{2} (F_{02}^{11} + F_{22}^{11}) - j k a^2 \hat{r}_\perp (\mathbf{C} \cdot \hat{r}_\perp) F_{22}^{11}\end{aligned}\quad (19.12.29)$$

These expressions reduce to those of Ref. [1364] for the case of incident plane waves.

Near-Field Approximation

Closed-form expressions for the near fields in the Bethe-Bouwkamp model have been derived for normal incidence by Bouwkamp [1322,1323] and Klimov and Letokhov [1350], and for more general incident plane waves, by Michalski and Mosig [1364].

Here, we follow the approach of [1364] in which the Hankel-type integrals, $F_{nm}^{pq}(\rho, z)$, in (19.12.29) are replaced by simple closed-form expressions when z is small. The limit $z \rightarrow 0$ corresponds in the Fourier domain to the limit $k_\rho \rightarrow \infty$, so that k_z can be replaced by its evanescent limit, $k_z = -j\sqrt{k_\rho^2 - k^2} \rightarrow -jk_\rho$, or, $jk_z = k_\rho$, and the Hankel integrals can be approximated by,

$$\begin{aligned} F_{nm}^{pq}(\rho, z) &= a^{p-q+1} \int_0^\infty \frac{(k_\rho)^p}{(jk_z)^q} J_n(k_\rho \rho) j_m(k_\rho a) e^{-jk_z z} dk_\rho \xrightarrow{\text{small } z} \\ &\approx a^{p-q+1} \int_0^\infty \frac{(k_\rho)^p}{(k_\rho)^q} J_n(k_\rho \rho) j_m(k_\rho a) e^{-k_\rho z} dk_\rho \\ &= a^{p-q+1} \int_0^\infty (k_\rho)^{p-q} J_n(k_\rho \rho) j_m(k_\rho a) e^{-k_\rho z} dk_\rho \end{aligned}$$

Defining the integrals,

$$I_{nm}^p(\rho, z) = a^{p+1} \int_0^\infty (k_\rho)^p J_n(k_\rho \rho) j_m(k_\rho a) e^{-k_\rho z} dk_\rho \quad (19.12.30)$$

it follows that the small- z limit of the Hankel integrals is,

$$F_{nm}^{pq}(\rho, z) \xrightarrow{\text{small } z} I_{nm}^{p-q}(\rho, z) \quad (19.12.31)$$

Under these approximations, all the terms in Eq. (19.12.29) admit a closed-form expression, with the exception of the last three terms of \mathbf{H}_\perp . However, because \mathbf{B} , \mathbf{C} are of order k , as is evident from Eq. (19.11.9), these three terms, being multiplied by ka^2 , will be of order $(ka)^2$ and can be ignored. Making the replacements (19.12.31), the *near-field approximation* then becomes,

$$\begin{aligned} \mathbf{E}_\perp &= \hat{\mathbf{r}}_\perp A I_{11}^1 + a \mathbf{B} I_{01}^0 + \frac{a\mathbf{C}}{2} (3I_{01}^0 - I_{00}^1 + I_{22}^1) - a \hat{\mathbf{r}}_\perp (\mathbf{C} \cdot \hat{\mathbf{r}}_\perp) I_{22}^1 \\ E_z &= A I_{01}^1 - a (\mathbf{B} \cdot \hat{\mathbf{r}}_\perp) I_{11}^0 - a (\mathbf{C} \cdot \hat{\mathbf{r}}_\perp) (3I_{11}^0 - I_{10}^1) \\ \eta H_z &= \frac{\hat{\mathbf{r}}_\perp \cdot (\mathbf{B} \times \hat{\mathbf{z}})}{jk} I_{11}^1 \\ \eta \mathbf{H}_\perp \times \hat{\mathbf{z}} &= jka \hat{\mathbf{r}}_\perp A I_{11}^0 + \frac{\mathbf{B}}{2jk} (I_{01}^1 - I_{21}^1) + \frac{\hat{\mathbf{r}}_\perp (\mathbf{B} \cdot \hat{\mathbf{r}}_\perp)}{jk} I_{21}^1 \end{aligned} \quad (19.12.32)$$

The required $I_{nm}^p(\rho, z)$ functions are given by the following closed-form expressions tabulated in [1364], and expressed in terms of oblate spheroidal coordinates,

$$\begin{aligned} I_{01}^0 &= u - uv \operatorname{acot}(v), & I_{01}^1 &= \operatorname{acot}(v) - \frac{v}{u^2 + v^2} \\ I_{10}^1 &= \frac{u}{u^2 + v^2}, & I_{11}^0 &= \frac{\rho}{2a} \left(\operatorname{acot}(v) - \frac{v}{1 + v^2} \right) \\ I_{10}^1 &= \frac{\rho}{a} \frac{v}{(u^2 + v^2)(1 + v^2)}, & I_{11}^1 &= \frac{\rho}{a} \frac{u}{(u^2 + v^2)(1 + v^2)} \\ I_{21}^1 &= \frac{v(1 - u^2)}{(u^2 + v^2)(1 + v^2)}, & I_{22}^1 &= \frac{u(1 - u^2)}{(u^2 + v^2)(1 + v^2)} \end{aligned} \quad (19.12.33)$$

where u, v range over, $0 \leq u \leq 1$ and $0 \leq v < \infty$, and are defined via,

$$z = auv, \quad \rho = a\sqrt{(1 - u^2)(1 + v^2)} \quad (19.12.34)$$

or, in terms of ρ, z ,

$$\begin{aligned} r^2 &= \rho^2 + z^2, & d^2 &= \sqrt{(r^2 - a^2)^2 + 4a^2 z^2} \\ u &= \sqrt{\frac{d^2 - (r^2 - a^2)}{2a^2}}, & v &= \sqrt{\frac{d^2 + (r^2 - a^2)}{2a^2}} \end{aligned} \quad (19.12.35)$$

On the $z = 0$ aperture plane, we have, $r^2 = \rho^2$, $d^2 = |\rho^2 - a^2|$, and

$$u = \sqrt{\frac{|\rho^2 - a^2| - (\rho^2 - a^2)}{2a^2}}, \quad v = \sqrt{\frac{|\rho^2 - a^2| + (\rho^2 - a^2)}{2a^2}}$$

It follows that on the conducting surface, $z = 0$ and $\rho > a$, we have $u = 0$, and Eqs. (19.12.33) imply that \mathbf{E}_\perp, H_z vanish, as required by the boundary conditions.

Similarly, on the aperture, $z = 0$ and $\rho \leq a$, we have $v = 0$ and $u = \Delta(\rho)/a$, and one can verify that \mathbf{E}_\perp is given by Eq. (19.11.8), and that E_z satisfies the condition $E_z = E_z^i$ in the following (Taylor expansion) sense,

$$E_z(\mathbf{r}_\perp, 0) = E_z^i(\mathbf{r}_\perp, 0) = E_z^i(0) + \mathbf{r}_\perp \cdot \nabla_\perp E_z^i(0) \quad (19.12.36)$$

Similarly, we find for \mathbf{H}_\perp ,

$$\mathbf{H}_\perp(\mathbf{r}_\perp, 0) = \mathbf{H}_\perp^i(0) + \frac{1}{2} jk \eta^{-1} E_z^i(0) \hat{\mathbf{z}} \times \mathbf{r}_\perp \quad (19.12.37)$$

So that at the aperture center, $\mathbf{H}_\perp(0, 0) = \mathbf{H}_\perp^i(0)$. The second term guarantees that the z -component of Maxwell's equation, $\nabla \times \eta \mathbf{H} = jk\mathbf{E}$, is satisfied at the center,

$$\partial_x H_y(0, 0) - \partial_y H_x(0, 0) = jk \eta^{-1} E_z(0) = jk \eta^{-1} E_z^i(0) \quad (19.12.38)$$

MATLAB Functions

The following three MATLAB functions calculate the E, H fields at any observation point (ρ, ϕ, z) to the right of the aperture, $z \geq 0$,

```
[Ex, Ey, Ez, Hx, Hy, Hz] = BBnum(EHi, k, a, rho, phi, z); % fields in Bethe-Bouwkamp model
[Ex, Ey, Ez, Hx, Hy, Hz] = BBnear(EHi, k, a, rho, phi, z); % near fields
[Ex, Ey, Ez, Hx, Hy, Hz] = BBfar(EHi, k, a, rho, phi, z); % far fields
```

The function BBnum implements Eqs. (19.12.29) for calculating the fields at any z . BBnear implements the near-field expressions (19.12.32) and (19.12.33), and BBfar implements the far-zone calculation based on Eqs. (19.11.35).

Their usage is illustrated in Example 19.12.1. In particular, the 1×5 input array, EHi, holds the five incident field values at the aperture center, $(x, y) = (0, 0)$,

$$EHi = [\eta H_x^i, \eta H_y^i, E_z^i, \partial_x E_z^i, \partial_y E_z^i]$$

The functions BBnum and BBnear require all five entries of EHi, whereas BBfar uses only the first three. In these functions, z is a scalar, but ρ, ϕ can be vectors of same size, or one of them a vector, the other a scalar. The outputs inherit the size of ρ or ϕ .

The numerical integration for the integrals F_{nm}^{pq} in BBnum are carried out by splitting the interval $0 \leq k_\rho < \infty$ in the two subintervals, $0 \leq k_\rho \leq k$ and $k \leq k_\rho < \infty$. The integral over $[0, k]$ is evaluated using the tanh-sinh double-exponential quadrature rule implemented by the MATLAB function QUADTS described in Appendix I. The integral over $[k, \infty)$ is approximated using Gauss-Legendre quadrature with the function QUADRS also from Appendix I. These work adequately for our purposes in this book. More accurate integration procedures are employed in [1364].

The implementation of BBnear is straightforward using the functions (19.12.33). For BBfar, we note that because the dipole moments M, P only have components M_x, M_y, P_z , we obtain the following explicit forms of Eqs. (19.11.35),

$$\begin{aligned} E_x &= P_z \partial_x \partial_z G + jk M_y \partial_z G \\ E_y &= P_z \partial_y \partial_z G - jk M_x \partial_z G \\ E_z &= k^2 P_z G + P_z \partial_z^2 G + jk (M_x \partial_y G - M_y \partial_x G) \\ \eta H_x &= k^2 M_x G + M_x \partial_x^2 G + M_y \partial_y \partial_x G + jk P_z \partial_y G \\ \eta H_y &= k^2 M_y G + M_x \partial_x \partial_y G + M_y \partial_y^2 G - jk P_z \partial_x G \\ \eta H_z &= M_x \partial_x \partial_z G + M_y \partial_y \partial_z G \end{aligned} \tag{19.12.39}$$

The required first and second derivatives of $G(r)$ are given as follows, for $\alpha, \beta = 1, 2, 3$, and implemented internally in BBfar,

$$\begin{aligned} \partial_\alpha G(\mathbf{r}) &= -\frac{x_\alpha}{r} \left(jk + \frac{1}{r} \right) G(\mathbf{r}) \\ \partial_\alpha \partial_\beta G(\mathbf{r}) &= \left[\left(jk + \frac{1}{r} \right) \frac{3x_\alpha x_\beta - r^2 \delta_{\alpha\beta}}{r^3} - k^2 \frac{x_\alpha x_\beta}{r^2} \right] G(\mathbf{r}) \end{aligned} \tag{19.12.40}$$

Example 19.12.1: We consider the same example of Ref. [1364]. The incident field is assumed to be TM, given by Eq. (19.11.55) with $E_0 = 0, \eta H_0 = 1$, and incident at an angle $\theta_i = 30^\circ$. Fig. 19.12.1 plots in log-log scales the field magnitudes $|\eta H_y|$ and $|E_x|$ along the aperture axis as a function of the distance z spanning the range $10^{-2} \leq z/a \leq 10^2$. The z -component is plotted in Fig. 19.12.2.

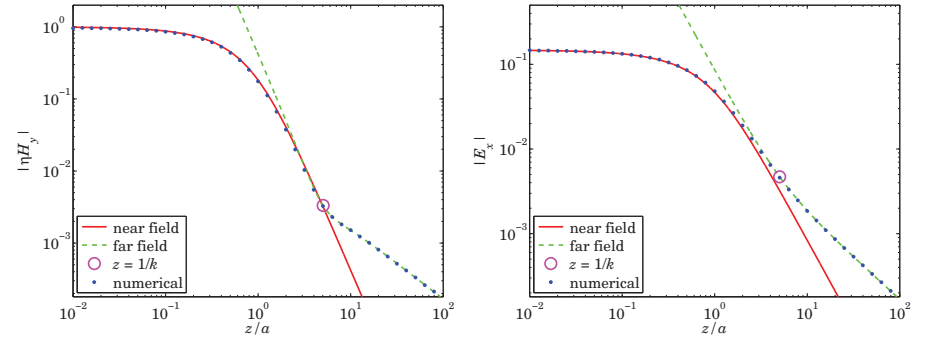


Fig. 19.12.1 Fields $\eta H_y, E_x$ at $x = y = 0$ versus distance z from aperture.

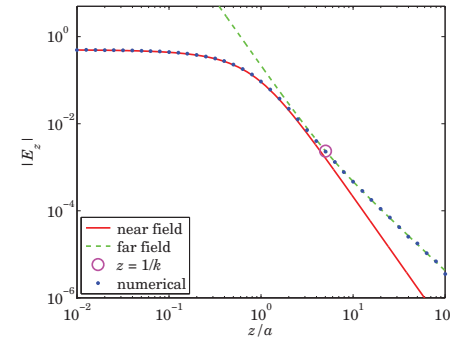


Fig. 19.12.2 Field E_z at $x = y = 0$ versus distance z from aperture.

The blue dots represent the numerical calculation using BBnum, the solid red lines are the near fields computed with BBnear, and the dashed green lines represent the far fields computed with BBfar. We note the point of transition at $z = 1/k$ between the far and radiation zones. The following MATLAB code illustrates the computation,

```
a=20; la=633; k=2*pi/la; thi=pi/6;
E0 = 0; H0 = 1;
kxi = k*sin(thi); kzi = k*cos(thi);
Hxi = -E0*kzi/k; Hyi = H0;
Ezi = -H0*kxi/k; dxEzi = -j*kxi*Ezi; dyEzi = 0;
EHi = [Hxi, Hyi, Ezi, dxEzi, dyEzi]; % input to BBnum
```

```

r=0; phi=0;
z = logspace(-2,2,2001)*a;
z1 = z(1:50:end); % subset of z's for BBnum
zk = 1/k; % turning point

for i=1:length(z1)
    [Ex(i),Ey(i),Ez(i),Hx(i),Hy(i),Hz(i))] = BBnum(EHi,k,a,r,phi,z1(i));
end

[Exn,Eyn,Ezn,Hxn,Hyn,Hzn] = BBnear(EHi,k,a,r,phi,z);
[Exf,Eyf,Ezf,Hxf,Hyf,Hzf] = BBfar(EHi,k,a,r,phi,z);
[Exk,Eyk,Ezk,Hxk,Hyk,Hzk] = BBfar(EHi,k,a,r,phi,zk);

figure; loglog(z/a,abs(Hyn),'b-', z/a,abs(HyF),'g--',...
    zk/a, abs(Hyk),'mo', z1/a,abs(Hy),'r. ');
figure; loglog(z/a,abs(Exn),'b-', z/a,abs(ExF),'g--',...
    zk/a, abs(Exk),'mo', z1/a,abs(Ex),'r. ');
    
```

Fig. 19.12.3 plots the real and imaginary parts of the fields, $\eta H_y, E_x, E_z$, at distance $z = a/10$, along the cross sections at $y = 0$ and $-3 \leq x/a \leq 3$, and $x = 0$ and $-3 \leq y/a \leq 3$. The following MATLAB code segment illustrates the computation,

```

x = linspace(-3,3,601)*a; y =0; % y = linspace(-3,3,601)*a; x =0;
r = sqrt(x.^2 + y.^2); ph = atan2(y,x);
z = a/10;

[Ex,Ey,Ez,Hx,Hy,Hz] = BBnum(EHi,k,a,r,ph,z);
% [Ex,Ey,Ez,Hx,Hy,Hz] = BBnear(EHi,k,a,r,ph,z); % alternative for small z

figure; plot(x/a,real(Ex),'b-', x/a,imag(Ex),'r--');
figure; plot(x/a,real(Hy),'b-', x/a,imag(Hy),'r--');
figure; plot(x/a,real(Ez),'b-', x/a,imag(Ez),'r--');
    
```

We should note that at the above short distance of $z = a/10$, the near-field approximation function `BBnear` could as well have been used to calculate the fields. \square

19.13 Babinet Principle

The Babinet principle for electromagnetic fields [1291,1316] applies to a flat conducting screen with an aperture cut in it.[†] The *complementary screen* is obtained by removing the conducting screen and replacing the aperture by a conductor, as shown in Fig. 19.13.1.

Let M, A denote the metallic part and the aperture of the original problem, making up the entire planar screen, $S = M + A$. Then the complementary screen has metallic part $M_c = A$ and aperture $A_c = M$, so that again, $S = M_c + A_c$.

We may assume that the aperture plane S is the xy plane, and suppose that the fields E^i, H^i are incident from the left on the original $M + A$ screen resulting in the diffracted fields E, H to the right of the aperture, $z \geq 0$. Consider also the fields E_c^i, H_c^i incident on the complementary screen $M_c + A_c$, resulting in the diffracted fields E_c, H_c . Then,

[†]For a recent review, see Ref. [1311].

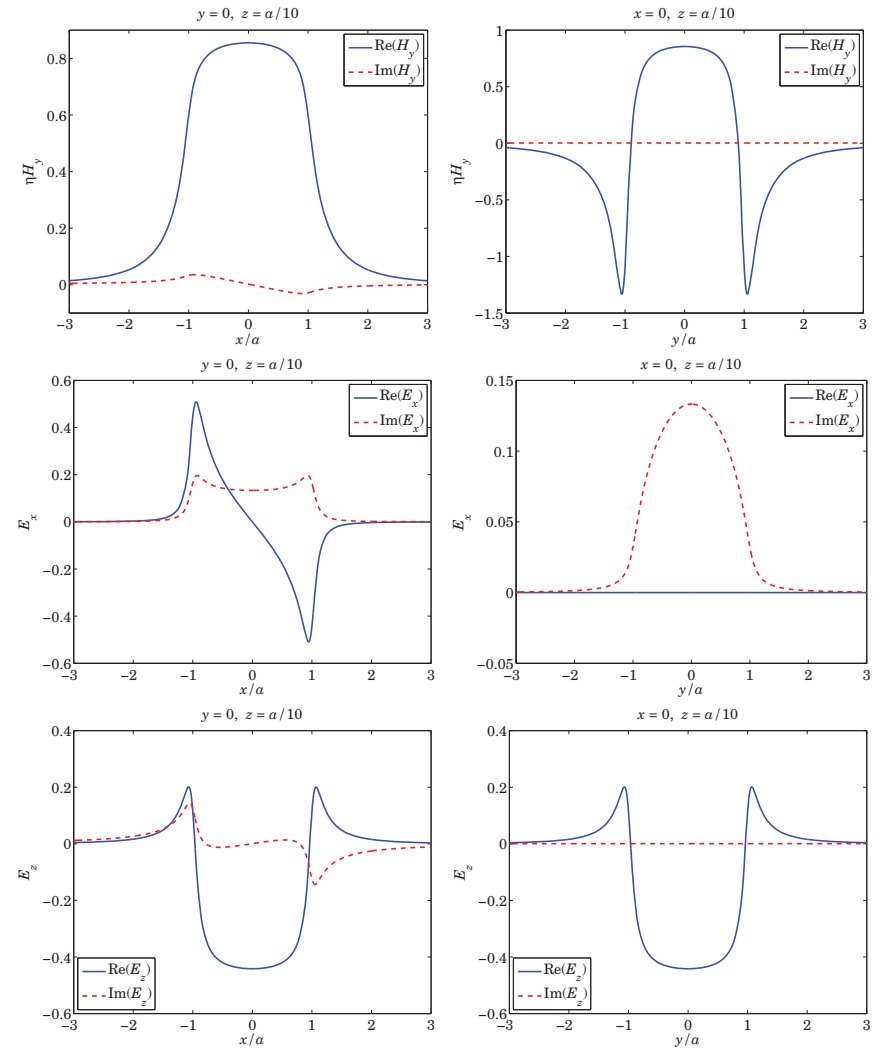


Fig. 19.12.3 Fields $\eta H_y, E_x, E_z$ at $z = a/10$ versus $-3 \leq x/a \leq 3$ and versus $-3 \leq y/a \leq 3$.

the boundary and symmetry conditions, Eqs. (19.9.2) and (19.9.4), imply the following conditions on the tangential electric and magnetic fields in the two problems,

$$\begin{aligned}
 \hat{z} \times E = 0, & \quad \text{on } M & \quad \left| & \quad \hat{z} \times E_c = 0, & \quad \text{on } M_c = A \\
 \hat{z} \times H = \hat{z} \times H^i, & \quad \text{on } A & \quad \left| & \quad \hat{z} \times H_c = \hat{z} \times H_c^i, & \quad \text{on } A_c = M
 \end{aligned} \tag{19.13.1}$$

Suppose now that the incident fields E_c^i, H_c^i are chosen to be the duals of the E^i, H^i

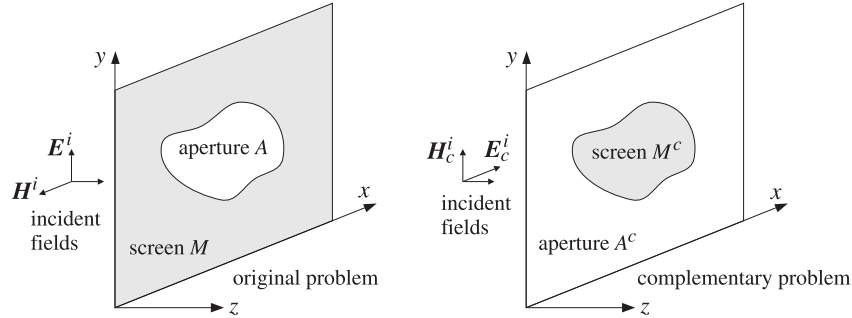


Fig. 19.13.1 Original and complementary metallic screen and aperture.

fields, that is, $E_c^i = -\eta H^i$ and $H_c^i = \eta^{-1} E^i$, or expressed in matrix form,

$$\begin{bmatrix} E_c^i \\ H_c^i \end{bmatrix} = \underbrace{\begin{bmatrix} 0 & -\eta \\ \eta^{-1} & 0 \end{bmatrix}}_D \begin{bmatrix} E^i \\ H^i \end{bmatrix} = D \begin{bmatrix} E^i \\ H^i \end{bmatrix} \quad (19.13.2)$$

Then, the last of Eqs. (19.13.1) implies that, $\hat{z} \times \eta H_c = \hat{z} \times \eta H_c^i = \hat{z} \times E^i$ on M , which can be added to the first equation, resulting in, $\hat{z} \times (E + \eta H_c) = \hat{z} \times E^i$ on M . Similarly, from the second and third equations, we have, $\hat{z} \times (H - \eta^{-1} E_c) = \hat{z} \times H^i - \eta^{-1} \hat{z} \times E_c = \hat{z} \times H^i$ on A . Thus, the original and complementary problems must satisfy the conditions,

$$\begin{aligned} \hat{z} \times (E + \eta H_c) &= \hat{z} \times E^i, & \text{on } M \\ \hat{z} \times (H - \eta^{-1} E_c) &= \hat{z} \times H^i, & \text{on } A \end{aligned} \quad (19.13.3)$$

These state that the tangential components of the total fields $E_{\text{tot}} = E + \eta H_c$ and $H_{\text{tot}} = H - \eta^{-1} E_c$ match those of the incident fields E^i, H^i over the entire xy plane, with the E -fields matching over M and the H -fields over A . As a consequence of the uniqueness theorem discussed below, it follows that the fields will match everywhere in the right half-space, that is, $E_{\text{tot}} = E^i, H_{\text{tot}} = H^i$, for $z \geq 0$,

$$\boxed{\begin{aligned} E + \eta H_c &= E^i \\ H - \eta^{-1} E_c &= H^i \end{aligned}} \quad (\text{electromagnetic Babinet principle}) \quad (19.13.4)$$

This is the Babinet principle for electromagnetic fields. Eq. (19.13.4) may also be written in matrix form with the help of the inverse of the duality matrix D of Eq. (19.13.2), that is, $D^{-1} = -D$,

$$\begin{bmatrix} E \\ H \end{bmatrix} + D^{-1} \begin{bmatrix} E_c \\ H_c \end{bmatrix} = \begin{bmatrix} E^i \\ H^i \end{bmatrix} \quad (19.13.5)$$

which, after multiplying both sides by D , can also be transformed into,

$$\begin{bmatrix} E_c \\ H_c \end{bmatrix} + D \begin{bmatrix} E \\ H \end{bmatrix} = \begin{bmatrix} E_c^i \\ H_c^i \end{bmatrix} \quad (19.13.6)$$

The operations of the Babinet principle are summarized pictorially in Fig. 19.13.2 in which F stands for $\begin{bmatrix} E \\ H \end{bmatrix}$, and the boxes labeled S, S_c represent the diffraction operations of the original and complementary problems, and D , the duality transformations.

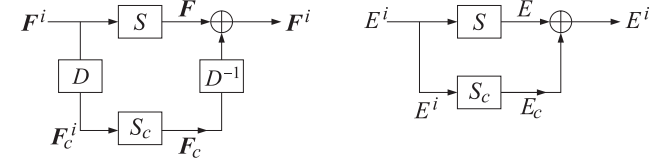


Fig. 19.13.2 Electromagnetic and scalar versions of the Babinet principle.

One may wonder why we formed the above particular linear combination of the H, E_c fields in defining H_{tot} ; the E_c could have been added with any weight and still satisfy (19.13.3). In fact, the form of H_{tot} is fixed by Maxwell's equations once E_{tot} is defined as $E_{\text{tot}} = E + \eta H_c$. Indeed, from Maxwell equations of the individual parts, we have,

$$H_{\text{tot}} = -\frac{\nabla \times E_{\text{tot}}}{jk\eta} = -\frac{\nabla \times E + \eta \nabla \times H_c}{jk\eta} = -\frac{-jk\eta H + \eta jk\eta^{-1} E_c}{jk\eta} = H - \eta^{-1} E_c$$

The proof of the Babinet principle rests on a particular form of the *uniqueness theorem* of electromagnetics [22] that states that the fields inside a volume are uniquely determined by the tangential E -fields over a part of the enclosing boundary surface and the tangential H -fields over the rest of that surface. In the problem at hand, the volume is taken to be the right half-space, bounded by the xy plane at $z = 0$ and an infinite hemispherical surface as shown below and in Fig. 19.1.1.

The proof of the uniqueness theorem relies on the following additional assumptions: (a) that there are no sources in the right half-space, (b) that the medium is slightly lossy, and (c) that the fields satisfy the (outgoing) Sommerfeld radiation condition, that is, having radial dependence of the form, e^{-jkr}/r , for large r .

The lossy medium can be represented by adding a small negative imaginary part to its dielectric constant and/or to its permittivity, that is, $\epsilon = \epsilon_R - j\epsilon_I$ and $\mu = \mu_R - j\mu_I$, and as a consequence, $k = k_R - jk_I$, where ϵ_I, μ_I, k_I are small positive constants. The lossless case is obtained in the limit of zero imaginary parts.

Working with the difference fields, $\delta E = E_{\text{tot}} - E^i$ and $\delta H = H_{\text{tot}} - H^i$, the conditions (19.13.3) become,

$$\begin{aligned} \delta E = E + \eta H_c - E^i &\Rightarrow \hat{z} \times \delta E = 0, & \text{on } M \\ \delta H = H - \eta^{-1} E_c - H^i &\Rightarrow \hat{z} \times \delta H = 0, & \text{on } A \end{aligned} \quad (19.13.7)$$

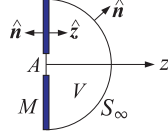
The fields $\delta E, \delta H$ satisfy the source-free Maxwell's equations in $z \geq 0$,

$$\nabla \times \delta E = -j\omega\mu\delta H, \quad \nabla \times \delta H = j\omega\epsilon\delta E \Rightarrow \nabla \times \delta H^* = -j\omega\epsilon^*\delta E^*$$

from which we obtain the divergence of the complex Poynting vector,

$$\nabla \cdot (\delta E \times \delta H^*) = \delta H^* \cdot \nabla \times \delta E - \delta E \cdot \nabla \times \delta H^* = -j\omega\mu |\delta H|^2 + j\omega\epsilon^* |\delta E|^2$$

Integrating over the right half-space V bounded by the xy plane, $M + A$, and the hemisphere S_∞ , and applying the divergence theorem, we obtain,

$$\begin{aligned} & \int_V \left[-j\omega\mu |\delta\mathbf{H}|^2 + j\omega\epsilon^* |\delta\mathbf{E}|^2 \right] dV = \\ & = \int_{M+A+S_\infty} \delta\mathbf{E} \times \delta\mathbf{H}^* \cdot \hat{\mathbf{n}} dS = \int_{S_\infty} \delta\mathbf{E} \times \delta\mathbf{H}^* \cdot \hat{\mathbf{n}} dS + \\ & + \int_M \hat{\mathbf{n}} \times \delta\mathbf{E} \cdot \mathbf{H}^* dS + \int_A \delta\mathbf{H}^* \times \hat{\mathbf{n}} \cdot \delta\mathbf{E} dS \end{aligned}$$


The surface integral over S_∞ is zero since the fields decay like $e^{-jkr}/r = e^{-jk_r r} e^{-k_i r}/r$ for large r . The surface integrals over M and A are zero because of Eqs. (19.13.7). Thus, we obtain the following complex-valued condition and its real part,

$$\begin{aligned} & \int_V \left[-j\omega\mu |\delta\mathbf{H}|^2 + j\omega\epsilon^* |\delta\mathbf{E}|^2 \right] dV = 0 \\ & \int_V \left[\omega\mu_I |\delta\mathbf{H}|^2 + \omega\epsilon_I |\delta\mathbf{E}|^2 \right] dV = 0 \end{aligned} \quad (19.13.8)$$

Since ϵ_I, μ_I are non-negative with at least one of them being non-zero, it follows from (19.13.8) that $\delta\mathbf{E} = \delta\mathbf{H} = 0$, which proves the Babinet principle. An equivalent way of stating the principle is in terms of the *scattered* fields, $\mathbf{E}^s = \mathbf{E} - \mathbf{E}^i$, $\mathbf{H}^s = \mathbf{H} - \mathbf{H}^i$ of the original problem, or, $\mathbf{E}_c^s = \mathbf{E}_c - \mathbf{E}_c^i$, $\mathbf{H}_c^s = \mathbf{H}_c - \mathbf{H}_c^i$, of the complementary problem,

$$\begin{array}{|l} \mathbf{E}^s = -\eta\mathbf{H}_c \\ \mathbf{H}^s = \eta^{-1}\mathbf{E}_c \end{array} \quad \text{and} \quad \begin{array}{|l} \mathbf{E}_c^s = \eta\mathbf{H} \\ \mathbf{H}_c^s = -\eta^{-1}\mathbf{E} \end{array} \quad (19.13.9)$$

and, in matrix form,

$$\begin{bmatrix} \mathbf{E}^s \\ \mathbf{H}^s \end{bmatrix} = D \begin{bmatrix} \mathbf{E}_c \\ \mathbf{H}_c \end{bmatrix} \quad \text{and} \quad \begin{bmatrix} \mathbf{E}_c^s \\ \mathbf{H}_c^s \end{bmatrix} = D^{-1} \begin{bmatrix} \mathbf{E} \\ \mathbf{H} \end{bmatrix} \quad (19.13.10)$$

In this form, it states that in order to find the scattered fields of the original problem, one can instead solve the dual complementary problem with inputs chosen as the duals of the incident fields of the original problem.

As an example, consider the problem of finding the scattered fields $\mathbf{E}_c^s, \mathbf{H}_c^s$ off a small circular conducting disk with given incident fields $\mathbf{E}_c^i, \mathbf{H}_c^i$. This is complementary to the problem of diffraction by a small hole whose solution was given by the Bethe-Bouwkamp model of the previous two sections. Thus, the solution of the scattering problem is obtained quickly by the following steps,

$$\begin{bmatrix} \mathbf{E}_c^i \\ \mathbf{H}_c^i \end{bmatrix} \xrightarrow{D^{-1}} \begin{bmatrix} \mathbf{E}^i \\ \mathbf{H}^i \end{bmatrix} \xrightarrow{\text{Bethe-Bouwkamp}} \begin{bmatrix} \mathbf{E} \\ \mathbf{H} \end{bmatrix} \xrightarrow{D^{-1}} \begin{bmatrix} \mathbf{E}_c^s \\ \mathbf{H}_c^s \end{bmatrix}$$

In particular, the \mathbf{E}, \mathbf{H} fields at any distance $z \geq 0$ are obtained from (19.12.29), the near-fields from (19.12.32), and the far-fields from (19.11.32)–(19.11.35). The required Bethe-Bouwkamp A, B, C parameters of (19.11.9) depend on E_z^i, H_x^i, H_y^i , which are obtained from the duality transformation, $\mathbf{E}^i = \eta\mathbf{H}_c^i$, $\mathbf{H}^i = -\eta^{-1}\mathbf{E}_c^i$, or,

$$E_z^i = \eta H_{cz}^i, \quad H_x^i = -\frac{1}{\eta} E_{cx}^i, \quad H_y^i = -\frac{1}{\eta} E_{cy}^i$$

In the radiation zone, the fields map as follows via Eq. (19.13.9), first, for the circular aperture as in (19.11.40), in spherical coordinates,

$$\begin{aligned} E_\theta &= \eta H_\phi = \frac{4a^3 k^2}{3\pi} \left(\eta H_x^i \sin\phi - \eta H_y^i \cos\phi - \frac{1}{2} E_z^i \sin\theta \right) \frac{e^{-jkr}}{r} \\ E_\phi &= -\eta H_\theta = \frac{4a^3 k^2}{3\pi} (\eta H_x^i \cos\phi + \eta H_y^i \sin\phi) \cos\theta \frac{e^{-jkr}}{r} \end{aligned} \quad (19.13.11)$$

second, for the scattered fields of the circular disk,

$$\begin{aligned} E_{c\phi}^s &= -\eta H_{c\theta}^s = \frac{4a^3 k^2}{3\pi} \left(-E_{cx}^i \sin\phi + E_{cy}^i \cos\phi - \frac{1}{2} \eta H_{cz}^i \sin\theta \right) \frac{e^{-jkr}}{r} \\ E_{c\theta}^s &= \eta H_{c\phi}^s = \frac{4a^3 k^2}{3\pi} (E_{cx}^i \cos\phi + E_{cy}^i \sin\phi) \cos\theta \frac{e^{-jkr}}{r} \end{aligned} \quad (19.13.12)$$

More generally, we can show that Eqs. (19.13.10) satisfy the required integral equations. In fact, Eqs. (19.9.13) for the original problem and (19.9.22) for the complementary problem are essentially the same. Indeed, we have for the two problems,

| on the aperture, A | on the conductor, $M_c = A$ |
|--|--|
| $k^2 \mathbf{F}^0 + \nabla_\perp (\nabla_\perp \cdot \mathbf{F}^0) = -jk\eta \mathbf{H}_\perp^i$ | $k^2 \mathbf{A}_c^0 + \nabla_\perp (\nabla_\perp \cdot \mathbf{A}_c^0) = -jk\eta^{-1} \mathbf{E}_{c\perp}^i$ |
| $\hat{\mathbf{z}} \cdot \nabla_\perp \times \mathbf{F}^0 = E_z^i$ | $\hat{\mathbf{z}} \cdot \nabla_\perp \times \mathbf{A}_c^0 = -H_{cz}^i$ |

(19.13.13)

where $\mathbf{F}^0, \mathbf{A}_c^0$ are defined as follows, with $R_0 = |\mathbf{r}_\perp - \mathbf{r}'_\perp|$, and $\mathbf{r}_\perp \in A$,

$$\begin{aligned} \mathbf{F}^0(\mathbf{r}_\perp) &= 2 \int_A [\hat{\mathbf{z}} \times \mathbf{E}_\perp(\mathbf{r}'_\perp, 0)] G(R_0) d^2 \mathbf{r}'_\perp \\ \mathbf{A}_c^0(\mathbf{r}_\perp) &= 2 \int_{M_c=A} [\hat{\mathbf{z}} \times \mathbf{H}_{c\perp}^s(\mathbf{r}'_\perp, 0^+)] G(R_0) d^2 \mathbf{r}'_\perp \end{aligned} \quad (19.13.14)$$

But if we set, $\mathbf{H}_c^s = -\eta^{-1}\mathbf{E}$, and, $\mathbf{E}_c^i = -\eta\mathbf{H}^i$, $\mathbf{H}_c^i = \eta^{-1}\mathbf{E}^i$, then we recognize that, $\mathbf{A}_c^0 = -\eta^{-1}\mathbf{F}^0$, and the two sets of integral equations in (19.13.13) become the same.

There is one minor difference between the aperture and the complementary scattering problem, namely, the *transmission cross-section* of the former is *half* as large as the *scattering cross-section* of the latter.

In both cases, the cross-section is defined as the ratio of the radiated power to the magnitude of the Poynting vector of the incident fields, as in Eq. (19.11.53),

$$\sigma = \frac{P_{\text{rad}}}{|\mathcal{P}^i|}, \quad |\mathcal{P}^i| = \left| \frac{1}{2} \text{Re}[\mathbf{E}^i \times \mathbf{H}^{i*}] \right| \quad (19.13.15)$$

The duality transformations between the two problems imply that the radiation intensity, $dP/d\Omega$, as well as $|\mathcal{P}^i|$ will be the same in the two problems, but the radiated power of the scattering problem is defined by integrating $dP/d\Omega$ over the entire sphere, whereas in the aperture case it is integrated over half of that, i.e., the right hemisphere.

Scalar Babinet Principle

The Babinet principle for scalar fields [638,1287] is more straightforward than the electromagnetic version, as it involves the same (rather than dual) incident fields on the original and complementary screens.

It can be proved quickly within the Kirchhoff approximation of Eq. (19.1.15). The screens are depicted in Fig. 19.13.1, except that now M, M_c are simply absorbing screens. With the field E^i incident from the left, the Rayleigh-Sommerfeld diffraction integrals for the original and complementary apertures, are,

$$\begin{aligned}
 E(\mathbf{r}_\perp, z) &= -2 \frac{\partial}{\partial z} \int_A E^i(\mathbf{r}'_\perp, 0) \frac{e^{-jkR}}{4\pi R} d\mathbf{r}'_\perp \\
 E_c(\mathbf{r}_\perp, z) &= -2 \frac{\partial}{\partial z} \int_{A_c} E^i(\mathbf{r}'_\perp, 0) \frac{e^{-jkR}}{4\pi R} d\mathbf{r}'_\perp
 \end{aligned}
 \tag{19.13.16}$$

with $R = \sqrt{|\mathbf{r}_\perp - \mathbf{r}'_\perp|^2 + z^2}$ and $z \geq 0$. Adding these up and invoking the Rayleigh-Sommerfeld integral for the field E^i itself relative to the entire xy -plane, we obtain,

$$\begin{aligned}
 E(\mathbf{r}_\perp, z) + E_c(\mathbf{r}_\perp, z) &= -2 \frac{\partial}{\partial z} \int_A E^i(\mathbf{r}'_\perp, 0) \frac{e^{-jkR}}{4\pi R} d\mathbf{r}'_\perp - 2 \frac{\partial}{\partial z} \int_{A_c} E^i(\mathbf{r}'_\perp, 0) \frac{e^{-jkR}}{4\pi R} d\mathbf{r}'_\perp \\
 &= -2 \frac{\partial}{\partial z} \int_{A+A_c} E^i(\mathbf{r}'_\perp, 0) \frac{e^{-jkR}}{4\pi R} d\mathbf{r}'_\perp = E^i(\mathbf{r}_\perp, z)
 \end{aligned}$$

These operations are depicted in Fig. 19.13.2. Thus the scalar Babinet principle is,

$$\boxed{E + E_c = E^i} \quad (\text{scalar Babinet principle}) \tag{19.13.17}$$

19.14 Problems

19.1 The following two expressions were derived for the radiated electric field, first in Eq. (19.6.1) using the stationary-phase method, and second in Eq. (19.11.23) applying the radiation field approximation to the Smythe formula,

$$\begin{aligned}
 E_{\text{rad}} &= 2jk \cos \theta \hat{\mathbf{E}}(\mathbf{k}_\perp) \cdot G(\mathbf{r}) \\
 E_{\text{rad}} &= -jk \hat{\mathbf{r}} \times [\hat{\mathbf{z}} \times \hat{\mathbf{E}}_\perp(\mathbf{k}_\perp)] \cdot G(\mathbf{r}), \quad G(\mathbf{r}) = \frac{e^{-jkr}}{4\pi r}
 \end{aligned}$$

where $\mathbf{k} = k \hat{\mathbf{r}}$. Show that these two expressions are equivalent.

19.2 Prove Eq. (19.11.48), and then show that if both terms are kept, the radiated power calculated by (19.11.50) will be given by,

$$P_{\text{rad}} = \frac{(ka)^2}{3} \cdot \pi a^2 \cdot \frac{1}{2\eta} [|E_\perp^i|^2 + k^2 D]$$

where the term D depends on the derivatives of the incident fields at the origin,

$$D = \frac{1}{80} [2 | \partial_x E_x^i + \partial_y E_y^i |^2 + | \partial_x E_y^i - \partial_y E_x^i |^2 + 3 \text{Re} [\partial_y E_x^i \partial_x E_y^{i*} - \partial_x E_x^i \partial_y E_y^{i*}]]$$

19.3 Derive Eqs. (19.11.58)–(19.11.63) regarding an incident plane wave on a circular aperture.
 19.4 Using the 2-D transform (19.12.12), and differentiating both sides with respect to k_x, k_y , derive the following transforms,

$$\begin{aligned}
 \int_A \frac{\chi_\alpha}{\Delta(\rho)} e^{jk_\perp \cdot \mathbf{r}_\perp} d^2 \mathbf{r}_\perp &= -j \frac{\partial}{\partial k_\alpha} \left[\int_A \frac{1}{\Delta(\rho)} e^{jk_\perp \cdot \mathbf{r}_\perp} d^2 \mathbf{r}_\perp \right] = 2\pi a^2 \cdot \frac{jk_\alpha}{k_\rho} j_1(k_\rho a) \\
 \int_A \frac{\chi_\alpha \chi_\beta}{\Delta(\rho)} e^{jk_\perp \cdot \mathbf{r}_\perp} d^2 \mathbf{r}_\perp &= -\frac{\partial^2}{\partial k_\alpha \partial k_\beta} \left[\int_A \frac{1}{\Delta(\rho)} e^{jk_\perp \cdot \mathbf{r}_\perp} d^2 \mathbf{r}_\perp \right] \\
 &= 2\pi a^2 \cdot \left[\delta_{\alpha\beta} \frac{j_1(k_\rho a)}{k_\rho} - \frac{k_\alpha k_\beta}{k_\rho^2} a j_2(k_\rho a) \right]
 \end{aligned}
 \tag{19.14.1}$$

where $\alpha, \beta = 1, 2$. Then, derive the 2-D transforms in Eqs. (19.12.11).